

N 62 54593

CASE FILE
COPY

NACA TN 2593

NATIONAL ADVISORY COMMITTEE
FOR AERONAUTICS

TECHNICAL NOTE 2593

DESIGN OF TWO-DIMENSIONAL CHANNELS WITH PRESCRIBED
VELOCITY DISTRIBUTIONS ALONG THE CHANNEL WALLS

I - RELAXATION SOLUTIONS

By John D. Stanitz

Lewis Flight Propulsion Laboratory
Cleveland, Ohio



Washington

January 1952

TECHNICAL NOTE 2593

DESIGN OF TWO-DIMENSIONAL CHANNELS WITH PRESCRIBED
VELOCITY DISTRIBUTIONS ALONG THE CHANNEL WALLS

I - RELAXATION SOLUTIONS

By John D. Stanitz

SUMMARY

A general method of design is developed for two-dimensional unbranched channels with prescribed velocities as a function of arc length along the channel walls. The method is developed for both incompressible and compressible, irrotational, nonviscous flow. Two types of compressible flow are considered: the general type, with the ratio of specific heats γ equal to 1.4, for example, and the linearized type in which γ is equal to -1.0. The design method gives complete information concerning the flow throughout the channel.

Five numerical examples are given including three elbow designs with the same prescribed velocity as a function of arc length along the channel walls but with incompressible, linearized compressible, and compressible flow. It is concluded that if a nonviscous gas with arbitrary γ (1.4, for example) were to flow through a channel designed for linearized compressible flow ($\gamma = -1.0$), the resulting velocity distribution along the channel walls would be nearly the velocity distribution prescribed for the linearized compressible flow, at least if the linearized flow were selected so that the densities are equal for both types of flow at the maximum and minimum velocities and if the ratio of these velocities is not too large (2:1 in the numerical examples).

INTRODUCTION

There are two general types of theoretical problem in two-dimensional fluid motion: (1) the direct problem, in which the distribution of velocity is determined for a prescribed shape of boundary, and (2) the inverse problem, in which the shape of boundary is determined for a prescribed distribution of velocity along the boundary. The direct problem is an analysis problem; the inverse problem is a design problem.

This report is concerned with the inverse, or design, problem for two-dimensional, irrotational flow in unbranched channels with prescribed velocities as a function of arc length along the channel walls.

The design of channels with prescribed velocities is important because: (1) Boundary-layer separation losses can be avoided by prescribed velocities that do not decelerate rapidly enough to cause separation, (2) shock losses in compressible flow and cavitation in incompressible flow can be avoided by prescribed velocities that do not exceed certain maximum values dictated by these phenomena, and (3) for compressible flow the desired flow rate can be assured by prescribed velocities that do not result in "choke flow" conditions.

Several methods of channel design have been developed for particular application (references 1 and 2, for example). In reference 1 a design method is developed for accelerating elbows in which the velocity increases monotonically along the channel walls. The method is developed for incompressible and linearized ($\gamma = -1.0$) compressible flow. The velocity distribution along the channel walls is not arbitrary and the design method applies to elbows only. In reference 2 a design method is developed for straight, symmetrical channels with contracting or expanding walls. The method is developed for incompressible flow and the velocities are prescribed not as a function of arc length along the channel walls but as a function of circle angle in the transformed circle plane. A more general design is suggested in reference 3 but no attempt is made to develop and apply the method.

In the present report a general method of design is developed for two-dimensional, unbranched channels with prescribed velocities as a function of arc length along the channel walls. The method is developed for both compressible and incompressible, irrotational, nonviscous flow and applies to the design of elbows, diffusers, nozzles, and so forth. Two types of compressible flow are considered: the general type with arbitrary value of γ (1.4, for example) and the linearized type with γ equal to -1.0. In general, if the prescribed velocity along one channel wall differs from that along the other, the channel turns so that the downstream flow direction is different from the upstream direction. This change in flow direction cannot be arbitrarily chosen but depends on the prescribed velocity distribution along the walls. Equations are developed for computing this change in flow direction for an arbitrary prescribed velocity distribution with incompressible or linearized compressible flow. Two methods of solution have been developed for the design method and are presented in separate reports. In this report (part I) solutions are obtained by relaxation methods (reference 4). This method of solution results in complete information concerning the distribution of flow conditions throughout the channel and, in addition, can be used to obtain nonlinear solutions for compressible flow with arbitrary values of γ . In reference 5 (part II)

solutions are obtained by means of a Green's function. This method of solution is limited to incompressible and linearized ($\gamma = -1.0$) compressible flow, but the method is more rapid than relaxation methods, provided information within the channel is not required.

The design method reported herein was developed at the NACA Lewis laboratory during 1950 and is part of a doctoral thesis conducted with the advice of Professor Ascher H. Shapiro of the Massachusetts Institute of Technology.

THEORY OF DESIGN METHOD

The design method is developed for two-dimensional channels with prescribed velocities along the channel walls. The prescribed velocity is arbitrary except that stagnation points (zero velocity) cannot be prescribed. This exception limits the design method to unbranched channels.

Preliminary Considerations

Assumptions. - The fluid is assumed to be nonviscous and either compressible or incompressible. The flow is assumed to be two-dimensional and irrotational.

The assumption of two-dimensional, nonviscous, irrotational motion limits the design method in practice to channels with thin (negligible) boundary layers, such as exist near the entrance to the channel or after a rapid acceleration of the flow through a contraction in the channel. Even if the boundary layer is thin, the design method is limited to (and finds its most useful application for) prescribed velocity distributions that, from boundary-layer theory, do not decelerate fast enough to result in separation of the boundary layer, which separation alters the "effective" shape of the channel and completely changes the character of the flow.

In some channels with fully developed turbulent boundary layers the design method might be expected to yield results that are satisfactory (although approximate) because for this type of flow the rotational motion occurs primarily in the regions close to the channel walls. In channel walls with thick or fully developed laminar boundary layers the design method cannot be used, because not only is the rotation of the flow important in most of the channel but, if the channel bends, important secondary flows develop that are not considered by the two-dimensional design method.

Flow field. - The flow field of the two-dimensional channel is considered to lie in the physical xy -plane where x and y are Cartesian coordinates expressed as ratios of a characteristic length equal to the constant channel width downstream at infinity. (All symbols are defined in appendix A.)

At each point in the channel (fig. 1) the velocity vector has a magnitude Q and a direction θ where Q is the fluid velocity expressed as the ratio of a characteristic velocity equal to the constant channel velocity downstream at infinity. For convenience, the velocity Q is related to a velocity q by

$$q = Qq_d \quad (1)$$

where q is the velocity expressed as a ratio of the stagnation speed of sound and the subscript d refers to conditions downstream at infinity.

The flow direction θ at each point in the channel is measured counterclockwise from the positive x -axis. From figure 1

$$dx = ds \cos \theta \quad (2a)$$

$$dy = ds \sin \theta \quad (2b)$$

where ds is a differential distance in the direction of Q , that is, along a streamline.

Stream function and velocity potential. - If the condition of continuity is satisfied a stream function ψ can be defined such that

$$d\psi = \rho Q \, dn \quad (3)$$

where ρ is the fluid density expressed as the ratio of a characteristic density equal to the stagnation density and where dn is a differential distance measured normal to the direction of Q , that is, normal to a streamline. Along a streamline, dn is zero so that from equation (3) the stream function ψ is constant.

If the condition of irrotational fluid motion is satisfied a velocity potential ϕ can be defined such that

$$d\phi = Q \, ds \quad (4)$$

Normal to a streamline, ds is zero so that from equation (4) the velocity potential ϕ is constant. Thus lines of constant ϕ and ψ are orthogonal in the physical xy -plane.

Outline of method. - Solutions for two-dimensional flow depend on known conditions imposed along the boundaries of the problem. In the inverse problem of channel design the geometry of the channel walls in the physical xy -plane is unknown. This unknown geometry apparently precludes the possibility of solving the problem in the physical plane and necessitates the use of some new set of coordinates, that is, a transformed plane, in which to solve the problem. These new coordinates must be such that the geometric boundaries along which the velocities are prescribed are known in the transformed plane. It is also desirable, for mathematical simplicity, that the coordinate system in the transformed plane be orthogonal in the physical plane. A set of coordinates that satisfies these requirements is provided by φ and ψ , which are orthogonal in the physical xy -plane and for which the geometric boundaries are known constant values of ψ in the transformed $\varphi\psi$ -plane. The distribution of velocity as a function of φ along these boundaries of constant ψ is known because, if

$$Q = Q(s)$$

is prescribed, equation (4) integrates to give

$$\varphi = \varphi(s)$$

From which equations,

$$Q = Q(\varphi)$$

The technique of the proposed method of channel design is therefore to obtain a differential equation for the distribution of velocity in the $\varphi\psi$ -plane. The velocity distribution obtained from the solution of this equation is then used to obtain the distribution of flow direction, from which distribution the channel walls in the physical xy -plane are obtained directly. The differential equation for the distribution of velocity in the $\varphi\psi$ -plane is nonlinear (for compressible flow with γ other than -1.0) and is solved by numerical methods (relaxation methods).

Differential Equation for Distribution of Velocity

in Transformed $\varphi\psi$ -Plane

The differential equation for the distribution of velocity in the transformed $\varphi\psi$ -plane is obtained from the equations for continuity and irrotational fluid motion expressed in terms of the transformed coordinates φ and ψ .

Continuity. - The continuity equation expressed in terms of φ and ψ becomes (appendix B):

$$\frac{1}{\rho} \left(\frac{\partial \log_e \rho}{\partial \varphi} + \frac{\partial \log_e Q}{\partial \varphi} \right) + \frac{\partial \theta}{\partial \psi} = 0 \quad (5)$$

Irrotational fluid motion. - The equation for irrotational fluid motion, expressed in terms of φ and ψ , becomes (appendix B):

$$\rho \frac{\partial \log_e Q}{\partial \psi} - \frac{\partial \theta}{\partial \varphi} = 0 \quad (6)$$

Differential equation for distribution of velocity. - The second order partial differential equation for the distribution of $\log_e Q$ in the transformed $\varphi\psi$ -plane is obtained by differentiating equations (5) and (6) with respect to φ and ψ , respectively, and combining to eliminate $\frac{\partial^2 \theta}{\partial \varphi \partial \psi}$. Thus,

$$\begin{aligned} \frac{\partial^2 \log_e \rho}{\partial \varphi^2} + \frac{\partial^2 \log_e Q}{\partial \varphi^2} - \frac{\partial \log_e \rho}{\partial \varphi} \left(\frac{\partial \log_e \rho}{\partial \varphi} + \frac{\partial \log_e Q}{\partial \varphi} \right) + \\ \rho^2 \frac{\partial \log_e Q}{\partial \psi} \frac{\partial \log_e \rho}{\partial \psi} + \rho^2 \frac{\partial^2 \log_e Q}{\partial \psi^2} = 0 \end{aligned} \quad (7)$$

Equation (7), together with a relation between ρ , Q , and q_d , determines the distribution of $\log_e Q$ in the $\varphi\psi$ -plane for compressible flow with a given value of q_d and for arbitrarily prescribed variations in $\log_e Q$ along the boundaries of constant ψ .

Density. - The density ρ is related to the velocity q by (reference 6, p. 26, for example)

$$\rho = \left(1 - \frac{\gamma-1}{2} q^2 \right)^{\frac{1}{\gamma-1}} \quad (8a)$$

which, from equation (1), becomes

$$\rho = \left(1 - \frac{\gamma-1}{2} Q^2 q_d^2 \right)^{\frac{1}{\gamma-1}} \quad (8b)$$

Equation (8b) relates the density ρ to the velocity Q for a given value of q_d .

Incompressible flow. - For incompressible flow ρ is constant and equal to 1.0 so that equation (7) becomes

$$\frac{\partial^2 \log_e Q}{\partial \varphi^2} + \frac{\partial^2 \log_e Q}{\partial \psi^2} = 0 \quad (9)$$

Equation (9) determines the distribution of $\log_e Q$ in the $\varphi\psi$ -plane for incompressible flow.

Channel Wall Geometry

After equation (7) or (9) has been solved to obtain the distribution of $\log_e Q$ in the transformed $\varphi\psi$ -plane (for arbitrary variations in $\log_e Q$ with φ along the boundaries of constant ψ), the geometry of the channel walls in the physical xy -plane can be determined from the resulting distribution of flow direction θ .

Flow direction θ . - The distribution of flow direction θ along a streamline (constant ψ) is obtained from equation (6), which integrates to give

$$\theta = \int_{\psi} \rho \frac{\partial \log_e Q}{\partial \psi} d\varphi \quad (10a)$$

where the subscript ψ indicates that the integration is taken along a line of constant ψ and where the constant of integration is selected to give a known value of θ at one value of φ along each streamline. The integrand in equation (10a) is obtained from the distribution of $\log_e Q$, which is known from the solution of equation (7) or (9).

The distribution of flow direction θ along a velocity-potential line (constant φ) is obtained from equation (5), which integrates to give

$$\theta = - \int_{\varphi} \frac{1}{\rho} \left(\frac{\partial \log_e \rho}{\partial \varphi} + \frac{\partial \log_e Q}{\partial \varphi} \right) d\psi \quad (10b)$$

where the subscript φ indicates that the integration is taken along a line of constant φ and where the constant of integration is selected to give a known value of θ at one value of ψ along each velocity-potential line. As for equation (10a), the integrand in equation (10b) is known from the distribution of $\log_e Q$ obtained from the solution of equation (7) or (9).

Channel wall coordinates. - The variation in x along a line of constant ψ in the $\varphi\psi$ -plane is given by

$$\frac{\partial x}{\partial \varphi} = \left(\frac{dx}{ds} \frac{ds}{d\varphi} \right)_{\psi}$$

which, combined with equations (2a) and (4), integrates to give

$$x = \int_{\psi} \frac{\cos \theta}{Q} d\varphi \quad (11a)$$

Likewise,

$$x = - \int_{\varphi} \frac{\sin \theta}{\rho Q} d\psi \quad (11b)$$

$$y = \int_{\psi} \frac{\sin \theta}{Q} d\varphi \quad (11c)$$

$$y = \int_{\varphi} \frac{\cos \theta}{\rho Q} d\psi \quad (11d)$$

where the constants of integration are selected to give known values of x or y at one value of φ along each streamline or at one value of ψ along each velocity-potential line. Equations (11a) to (11d) determine the distribution of x and y in the transformed $\varphi\psi$ -plane or, which is the same thing, the shape of the streamlines and velocity-potential lines in the physical xy -plane. In particular, equations (11a) and (11c) when integrated along the boundaries of constant ψ in the $\varphi\psi$ -plane determine the shape of the channel walls.

Turning angle. - In general, if the prescribed velocity distribution along one channel wall differs from the distribution along the other wall, the channel deflects an amount $\Delta\theta$, which is the difference in flow direction far downstream and far upstream of the region in which the prescribed velocity distribution varies. In reference 5 it is shown that for incompressible flow the turning angle $\Delta\theta$ is given by

$$\Delta\theta = \theta_d - \theta_u$$

$$= -\int_{-\infty}^{\infty} \varphi \left[\left(\frac{\partial \log_e Q}{\partial \varphi} \right)_{1.0} - \left(\frac{\partial \log_e Q}{\partial \varphi} \right)_0 \right] d\varphi \quad (12)$$

where the subscript u refers to conditions upstream at infinity and where the subscripts 0 and 1.0 refer to the channel boundaries along which ψ equals 0 and 1.0, respectively. A similar equation will be given later for the case of linearized compressible flow.

Linearized Compressible Flow

The nonlinear differential equation (7) for the distribution of velocity in the $\varphi\psi$ -plane with compressible flow becomes linear and is considerably simplified if a linear variation in pressure with specific volume ($1/\rho$) is assumed. This linear relation between pressure and specific volume was first suggested by Chaplygin (reference 7) in order to linearize the differential equations for two-dimensional compressible flow in the hodograph plane.

Density. - If a linear variation in pressure with specific volume is assumed, the density ρ^* is related to the velocity q^* by (appendix C)

$$\rho^* = (1 + q^{*2})^{-1/2} \quad (13)$$

where

$$\rho^* = k_1 \rho \quad (13a)$$

and

$$q^* = k_2 q \quad (13b)$$

where the constants k_1 and k_2 have been determined so that values of ρ given by equation (13) equal the values of ρ given by equation (8a) for any two selected values of q (designated by q_a and q_b). Thus,

$$k_1 = \frac{1}{\rho_a} \sqrt{\frac{1 - \left(\frac{\rho_a q_a}{\rho_b q_b}\right)^2}{1 - \left(\frac{q_a}{q_b}\right)^2}} \quad (14a)$$

and

$$k_2 = \frac{1}{q_b} \sqrt{\frac{\left(\frac{\rho_a}{\rho_b}\right)^2 - 1}{1 - \left(\frac{\rho_a q_a}{\rho_b q_b}\right)^2}} \quad (14b)$$

where ρ_a and ρ_b are determined by equation (8a) for the selected values of q_a and q_b , respectively. A discussion of the selection of q_a and q_b is given later. It will be noted that, if γ is equal to -1.0, equation (8a) has the same form as equation (13).

Stream function and velocity potential. - For the case of linearized compressible flow it is convenient to define the stream function ψ^* and the velocity potential φ^* by

$$d\psi^* = \rho^* q^* dn \quad (15)$$

and

$$d\varphi^* = q^* ds \quad (16)$$

Continuity. - The continuity equation expressed in terms of φ^* and ψ^* becomes (appendix D)

$$\frac{\partial \log_e u}{\partial \varphi^*} + \frac{\partial \theta}{\partial \psi^*} = 0 \quad (17)$$

where

$$u = \frac{q^*}{1 + \sqrt{1 + q^{*2}}} \quad (18)$$

or, conversely

$$q^* = \frac{2u}{1 - u^2} \tag{19}$$

Irrotational fluid motion. - The equation for irrotational fluid motion, expressed in terms of φ^* and ψ^* becomes (appendix D)

$$\frac{\partial \log_e u}{\partial \psi^*} - \frac{\partial \theta}{\partial \varphi^*} = 0 \tag{20}$$

Differential equation for distribution of $\log_e u$. - The partial differential equation for the distribution of $\log_e u$ in the $\varphi^*\psi^*$ -plane is obtained by differentiating equations (17) and (20) with respect to φ^* and ψ^* , respectively, and combining to eliminate $\frac{\partial^2 \theta}{\partial \varphi^* \partial \psi^*}$. Thus

$$\frac{\partial^2 \log_e u}{\partial \varphi^{*2}} + \frac{\partial^2 \log_e u}{\partial \psi^{*2}} = 0 \tag{21}$$

Equation (21) determines the distribution of $\log_e u$ in $\varphi^*\psi^*$ -plane for linearized compressible flow with a given value of q_d and for arbitrarily prescribed variations in $\log_e Q$, related to $\log_e u$ by equations (1), (13b), and (18), along the boundaries of constant ψ^* . Equation (21) is linear and is, like equation (9) for the case of incompressible flow, the equation of Laplace. Thus an incompressible flow solution for the distribution of $\log_e Q$ in the $\varphi\psi$ -plane is also a linearized compressible flow solution for the distribution of $\log_e u$ in the $\varphi^*\psi^*$ -plane. The transformation from the $\varphi\psi$ -plane is different, however, from the transformation from the $\varphi^*\psi^*$ -plane so that different channel shapes result in the xy -plane.

Flow direction θ . - The distribution of flow direction θ along a streamline (constant ψ^*) is obtained from equation (20), which integrates to give

$$\theta = \int_{\psi^*} \frac{\partial \log_e u}{\partial \psi^*} d\varphi^* \tag{22a}$$

2306

Likewise, the distribution of flow direction θ along a velocity-potential line (constant φ^*) is obtained from equation (17), which integrates to give

$$\theta = - \int_{\varphi^*} \frac{\partial \log_e u}{\partial \varphi^*} d\psi^* \quad (22b)$$

Equations (22a) and (22b) for linearized compressible flow correspond to, and are used in the same manner as, equations (10a) and (10b) for the usual type of compressible or incompressible flow.

Channel wall coordinates. - The variation in x along a line of constant ψ^* in the $\varphi^*\psi^*$ -plane is given by

$$\frac{\partial x}{\partial \varphi^*} = \left(\frac{dx}{ds} \frac{ds}{d\varphi^*} \right)_{\psi^*}$$

which combined with equations (2a) and (16) integrates to give

$$x = \int_{\psi^*} \frac{\cos \theta}{q^*} d\varphi^* \quad (23a)$$

Likewise,

$$x = - \int_{\varphi^*} \frac{\sin \theta}{\rho^* q^*} d\psi^* \quad (23b)$$

$$y = \int_{\psi^*} \frac{\sin \theta}{q^*} d\varphi^* \quad (23c)$$

$$y = \int_{\varphi^*} \frac{\cos \theta}{\rho^* q^*} d\psi^* \quad (23d)$$

Equations (23a) to (23d) determine the distribution of x and y in the transformed $\varphi^*\psi^*$ -plane or, which is the same thing, the shape of the streamline and velocity-potential lines in the physical xy -plane. In

particular, equations (23a) and (23c), when integrated along the boundaries of constant ψ^* in the $\varphi^*\psi^*$ -plane, determine the shape of the channel walls. Equations (23a) to (23d) for linearized compressible flow correspond to, and are used in the same manner as, equations (11a) to (11d) for the usual type of compressible or incompressible flow.

Turning angle. - In reference 5 it is shown that for linearized compressible flow the turning angle, or difference in flow direction far downstream and far upstream of the region in which the prescribed velocity distribution varies along the channel walls, is given by

$$\Delta\theta = \frac{-1}{\Delta\psi^*} \int_{-\infty}^{\infty} \varphi^* \left[\left(\frac{\partial \log_e u}{\partial \varphi^*} \right)_{\Delta\psi^*} - \left(\frac{\partial \log_e u}{\partial \varphi^*} \right)_0 \right] d\varphi^* \quad (24)$$

where $\Delta\psi^*$ is the value of ψ^* along the left boundary (channel wall) when faced in the direction of flow if the value of ψ^* along the right boundary is zero and where the subscript $\Delta\psi^*$ refers to the boundary along which ψ^* is equal to $\Delta\psi^*$.

NUMERICAL PROCEDURE

The channel design method of this report was developed for three types of fluid flow: (1) compressible, (2) incompressible, and (3) linearized compressible. Although the numerical procedures of the design method are similar for each type of fluid, the procedures differ in detail and are therefore considered separately in this section.

Compressible Flow

The numerical procedure for channel design with compressible flow ($\gamma = 1.4$, for example) is as follows:

(1) The velocity is specified as a function of arc length along that portion of the channel walls over which the velocity varies

$$q = q(s)$$

or q_d is specified and

$$Q = Q(s) \quad (25)$$

where s is arbitrarily equal to zero at that point along one channel wall where the velocity first begins to vary.

(2) The channel wall boundaries of the flow field in the transformed $\varphi\psi$ -plane are straight and parallel lines of constant ψ extending indefinitely far upstream and downstream between φ equals $\pm\infty$ where φ is arbitrarily equal to zero at that point on the channel wall at which s is equal to zero. The value of ψ along the right channel wall when faced in the direction of flow (direction of positive φ) is arbitrarily set equal to zero in which case the value of ψ along the left channel wall ($\Delta\psi$) is obtained by integrating equation (3) across the channel at a position far downstream where flow conditions are uniform

$$\Delta\psi = \rho_d \quad (26)$$

(3) The distribution of $\log_e Q$ as a function of φ along the boundaries in the $\varphi\psi$ -plane is obtained by integrating equation (4) between limits so that

$$\varphi = \int_0^s Q \, ds = \varphi(s) \quad (27)$$

which together with equation (25) gives the distribution of $\log_e Q$ along the boundaries in the $\varphi\psi$ -plane

$$\log_e Q = f(\varphi) \quad (28)$$

The integration indicated by equation (27) is carried out numerically for arbitrary distributions of Q as a function of s .

(4) If the velocities prescribed along one channel wall differ from those along the other wall, the channel will, in general, turn the flow. This turning angle cannot be determined exactly for compressible flow until the channel design is completed. However, it will be shown that this turning angle is only slightly greater than that resulting for linearized compressible flow with the same prescribed velocity and with a suitable selection for q_a and q_b in equations (14a) and (14b). This latter turning angle for linearized compressible flow is given by equation (24), which can be integrated numerically for the arbitrary distribution of $\log_e u = f(\varphi)$ corresponding to equation (28).

(5) In order to solve equation (7) for the distribution of $\log_e Q$ in the $\varphi\psi$ -plane it is convenient to eliminate the density terms from equation (7) by means of equation (8b). Thus, equation (7) becomes

$$A \frac{\partial^2 \log_e q}{\partial \phi^2} + B \frac{\partial^2 \log_e q}{\partial \psi^2} + 4C \left(\frac{\partial \log_e q}{\partial \phi} \right)^2 + 4D \left(\frac{\partial \log_e q}{\partial \psi} \right)^2 = 0 \quad (29)$$

where

$$A = \frac{1 - \frac{\gamma+1}{2} q^2}{\left(1 - \frac{\gamma-1}{2} q^2 \right)^{\frac{\gamma+1}{\gamma-1}}}$$

$$B = 1.0$$

$$4C = \frac{-q^2 \left(1 + \frac{\gamma+1}{2} q^2 \right)}{\left(1 - \frac{\gamma-1}{2} q^2 \right)^{\frac{2\gamma}{\gamma-1}}}$$

and

$$4D = \frac{-q^2}{\left(1 - \frac{\gamma-1}{2} q^2 \right)}$$

Although equation (29) is nonlinear, it can be solved by relaxation methods (references 4 and 8, for example). A grid of equally spaced points, at each of which the value of $\log_e Q$ is to be determined, is placed in the flow field between the channel wall boundaries. The grid is extended upstream and downstream sufficiently far so that constant values of $\log_e Q$ are obtained across the channel by the relaxation methods. In the numerical examples to be presented six or eight grid spaces were used across the channel. In example III the number of grid spaces was reduced from eight to four with negligible effect upon the resulting channel design. The values of $\log_e Q$ at each grid point were relaxed to five significant figures. If the same velocity distribution is prescribed along both walls, the channel is symmetrical so that the velocity distribution in only one half of the channel need be determined by relaxation methods.

(6) After $\log_e Q$ has been determined at each grid point in the $\varphi\psi$ -plane the distribution of θ is determined by equations (10a) and (10b), which are integrated numerically. The constants of integration in equations (10a) and (10b) are determined to give a specified value of θ at one point in the channel (far upstream, for example). The integrands in equations (10a) and (10b) are determined by numerical methods (tables I to VII, reference 4, for example) from the known values of ρ and $\log_e Q$ at each of the grid points. If it is desired to know the flow direction along the channel walls only, equation (10a) can be solved along the channel wall boundaries $\psi = 0$ and $\psi = \Delta\psi$ only. If it is desired to know θ everywhere in the channel, the recommended procedure is to determine the variation in θ along the mean streamline ($\psi = (\Delta\psi)/2$) by equation (10a) and to determine the variation in θ along each velocity-potential line from the previously determined values on the mean streamline by equation (10b).

(7) After the distribution of $\log_e Q$ and θ are known in the $\varphi\psi$ -plane, the shapes of the streamlines and the velocity-potential lines in the physical xy -plane or, which is the same thing, the distributions of x and y in the transformed $\varphi\psi$ -plane are determined by the numerical integration of equations (11a) to (11d). The constants of integration in these equations are determined so that specified values of x and y occur at one point in the flow field. The recommended procedure is to determine the variation in x and y along the mean streamline by equations (11a) and (11c) and to determine the variation in x and y along each velocity-potential line for the previously determined values on the mean streamline by equations (11b) and (11d). If it is desired to know the x and y coordinates from the channel walls only, equations (11a) and (11c) can be solved along the channel wall boundaries $\psi = 0$ and $\psi = \Delta\psi$ only.

Incompressible Flow

The numerical procedure for channel design with incompressible flow ($\rho = 1$) is similar to that just outlined for compressible flow, but with the following differences:

(1) The velocity is specified as a function of arc length by equation (25) alone. The constant q_d is not considered, because it does not exist.

(2) The value of ψ along the left channel wall ($\Delta\psi$) is equal to 1.0 instead of the value given by equation (26).

(3) The distribution of $\log_e Q$ as a function of φ along the channel wall boundaries in the $\varphi\psi$ -plane is the same as that obtained from equations (25) and (27) and given by equation (28).

(4) The turning angle $\Delta\theta$ of the channel is given by equation (12).

(5) The distribution of $\log_e Q$ in the $\phi\psi$ -plane is obtained from the solution of equation (9) by relaxation methods.

(6) After $\log_e Q$ has been determined at each grid point between the channel wall boundaries in the $\phi\psi$ -plane, the distribution of θ is determined by equations (10a) and (10b) as indicated previously for compressible flow, but with ρ equal to unity.

(7) After the distribution of $\log_e Q$ and θ are known in the $\phi\psi$ -plane, the shapes of the streamlines and velocity-potential lines in the physical xy -plane are determined by equations (11a) to (11d) as indicated previously for compressible flow, but with ρ equal to unity.

Linearized Compressible Flow

The numerical procedure for channel design with linearized compressible flow ($\gamma = -1.0$) is similar to that previously outlined for compressible flow, but with the following differences:

(1) The velocity q is specified as a function of arc length along the channel walls by $q(s)$ or by q_a and equation (25). For each prescribed velocity there are an infinite number of linearized compressible flow solutions depending on the selected values of q_a and q_b in equations (14a) and (14b). However, for values of q_a and q_b within the range of q prescribed along the channel walls (and therefore everywhere in the channel), the solutions, that is, channel shapes, probably differ only in small detail. The best solution is that most nearly like the nonlinear compressible solution with arbitrary value of γ (1.4, for example). In the numerical examples of this report it is shown that if q_a and q_b are equal to the maximum and minimum values of q a good solution results, at least if the ratio of these prescribed velocities is not too large (2:1 in the numerical examples). On the other hand, if continuity is to be satisfied for a gas with the correct value of γ (1.4, for example) upstream and downstream of the region of the channel in which the prescribed velocities vary, then q_a and q_b must equal q_u and q_d .

After q_a and q_b have been selected the velocity distribution $q(s)$ is expressed as $q^*(s)$ by equation (13b) where k_2 is given by equation (14b) so that

$$q^* = q^*(s) \quad (30)$$

The velocity q^* is then expressed as u by equation (18) so that

$$u = u(s) \quad (31)$$

In the particular case where the selected value of q_a is equal to q_b the value of k_2 is given by equation (C4b) in appendix C where the significance of this particular case is also discussed.

(2) The solution is obtained in the transformed $\varphi^*\psi^*$ -plane where φ^* and ψ^* are defined by equations (16) and (15), respectively. If the value of ψ^* along the right channel wall when faced in the direction of q^* is zero, the value of ψ^* along the left wall ($\Delta\psi^*$) is obtained by integrating equation (15) across the channel at a position far downstream where flow conditions are uniform

$$\Delta\psi^* = \rho_d^* q_d^* \quad (32)$$

(3) The distribution of $\log_e u$ as a function of φ^* along the channel wall boundaries in the $\varphi^*\psi^*$ -plane is obtained by integrating equation (16) between limits similar to those discussed previously for compressible flow so that

$$\varphi^* = \int_0^s q^* ds = \varphi^*(s) \quad (33)$$

which together with equation (31) determines the distribution of $\log_e u$ along the channel wall boundaries in the $\varphi^*\psi^*$ -plane

$$\log_e u = f(\varphi^*) \quad (34)$$

(4) The turning angle $\Delta\theta$ of the channel is given by equation (24).

(5) The distribution of $\log_e u$ in the $\varphi^*\psi^*$ -plane is obtained from the solution of equation (21) by relaxation methods.

(6) After $\log_e u$ has been determined at each grid point between the channel wall boundaries in the $\varphi^*\psi^*$ -plane, the distribution of θ is determined by equations (22a) and (22b) in a manner similar to that outlined previously for compressible flow.

(7) After the distribution of $\log_e u$ and θ are known in the $\varphi^*\psi^*$ -plane, the shapes of the streamlines and the velocity-potential lines in the physical xy -plane are determined by equations (23a) to (23d) in a manner similar to that outlined previously for compressible flow. The velocities q^* in equations (23) are obtained from the known values of u and the densities ρ^* are given by equation (13).

NUMERICAL EXAMPLES

The channel design method has been applied to five examples listed below:

Examples	Type of channel	Type of flow
I	Reducing section	Incompressible
II	Converging section	Incompressible
III	Elbow	Incompressible
IV	Elbow	Linearized compressible
V	Elbow	Compressible ($\gamma = 1.4$)

Example I

The first numerical example is the design of a reducing section in a straight channel such that the upstream velocity is half the downstream velocity. The solution is for incompressible flow.

Prescribed velocity distribution. - The prescribed velocity as a function of arc length s along both channel walls is given by

$$\left. \begin{aligned}
 Q &= 0.5 && (s \leq 0) \\
 Q &= \frac{1}{2} + \frac{s^2}{6} - \frac{s^3}{27} && (0 \leq s \leq 3.0) \\
 Q &= 1.0 && (s \leq 3.0)
 \end{aligned} \right\} \quad (35)$$

The prescribed velocity given by equation (35) is plotted in figure 2.

Equation (35) together with equation (27) results in

$$\left. \begin{aligned}
 \varphi &= 0.5 s && (s \leq 0) \\
 \varphi &= \frac{s}{2} + \frac{s^3}{18} - \frac{s^4}{108} && (0 \leq s \leq 3.0) \\
 \varphi &= -0.75 + s && (s \leq 3.0)
 \end{aligned} \right\} \quad (36)$$

From equations (35) and (36), $\log_e Q$ is a known function of φ , which function is plotted in figure 3.

2306

Results. - The results of example I are presented in figures 4 to 7.

In figure 4 lines of constant velocity Q and flow direction θ are plotted in the transformed $\phi\psi$ -plane. The flow direction θ is constant and equal to zero along the mean streamline ($\psi = 0.5$) indicating that the center line of the channel is straight. The maximum absolute values of θ occur along the channel walls. The solution is symmetrical about the mean streamline. The lines of constant Q and θ are orthogonal (see appendix E). If $(\delta S)_Q$ is the spacing of lines of constant θ measured along lines of constant Q and if $(\delta S)_\theta$ is the spacing of lines of constant Q measured along lines of constant θ , equation (F5) in appendix F gives

$$\frac{(\delta S)_Q}{(\delta S)_\theta} = \left(\frac{\delta \theta}{\delta Q} \right) Q = \left(\frac{2\pi/180}{0.03} \right) Q = \frac{\pi}{2.7} Q \quad (37)$$

In figure 5 lines of constant x and y are plotted on the transformed $\phi\psi$ -plane. Along the mean streamline ($\psi = 0.5$) the value of y is constant and equal to zero indicating, as before, that the center line of the channel is straight. The lines of constant x and y are orthogonal (appendix E). The solution is symmetrical. The ratio of the spacing of lines of constant x and y is given by equation (F6) of appendix F

$$\frac{(\delta S)_x}{(\delta S)_y} = \frac{\delta y}{\delta x} = \frac{0.2}{0.2} = 1.0$$

so that the system of curves forms a square network.

In figure 6 lines of constant ϕ and ψ (velocity potential and streamlines, respectively) are plotted in the physical xy -plane. The shape of the channel walls is that required to result in the prescribed velocity distribution given by equation (35) and plotted in figure 2. The downstream channel width is 1.0 by definition. The upstream channel width is 2.0 in order that the upstream velocity be half the downstream velocity. As usual the streamlines and velocity potential lines are orthogonal (appendix E) and, for equal increments of ϕ and ψ , form a square network (equation (F7), appendix F, with ρ equal to 1.0).

In figure 7 lines of constant Q and θ are plotted in the physical xy -plane. The lines of constant Q and θ are orthogonal (appendix E). The ratio of the spacing of lines of constant Q and θ is given by equation (F8) of appendix F

$$\frac{(\delta S)_Q}{(\delta S)_\theta} = \left(\frac{\delta \theta}{\delta Q} \right) Q = \left(\frac{2\pi/180}{0.03} \right) Q = \frac{\pi}{2.7} Q$$

which is the same as that for the same lines of constant Q and θ in the $\varphi\psi$ -plane (see equation (37)).

Example II

The second numerical example is the design of a converging section that funnels the fluid from an infinite expanse into a straight channel of unit width. Far upstream the channel walls are straight and converge at a 90° angle. The solution is for incompressible flow.

Prescribed velocity. - The prescribed velocity as a function of arc length s along both channel walls is given by

$$\left. \begin{aligned} Q &= \frac{-2}{\pi(s-2)} && (s \leq 0) \\ Q &= \frac{1}{\pi} + \frac{1}{2\pi} s - \frac{1}{8} \left(\frac{7}{2\pi} - \frac{3}{2} \right) s^2 + \frac{1}{32} \left(\frac{2}{\pi} - 1 \right) s^3 && (0 \leq s \leq 4) \\ Q &= 1.0 && (s \geq 4) \end{aligned} \right\} (38)$$

The prescribed velocity given by equation (38) is plotted in figure 8.

Equation (38) together with equation (27) results in

$$\left. \begin{aligned} \varphi &= \frac{-2}{\pi} \log_e \left(1 - \frac{s}{2} \right) && (s \leq 0) \\ \varphi &= \frac{1}{\pi} s + \frac{1}{2\pi} \frac{s^2}{2} - \frac{1}{8} \left(\frac{7}{2\pi} - \frac{3}{2} \right) \frac{s^3}{3} + \frac{1}{32} \left(\frac{2}{\pi} - 1 \right) \frac{s^4}{4} && (0 \leq s \leq 4) \\ \varphi &= \frac{8}{3\pi} - 2 + s && (s \geq 4) \end{aligned} \right\} (39)$$

From equations (38) and (39), $\log_e Q$ is a known function of φ , which function is plotted in figure 9.

Results. - The results of example II are presented in figures 10 to 12.

In figure 10 lines of constant velocity Q and flow direction θ are plotted in the transformed $\varphi\psi$ -plane. The flow direction θ is constant and equal to zero along the mean streamline ($\psi = 0.5$) indicating that the center line of the channel is straight. The solution is symmetrical about the mean streamline. As for example I the lines of constant Q and θ are orthogonal. The ratio of the spacing of lines of constant Q and θ is given by equation (F5) in appendix F

$$\frac{(\delta S)_Q}{(\delta S)_\theta} = \left(\frac{\delta \theta}{\delta Q} \right) Q = \left(\frac{4\pi/180}{0.05} \right) Q = \frac{4\pi}{9} Q \quad (40)$$

In figure 11 lines of constant φ and ψ are plotted in the physical xy -plane. The shape of the channel walls is that required to result in the prescribed velocity distribution given by equation (38) and plotted in figure 8. As usual the streamlines and velocity potential lines are orthogonal (appendix E) and, for incompressible flow with equal increments of φ and ψ , form a square network (appendix F).

In figure 12 lines of constant Q and θ are plotted in the physical xy -plane. The lines of constant Q and θ are orthogonal (appendix E), and the ratio of the spacing of lines of constant Q and θ is the same as that given for the same lines of constant Q and θ in the $\varphi\psi$ -plane (equation (40)).

Example III

The third numerical example is the design of an elbow for which the upstream velocity is half the downstream velocity. The prescribed velocities are such that no deceleration occurs anywhere along the channel walls. The solution is for incompressible flow.

Prescribed velocity distribution. - Along both walls upstream of the elbow the velocity Q is equal to 0.5, and along both walls downstream of the elbow Q is equal to 1.0. The transition from Q equals 0.5 to 1.0 along both walls of the elbow will be the prescribed velocity distribution as a function of arc length given by equation (35) for example I and plotted in figure 2. In terms of $\log_e Q$ as a function of φ this prescribed velocity distribution is given by equation (36) and is plotted in figure 3. Although this velocity distribution is the same for both walls, the distribution on the outer wall (wall with larger radius of curvature) is shifted in the positive φ direction an amount equal to 2.25 relative to the distribution on the inner wall. Thus, a velocity difference exists on the two walls at equal values of φ , as shown in figure 13. The greater this difference in velocity and the greater the range in φ over which velocity differences exist, the greater is the elbow turning angle. For the prescribed

velocity distribution given in figure 13 the elbow turning angle given by equation (12) was 89.37 degrees compared with a value of 89.36 degrees obtained from the relaxation solution.

Results. - The results of example III are presented in figures 14 to 16 and in tables I and II. (The numerical results for examples III, IV, and V are tabulated in tables I to VI to enable a detailed comparison of the three elbow designs with the same prescribed velocity Q distribution as a function of arc length but with incompressible (example III), linearized compressible (example IV), and compressible (example V) flow.)

In figure 14 lines of constant Q and θ are plotted in the $\varphi\psi$ -plane. The flow direction θ varies along the mean streamline ($\psi = 0.5$) indicating that the channel is curved. The solution is unsymmetrical. As for examples I and II, the lines of constant Q and θ are orthogonal (appendix E). The ratio of the spacing of lines of constant Q and θ is given by equation (F5) in appendix F

$$\frac{(\delta S)_Q}{(\delta S)_\theta} = \left(\frac{\delta \theta}{\delta Q} \right) Q = \left(\frac{4\pi/180}{0.03} \right) Q = \frac{2\pi}{2.7} Q \quad (41)$$

In figure 15 lines of constant φ and ψ are plotted in the physical xy -plane. The shape of the channel walls is that required to result in the prescribed velocity distribution given by equations (35) and (36) and plotted in figures 2 and 13. The upstream channel width is twice the downstream width in order that the upstream velocity be half the downstream velocity. It is interesting to note that, before curving in the direction of the elbow turning angle, the inner wall first curves in the opposite direction. This behavior of the inner wall geometry is necessary in order to maintain the prescribed constant velocity along the outer wall where the velocity would otherwise decelerate because of the necessary curvature in the direction of elbow turning. This feature of the elbow geometry will also be noted in examples IV and V. As usual the streamlines and velocity-potential lines are orthogonal (appendix E), and, for equal increments of φ and ψ , form a square network (equation (F7), appendix F, with ρ equal to 1.0).

In figure 16 lines of constant Q and θ are plotted in the physical xy -plane. The lines of constant Q and θ are orthogonal (appendix E), and the ratio of the spacing of lines of constant Q and θ is the same as that given for the same lines of constant Q and θ in the $\varphi\psi$ -plane (equation (41)).

Example IV

The fourth numerical example is the design of an elbow with the same prescribed velocity Q , as a function of arc length, used in example III but for linearized compressible flow ($\gamma = -1.0$).

Prescribed velocity distribution. - The prescribed velocity distribution Q is the same as that for example III and with q_d equal to 0.80176. The variation in Q with s along one channel wall is plotted in figure 2. The values of q_a and q_b in equations (14a) and (14b) are equal to q_u and q_d , or 0.40088 and 0.80176, respectively. For these values of q_a and q_b and for the prescribed velocity distribution with linearized compressible flow, the elbow turning angle given by equation (24) was 104.08° compared with a value of 104.07° obtained from the relaxation solution and a value of 89.36° obtained for incompressible flow (example III).

Results. - The results of example IV are presented in figures 17 to 19 and in tables III and IV.

In figure 17 lines of constant q and θ are plotted in the transformed $\phi^*\psi^*$ -plane. The solution is unsymmetrical. The lines of constant q and θ are orthogonal (appendix E), and the ratio of the spacing of lines of constant q and θ is given by equation (F9) in appendix F.

$$\frac{(\delta s)_q}{(\delta s)_\theta} = \left(\frac{\delta \theta}{\delta q} \right) \frac{q}{\rho^*} = \left(\frac{4\pi/180}{0.02} \right) \frac{q}{\rho^*} = \frac{\pi}{0.9} \frac{q}{\rho^*}$$

where ρ^* is related to q by equations (13) and (13b).

In figure 18 lines of constant $\phi^*/\Delta\psi^*$ and $\psi^*/\Delta\psi^*$ are plotted in the physical xy -plane (where the constant $\Delta\psi^*$ is given by equation (32) and is equal to 0.73782 for q_d equal to 0.80176). The shape of the channel walls is that required to result in the prescribed velocity distribution used in example III but with linearized compressible flow and for q_d equal to 0.80176. From continuity considerations the upstream channel width is 1.5385 times the downstream width. As in example III the inner wall of the elbow first turns in the opposite direction to the elbow turning angle. As usual the streamlines and velocity-potential lines are orthogonal (appendix E). The ratio of the spacing of the lines of constant $\phi^*/\Delta\psi^*$ and $\psi^*/\Delta\psi^*$ is given by equation (F10) in appendix F.

$$\frac{(\delta S)_{\varphi^*}}{(\delta S)_{\psi^*}} = \left(\frac{\delta \psi^*}{\delta \varphi^*} \right) \frac{1}{\rho^*} = \frac{1/6}{1/6} \frac{1}{\rho^*} = \frac{1}{\rho^*}$$

Thus the ratio of the spacing of lines of constant $\varphi^*/\Delta\psi^*$ and $\psi^*/\Delta\psi^*$ in figure 18 is a measure of the density ρ^* .

In figure 19 lines of constant q and θ are plotted in the physical xy -plane. The lines of constant q and θ are not in general orthogonal (appendix E).

Example V

The fifth numerical example is the design of an elbow with the same prescribed velocity Q , as a function of arc length, used in examples III and IV but for compressible flow ($\gamma = 1.4$).

Prescribed velocity distribution. - The prescribed velocity distribution Q is the same as that for examples III and IV but with q_d equal to 0.79927. The variation in Q with s along one channel wall is plotted in figure 2.

Results - The results of example V are presented in figures 20 and 21 and in tables V and VI.

In figure 20 lines of constant $\varphi/\Delta\psi$ and $\psi/\Delta\psi$ are plotted in the physical xy -plane (where the constant $\Delta\psi$ is given by equation (26) and is equal to 0.71054 for q_d equal to 0.79927). The shape of the channel walls is that required to result in the prescribed velocity distribution used in examples III and IV but with compressible flow ($\gamma \approx 1.4$) and for q_d equal to 0.79927. The upstream channel width is 1.5412 times the downstream width, and the turning angle is 105.31° compared with 104.07° for linearized compressible flow (example IV) and 89.36° for incompressible flow (example III). The streamlines and velocity-potential lines are orthogonal, and from equation (F7) of appendix F the ratio of the spacing of the lines of constant $\varphi/\Delta\psi$ and $\psi/\Delta\psi$ is given by

$$\frac{(\delta S)_{\varphi}}{(\delta S)_{\psi}} = \left(\frac{\delta \psi}{\delta \varphi} \right) \frac{1}{\rho} = \frac{1/6}{1/6} \frac{1}{\rho} = \frac{1}{\rho}$$

Thus, as for linearized compressible flow (example IV), the ratio of the spacing of lines of constant $\phi/\Delta\psi$ and $\psi/\Delta\psi$ in figure 20 for equal increments of $\phi/\Delta\psi$ and $\psi/\Delta\psi$ is a measure of the density ρ .

The shape of the elbow for compressible flow (example V, fig. 20) is nearly the same as the shape of the elbow for linearized compressible flow (example IV, fig. 18). Therefore, in figure 21 the contours of the walls for both examples are compared. The difference in contours is very small and it is concluded that, if a nonviscous gas with arbitrary γ (1.4, for example) were to flow through a channel designed for linearized compressible flow ($\gamma = -1.0$), the resulting velocity distribution along the channel walls would be nearly the velocity distribution prescribed for the linearized compressible flow, at least if the linearized flow were selected (by the choice of q_a and q_b) so that the densities were equal for both types of flow at the maximum and minimum velocities and if the ratio of these prescribed velocities is not too large (2:1 in the numerical examples). This conclusion is important because the design method for linearized compressible flow is considerably faster than the design method for compressible flow with γ other than -1.0.

SUMMARY OF RESULTS AND CONCLUSIONS

A general method of design is developed for two-dimensional unbranched channels with prescribed velocities as a function of arc length along the channel walls. The method is developed for both compressible and incompressible, irrotational, nonviscous flow and applies to the design of elbows, diffusers, nozzles, and so forth. Two types of compressible flow are considered: the general type with arbitrary value for the ratio of specific heats γ (1.4, for example) and the linearized type in which γ is equal to -1.0. In this report (part I) solutions are obtained by relaxation methods on a transformed plane the coordinates of which are the streamlines and velocity-potential lines in the physical plane; in part II solutions are obtained by a Green's function. The present method of solution gives complete information concerning the flow throughout the channel.

Five numerical examples are given and the results presented in plots of lines of constant velocity and flow direction or lines of constant physical coordinates in the transformed plane and streamlines and velocity-potential lines or lines of constant velocity and flow direction in the physical plane. Among the five examples are three elbow designs for the same prescribed velocity as a function of arc length along the channel walls but with incompressible, linearized compressible, and compressible flow. The numerical results of these three elbow designs are tabulated to enable a detailed comparison of the three designs.

2306

The shapes of the elbows for compressible flow and for linearized compressible flow are very nearly the same and it is concluded that, if a nonviscous gas with arbitrary γ (1.4, for example) were to flow through a channel designed for linearized compressible flow ($\gamma = -1.0$), the resulting velocity distribution along the channel walls would be nearly the velocity distribution prescribed for the linearized compressible flow, at least if the linearized flow were selected so that the densities are equal for both types of flow at the maximum and minimum velocities and if the ratio of these velocities is not too large (2:1 in the numerical examples). This conclusion is important because the design method for linearized compressible flow is considerably faster than that for compressible flow.

Lewis Flight Propulsion Laboratory
National Advisory Committee for Aeronautics
Cleveland, Ohio, July 25, 1951

APPENDIX A

Symbols

The following symbols are used in this report:

A,B,C,D	coefficients, equation (29)
A,B	arbitrary constants, equation (14a)
k_1	coefficient, equation (14a)
k_2	coefficient, equation (14b)
n	distance in xy-plane measured normal to direction of flow (expressed as ratio of characteristic length equal to channel width downstream at infinity)
p	static pressure (expressed as ratio of stagnation density multiplied by stagnation speed of sound squared)
Q	velocity (expressed as ratio of characteristic velocity equal to constant channel velocity downstream at infinity)
q	velocity (expressed as ratio of stagnation speed of sound)
q^*	velocity used in linearized compressible flow and related to q by equation (13b)
S	spacing between lines in xy- or $\phi\psi$ -plane
s	distance in xy-plane measured along direction of flow (expressed as ratio of characteristic length equal to channel width downstream at infinity)
u	velocity parameter related to q^* by equation (18)
x,y	Cartesian coordinates in physical plane (expressed as ratios of characteristic length equal to channel width downstream at infinity)
γ	ratio of specific heats
δ	increment of
θ	flow direction in physical xy-plane (measured in counter-clockwise direction from positive x-axis).

$\Delta\theta$	channel turning angle, equation (12)
ρ	density (expressed as ratio of stagnation density)
ρ^*	density used in linearized compressible flow and related to ρ by equation (13a)
φ, ψ	velocity potential and stream function, respectively, used as Cartesian coordinates in transformed plane, defined by equations (3) and (4)
$\Delta\psi$	boundary value of ψ along left channel wall when faced in the direction of flow, equation (26)
φ^*, ψ^*	velocity potential and stream function, respectively, for linearized compressible flow and used as Cartesian coordinates in the transformed $\varphi^*\psi^*$ -plane, defined by equations (15) and (16)
$\Delta\psi^*$	boundary value of ψ^* , for linearized compressible flow, along left channel wall when faced in the direction of flow, equation (32)

Subscripts:

a, b	quantities related to two velocities (q_a and q_b , respectively) for which density given by equation (8a) is equal to density ρ given by equations (13), (13a), and (13b)
d	conditions downstream at infinity
Q, q	along lines of constant Q and q , respectively
u	conditions upstream at infinity
x, y	along lines of constant x and y , respectively
$\Delta\psi^*$	left channel wall, when faced in direction of flow, along which ψ^* is equal to $\Delta\psi^*$
θ	along lines of constant θ
$\varphi, \psi, \varphi^*, \psi^*$	along lines of constant φ , ψ , φ^* , and ψ^* , respectively
0	right channel wall, when faced in direction of flow, along which ψ or ψ^* is equal to 0
1.0	left channel wall, when faced in direction of flow, along which ψ is equal to 1.0

APPENDIX B

EQUATIONS OF CONTINUITY AND IRROTATIONAL FLUID MOTION IN TERMS
OF TRANSFORMED φ, ψ COORDINATES

Consider the two-dimensional irrotational motion of a fluid particle in the physical xy -plane. The fluid particle is defined by adjacent streamlines (constant ψ) and velocity-potential lines (constant φ) spaced δn and δs apart as indicated in figure 22. The velocity Q is parallel to the streamlines and normal to the velocity-potential lines.

Continuity. - From continuity considerations of the fluid particle in figure 22

$$\frac{\partial}{\partial s} (\rho Q \delta n) = 0$$

or

$$\frac{\partial \log_e \rho}{\partial s} + \frac{\partial \log_e Q}{\partial s} + \frac{1}{\delta n} \frac{\partial(\delta n)}{\partial s} = 0 \quad (\text{B1})$$

But, from geometrical considerations (reference 6, p. 167, for example)

$$\frac{1}{\delta n} \frac{\partial(\delta n)}{\partial s} = \frac{\partial \theta}{\partial n} \quad (\text{B2a})$$

and

$$\frac{1}{\delta s} \frac{\partial(\delta s)}{\partial n} = - \frac{\partial \theta}{\partial s} \quad (\text{B2b})$$

so that equation (B1) becomes

$$\frac{\partial \log_e \rho}{\partial s} + \frac{\partial \log_e Q}{\partial s} + \frac{\partial \theta}{\partial n} = 0$$

or

$$\frac{\partial \log_e \rho}{\partial \varphi} \frac{d\varphi}{ds} + \frac{\partial \log_e Q}{\partial \varphi} \frac{d\varphi}{ds} + \frac{\partial \theta}{\partial \psi} \frac{d\psi}{dn} = 0$$

which, combined with equations (3) and (4), becomes

$$\frac{1}{\rho} \left(\frac{\partial \log_e \rho}{\partial \varphi} + \frac{\partial \log_e Q}{\partial \varphi} \right) + \frac{\partial \theta}{\partial \psi} = 0 \quad (5)$$

Equation (5) is the continuity equation expressed in terms of φ, ψ coordinates.

Irrotational fluid motion. - For irrotational motion of the fluid particle in figure 22

$$\frac{\partial}{\partial n} (Q \delta s) = 0$$

or

$$\frac{\partial \log_e Q}{\partial n} + \frac{1}{\delta s} \frac{\partial (\delta s)}{\partial n} = 0 \quad (B3)$$

But, from equations (B2b) and (B3)

$$\frac{\partial \log_e Q}{\partial n} - \frac{\partial \theta}{\partial s} = 0$$

or

$$\frac{\partial \log_e Q}{\partial \psi} \frac{d\psi}{dn} - \frac{\partial \theta}{\partial \varphi} \frac{d\varphi}{ds} = 0$$

which, combined with equations (3) and (4), becomes

$$\rho \frac{\partial \log_e Q}{\partial \psi} - \frac{\partial \theta}{\partial \varphi} = 0 \quad (6)$$

Equation (6) is the equation for irrotational fluid motion expressed in terms of the φ, ψ coordinates. Equations (5) and (6) were originally derived in modified forms by Chaplygin (reference 7) and are given in reference 6, page 169.

APPENDIX C

RELATION BETWEEN VELOCITY AND DENSITY ASSUMING LINEAR VARIATION
IN PRESSURE WITH SPECIFIC VOLUME

The approximate, linear relation between pressure p and specific volume $1/\rho$ first suggested by Chaplygin (reference 7) is given by

$$p = A - \frac{B}{\rho} \quad (C1a)$$

from which

$$\frac{dp}{d\rho} = \frac{B}{\rho^2} \quad (C1b)$$

where A and B are arbitrary constants.

If p denotes the static pressure expressed as a ratio of the stagnation density multiplied by the stagnation speed of sound squared, Bernoulli's equation is

$$\frac{dp}{\rho} + q \, dq = 0$$

which combined with equation (C1b) integrates to give the approximate relation between velocity and density

$$\frac{B}{2\rho^2} - \frac{q^2}{2} = \text{constant} \quad (C2)$$

For convenience equation (C2) can be written as

$$\frac{1}{\rho^*} - q^{*2} = 1$$

or

$$\rho^* = (1 + q^{*2})^{-1/2} \quad (13)$$

where

$$\rho^* = k_1 \rho \quad (13a)$$

and

$$q^* = k_2 q \quad (13b)$$

The constants k_1 and k_2 replace the two arbitrary constants in equation (C2) and their values are determined so that for any two arbitrary values of q (designated by q_a and q_b) the values of ρ given by equation (13) equal the values of ρ given by equation (8a). Thus the values of ρ given by equation (13) for q equal to q_a or q_b are correct; for all other values of q the values of ρ are approximate. The constants k_1 and k_2 are determined from the conditions

$$\left. \begin{aligned} \rho_a^* &= k_1 \rho_a \\ q_a^* &= k_2 q_a \\ \rho_b^* &= k_1 \rho_b \\ q_b^* &= k_2 q_b \end{aligned} \right\} \quad (C3)$$

From equation (13) and the conditions given by equation (C3)

$$k_1 = \frac{1}{\rho_a} \sqrt{\frac{1 - \left(\frac{\rho_a q_a}{\rho_b q_b}\right)^2}{1 - \left(\frac{q_a}{q_b}\right)^2}} \quad (14a)$$

and

$$k_2 = \frac{1}{q_b} \sqrt{\frac{\left(\frac{\rho_a}{\rho_b}\right)^2 - 1}{1 - \left(\frac{\rho_a q_a}{\rho_b q_b}\right)^2}} \quad (14b)$$

where ρ_a and ρ_b are determined by equation (8a) for the selected values of q_a and q_b , respectively.

The values of q_a and q_b might, for example, be selected to equal the maximum and minimum values of q (which values of q must occur on the channel walls and are therefore known). Also, the values of q_a and q_b might be selected to equal the upstream and downstream velocities q_u and q_d . In this case the upstream and downstream channel widths would then satisfy continuity for a gas with the correct value of γ (1.4, for example). If the upstream and downstream velocities are equal, their value and the value of some other velocity (the maximum or minimum velocity, for example) can be selected for q_a and q_b or, if desired, q_a can be equal to q_b in which case if

$$q_a = q + \epsilon \quad \text{where } \epsilon \rightarrow 0$$

$$q_b = q$$

it can be shown from equations (14a) and (14b) that

$$k_1 = \frac{1}{\rho} \sqrt{\frac{1 - \frac{\gamma+1}{2} q^2}{1 - \frac{\gamma-1}{2} q^2}} \quad (C4a)$$

and

$$k_2 = \sqrt{\frac{1}{1 - \frac{\gamma+1}{2} q^2}} \quad (C4b)$$

This latter case, in which $q_a = q_b = q$, corresponds to the method used by Chaplygin (reference 7) and Kármán-Tsien (reference 9) in which the correct relation between p and $\frac{1}{\rho}$ is replaced by a straight line (equation (C1a)) that is tangent to the correct relation at one point (where $q_a = q_b$).

APPENDIX D

EQUATIONS OF CONTINUITY AND IRROTATIONAL FLUID MOTION IN
TERMS OF TRANSFORMED φ^*, ψ^* COORDINATES

Consider the two-dimensional irrotational motion of a fluid particle in the physical xy -plane. The fluid particle is defined by adjacent streamlines (constant ψ^*) and velocity-potential lines (constant φ^*) spaced δn and δs apart as indicated in figure 22. The velocity q^* is parallel to the streamlines and normal to the velocity-potential lines.

Continuity. - From continuity considerations of the fluid particle in figure 22

$$\frac{\partial}{\partial s} (\rho^* q^* \delta n) = 0$$

or

$$\frac{\partial \log_e \rho^*}{\partial s} + \frac{\partial \log_e q^*}{\partial s} + \frac{1}{\delta n} \frac{\partial(\delta n)}{\partial s} = 0$$

which combined with equation (B2a) becomes

$$\frac{\partial \log_e \rho^*}{\partial \varphi^*} \frac{d\varphi^*}{ds} + \frac{\partial \log_e q^*}{\partial \varphi^*} \frac{d\varphi^*}{ds} + \frac{\partial \theta}{\partial \psi^*} \frac{d\psi^*}{dn} = 0$$

or, from equations (15) and (16)

$$\frac{1}{\rho^*} \left(\frac{\partial \log_e \rho^*}{\partial \varphi^*} + \frac{\partial \log_e q^*}{\partial \varphi^*} \right) + \frac{\partial \theta}{\partial \psi^*} = 0 \tag{D1}$$

But, from equation (13)

$$\frac{1}{\rho^*} \frac{\partial \log_e \rho^*}{\partial \varphi^*} = \frac{-q^{*2}}{\sqrt{1+q^{*2}}} \frac{\partial \log_e q^*}{\partial \varphi^*}$$

so that equation (D1) becomes

$$\frac{1}{\sqrt{1+q^{*2}}} \frac{\partial \log_e q^*}{\partial \varphi^*} + \frac{\partial \theta}{\partial \psi^*} = 0 \tag{D2}$$

2306

Finally, if

$$u = \frac{q^*}{1 + \sqrt{1 + q^{*2}}} \quad (18)$$

then

$$\frac{\partial \log_e q^*}{\sqrt{1 + q^{*2}}} = \partial \log_e u \quad (D3)$$

so that equation (D2) becomes

$$\frac{\partial \log_e u}{\partial \varphi^*} + \frac{\partial \theta}{\partial \psi^*} = 0 \quad (17)$$

Equation (17) is the continuity equation expressed in terms of φ^*, ψ^* coordinates and $\log_e u$.

Irrotational fluid motion. - For irrotational motion of the fluid particle in figure 22

$$\frac{\partial}{\partial n} (q^* \delta s) = 0$$

or

$$\frac{\partial \log_e q^*}{\partial n} + \frac{1}{\delta s} \frac{\partial (\delta s)}{\partial n} = 0$$

which combined with equation (B2b) becomes

$$\frac{\partial \log_e q^*}{\partial \psi^*} \frac{d\psi^*}{dn} - \frac{\partial \theta}{\partial \varphi^*} \frac{d\varphi^*}{ds} = 0$$

or, from equations (13), (15), and (16)

$$\frac{1}{\sqrt{1 + q^{*2}}} \frac{\partial \log_e q^*}{\partial \psi^*} - \frac{\partial \theta}{\partial \varphi^*} = 0 \quad (D4)$$

Finally, from equations (D3) and (D4)

$$\frac{\partial \log_e u}{\partial \psi^*} - \frac{\partial \theta}{\partial \varphi^*} = 0 \quad (20)$$

Equation (20) is the equation for irrotational fluid motion expressed in terms of φ^*, ψ^* coordinates and $\log_e u$.

APPENDIX E

ORTHOGONAL CURVES IN $\varphi\psi$ - AND xy -PLANES

If, for example, lines of constant Q and θ are orthogonal in the $\varphi\psi$ -plane the product of their tangents equals -1.0. This condition is satisfied if

$$\frac{\partial Q}{\partial \varphi} \frac{\partial \theta}{\partial \varphi} + \frac{\partial Q}{\partial \psi} \frac{\partial \theta}{\partial \psi} = 0 \quad (E1)$$

But, from equations (5) and (6)

$$\frac{\partial Q}{\partial \varphi} \frac{\partial \theta}{\partial \varphi} + \frac{\partial Q}{\partial \psi} \frac{\partial \theta}{\partial \psi} = Q \left[\left(\frac{1}{\rho} - \rho \right) \frac{\partial \theta}{\partial \psi} \frac{\partial \theta}{\partial \varphi} - \frac{\partial \log_e \rho}{\partial \varphi} \frac{\partial \theta}{\partial \psi} \right] \quad (E2)$$

so that for compressible flow equation (E1) is not, in general, satisfied and therefore lines of constant Q (or q) and θ are not orthogonal in the $\varphi\psi$ -plane. For incompressible flow ρ is equal to 1.0 and the right side of equation (E2) is zero so that equation (E1) is satisfied and therefore lines of constant Q and θ are orthogonal in the $\varphi\psi$ -plane.

From equations (11a) to (11d) in differential form

$$\frac{\partial x}{\partial \varphi} = \frac{\cos \theta}{Q} = \rho \frac{\partial y}{\partial \psi}$$

$$\frac{\partial y}{\partial \varphi} = \frac{\sin \theta}{Q} = -\rho \frac{\partial x}{\partial \psi}$$

so that

$$\frac{\partial x}{\partial \varphi} \frac{\partial y}{\partial \varphi} + \frac{\partial x}{\partial \psi} \frac{\partial y}{\partial \psi} = (1 - \rho^2) \frac{\partial x}{\partial \psi} \frac{\partial y}{\partial \psi} \quad (E3)$$

For compressible flow the right side of equation (E3) is not, in general, zero so that lines of constant x and y are not orthogonal in the $\varphi\psi$ -plane. For incompressible flow the right side of equation (E3) becomes zero so that lines of constant x and y are orthogonal in the $\varphi\psi$ -plane.

From the usual definitions of φ and ψ

$$\frac{\partial \varphi}{\partial x} = Q \cos \theta = \frac{1}{\rho} \frac{\partial \psi}{\partial y}$$

$$\frac{\partial \varphi}{\partial y} = Q \sin \theta = -\frac{1}{\rho} \frac{\partial \psi}{\partial x}$$

so that

$$\frac{\partial \varphi}{\partial x} \frac{\partial \psi}{\partial x} + \frac{\partial \varphi}{\partial y} \frac{\partial \psi}{\partial y} = 0$$

Thus, for both compressible and incompressible flow lines of constant φ and ψ are orthogonal in the xy -plane.

In terms of Q and θ the equations for continuity and irrotational motion in the xy -plane reduce to

$$\frac{\partial \log_e Q}{\partial x} + \frac{\partial \theta}{\partial y} = -\sin \theta \cos \theta \frac{\partial \log_e \rho}{\partial y} - \cos^2 \theta \frac{\partial \log_e \rho}{\partial x}$$

$$\frac{\partial \log_e Q}{\partial y} - \frac{\partial \theta}{\partial x} = -\sin \theta \cos \theta \frac{\partial \log_e \rho}{\partial x} - \sin^2 \theta \frac{\partial \log_e \rho}{\partial y}$$

so that

$$\begin{aligned} & \frac{\partial Q}{\partial x} \frac{\partial \theta}{\partial x} + \frac{\partial Q}{\partial y} \frac{\partial \theta}{\partial y} = \\ & - Q \frac{\partial \theta}{\partial x} \left(\sin \theta \cos \theta \frac{\partial \log_e \rho}{\partial y} + \cos^2 \theta \frac{\partial \log_e \rho}{\partial x} \right) \\ & - Q \frac{\partial \theta}{\partial y} \left(\sin \theta \cos \theta \frac{\partial \log_e \rho}{\partial x} + \sin^2 \theta \frac{\partial \log_e \rho}{\partial y} \right) \end{aligned} \quad (E4)$$

For compressible flow the right side of equation (E4) is not, in general, zero so that lines of constant Q (or q) and θ are not orthogonal in the xy -plane. For incompressible flow the right side of equation (E4) becomes zero so that lines of constant Q and θ are orthogonal in the $\varphi\psi$ -plane.

Likewise for linearized compressible flow it can be shown that

$$\frac{\partial q}{\partial \varphi^*} \frac{\partial \theta}{\partial \varphi^*} + \frac{\partial q}{\partial \psi^*} \frac{\partial \theta}{\partial \psi^*} = 0 \tag{E5}$$

$$\frac{\partial x}{\partial \varphi^*} \frac{\partial y}{\partial \varphi^*} + \frac{\partial x}{\partial \psi^*} \frac{\partial y}{\partial \psi^*} = (1 - \rho^{*2}) \frac{\partial x}{\partial \psi^*} \frac{\partial y}{\partial \psi^*} \tag{E6}$$

$$\frac{\partial \varphi^*}{\partial x} \frac{\partial \psi^*}{\partial x} + \frac{\partial \varphi^*}{\partial y} \frac{\partial \psi^*}{\partial y} = 0 \tag{E7}$$

and

$$\begin{aligned} & \frac{\partial q}{\partial x} \frac{\partial \theta}{\partial x} + \frac{\partial q}{\partial y} \frac{\partial \theta}{\partial y} = \\ & - q \frac{\partial \theta}{\partial x} \left(\sin \theta \cos \theta \frac{\partial \log_e \rho^*}{\partial y} + \cos^2 \theta \frac{\partial \log_e \rho^*}{\partial x} \right) \\ & - q \frac{\partial \theta}{\partial y} \left(\sin \theta \cos \theta \frac{\partial \log_e \rho^*}{\partial x} + \sin^2 \theta \frac{\partial \log_e \rho^*}{\partial y} \right) \end{aligned} \tag{E8}$$

Thus, from equation (E5) lines of constant q and θ are orthogonal in the $\varphi^*\psi^*$ -plane and from equation (E7) lines of constant φ^* and ψ^* are orthogonal in the xy -plane. But from equation (E6) lines of constant x and y are not orthogonal in the $\varphi^*\psi^*$ -plane and from equation (E8) lines of constant q and θ are not orthogonal in the xy -plane.

APPENDIX F

RATIO OF CURVE SPACING FOR SETS OF ORTHOGONAL CURVES

IN $\varphi\psi$ - AND xy -PLANES

Consider for example the case of orthogonal lines of constant Q and θ in the $\varphi\psi$ -plane (incompressible flow, appendix E). If $(ds)_\theta$ is the differential distance along a line of constant θ between two curves of constant Q

$$(ds)_\theta^2 = (d\varphi)_\theta^2 + (d\psi)_\theta^2 \quad (F1)$$

where the subscripts θ indicate that the changes are made along a line of constant θ . The change in Q along $(ds)_\theta$ is

$$dQ = \frac{\partial Q}{\partial \varphi} (d\varphi)_\theta + \frac{\partial Q}{\partial \psi} (d\psi)_\theta \quad (F2)$$

Also, because $d\theta$ is zero along $(ds)_\theta$

$$0 = \frac{\partial \theta}{\partial \varphi} (d\varphi)_\theta + \frac{\partial \theta}{\partial \psi} (d\psi)_\theta \quad (F3)$$

From equations (F1) to (F3)

$$(ds)_\theta^2 = (dQ)^2 \left[\frac{\left(\frac{\partial \theta}{\partial \varphi}\right)^2 + \left(\frac{\partial \theta}{\partial \psi}\right)^2}{\left(\frac{\partial Q}{\partial \varphi} \frac{\partial \theta}{\partial \psi} - \frac{\partial \psi}{\partial \varphi} \frac{\partial \theta}{\partial \psi}\right)^2} \right] \quad (F4a)$$

Likewise, if $(ds)_Q$ is the differential distance along a line of constant Q between two curves of constant θ

$$(ds)_Q^2 = (d\theta)^2 \left[\frac{\left(\frac{\partial Q}{\partial \varphi}\right)^2 + \left(\frac{\partial Q}{\partial \psi}\right)^2}{\left(\frac{\partial Q}{\partial \varphi} \frac{\partial \theta}{\partial \psi} - \frac{\partial \psi}{\partial \varphi} \frac{\partial \theta}{\partial \psi}\right)^2} \right] \quad (F4b)$$

Thus, from equations (F4a) and (F4b) the ratio of curve spacing for orthogonal lines of constant Q and θ in the $\varphi\psi$ -plane becomes

$$\frac{(\delta S)_Q}{(\delta S)_\theta} = \frac{\delta\theta}{\delta Q} \left[\frac{\left(\frac{\partial Q}{\partial\varphi}\right)^2 + \left(\frac{\partial Q}{\partial\psi}\right)^2}{\left(\frac{\partial\theta}{\partial\varphi}\right)^2 + \left(\frac{\partial\theta}{\partial\psi}\right)^2} \right]^{1/2}$$

which, from equations (5) and (6) with ρ equal to 1.0, becomes

$$\frac{(\delta S)_Q}{(\delta S)_\theta} = \left(\frac{\delta\theta}{\delta Q}\right)_Q \quad (F5)$$

Likewise it can be shown that for incompressible flow in the $\varphi\psi$ -plane with lines of constant x and y

$$\frac{(\delta S)_x}{(\delta S)_y} = \frac{\delta y}{\delta x} \quad (F6)$$

For both compressible and incompressible flow in the xy -plane with lines of constant φ and ψ

$$\frac{(\delta S)_\varphi}{(\delta S)_\psi} = \left(\frac{\delta\psi}{\delta\varphi}\right) \frac{1}{\rho} \quad (F7)$$

For incompressible flow in the xy -plane with lines of constant Q and θ

$$\frac{(\delta S)_Q}{(\delta S)_\theta} = \left(\frac{\delta\theta}{\delta Q}\right)_Q \quad (F8)$$

For linearized compressible flow in the $\varphi^*\psi^*$ -plane with lines of constant q and θ

$$\frac{(\delta S)_q}{(\delta S)_\theta} = \left(\frac{\delta\theta}{\delta q}\right) \frac{q}{\rho^*} \quad (F9)$$

And for linearized compressible flow in the xy -plane with lines of constant φ^* and ψ^*

$$\frac{(\delta S)_{\varphi^*}}{(\delta S)_{\psi^*}} = \left(\frac{\delta\psi^*}{\delta\varphi^*}\right) \frac{1}{\rho^*} \quad (F10)$$

REFERENCES

1. Carrier, G. F.: Elbows for Accelerated Flow. Jour. Appl. Mech., vol. 14, no. 2, June 1947, pp. A-108-A-112.
2. Lighthill, M. J.: A New Method of Two-Dimensional Aerodynamic Design. R. & M. No. 2112, British A.R.C., 1945.
3. Clauser, Francis H.: Two-Dimensional Compressible Flows Having Arbitrarily Specified Pressure Distributions for Gases with Gamma Equal to Minus One. Rep. NOLR 1132, Symposium on Theoretical Compressible Flow, U. S. Naval Ordnance Lab., June 28, 1949, pp. 1-33.
4. Southwell, R. V.: Relaxation Methods in Theoretical Physics. Clarendon Press (Oxford), 1946.
5. Stanitz, John D.: Design of Two-Dimensional Channels with Prescribed Velocity Distributions along the Channel Walls. II - Solution by Green's Function. NACA TN 2595, 1952.
6. Liepmann, Hans Wolfgang, and Puckett, Allen E.: Introduction to Aerodynamics of a Compressible Fluid. John Wiley & Sons, Inc., 1947.
7. Chaplygin, S.: Gas Jets. NACA TM 1063, 1944.
8. Emmons, Howard W.: The Numerical Solution of Partial Differential Equations. Quart. Appl. Math., vol. II, no. 3, Oct. 1944, pp. 173-195.
9. Tsien, Hsue-Shen: Two-Dimensional Subsonic Flow of Compressible Fluids. Jour. Aero. Sci., vol. 6, no. 10, Aug. 1939, pp. 399-407.

TABLE I - DISTRIBUTION OF VELOCITY Q AND FLOW DIRECTION θ IN TRANSFORMED φψ-PLANE FOR EXAMPLE III (ELBOW WITH INCOMPRESSIBLE FLOW)

[Prescribed variation in Q with arc length s along channel walls plotted in fig 2, $Q_1 = 0.5$, $Q_2 = 1.0$, $\Delta\theta = 89.36^\circ$]

φ \ ψ	0		0 125		0 250		0 375		0 500		0 625		0 750		0 875		1 000	
	Q	θ	Q	θ	Q	θ	Q	θ	Q	θ	Q	θ	Q	θ	Q	θ	Q	θ
0 000	0 5000	0	0 5000	0	0 5000	0	0 5000	0	0 5000	0	0 5000	0	0 5000	0	0 5000	0	0 5000	0
-1 875	5000	01	5000	01	5000	00	5000	00	5000	00	5000	00	5000	00	5000	-01	5000	-01
-1 750	5000	01	5000	01	5000	01	5000	00	5000	00	5000	00	5000	-01	5000	-01	5000	-01
-1 625	5000	01	5000	01	5001	01	5001	01	5001	00	5001	-01	5001	-01	5000	-01	5000	-01
-1 500	5000	02	5001	02	5001	01	5001	01	5001	00	5001	-01	5001	-01	5001	-02	5000	-02
-1 375	5000	03	5001	03	5002	02	5002	01	5002	00	5002	-01	5002	-02	5001	-03	5000	-03
-1 250	5000	04	5001	04	5002	03	5003	02	5003	00	5003	-02	5002	-03	5001	-04	5000	-04
-1 125	5000	06	5002	06	5004	04	5005	03	5005	00	5005	-03	5004	-05	5002	-06	5000	-06
-1 000	5000	09	5003	08	5006	07	5007	04	5008	00	5007	-04	5005	-07	5003	-08	5000	-09
-875	5000	14	5005	12	5009	10	5011	05	5012	00	5011	-06	5008	-10	5004	-12	5000	-14
-750	5000	20	5007	18	5013	14	5016	08	5017	-01	5016	-09	5012	-14	5006	-18	5000	-20
-625	5000	30	5011	27	5019	21	5025	11	5026	-01	5023	-13	5018	-21	5009	-27	5000	-30
-500	5000	45	5016	40	5029	30	5037	16	5038	-02	5034	-19	5026	-31	5014	-39	5000	-42
-375	5000	69	5025	60	5044	45	5055	24	5056	-04	5050	-28	5037	-45	5019	-56	5000	-61
-250	5000	1 04	5039	89	5068	65	5082	32	5083	-09	5072	-43	5053	-67	5028	-83	5000	-89
-125	5000	1 63	5065	1 34	5107	94	5124	44	5121	-17	5103	-64	5074	-98	5039	-1 19	5000	-1 26
0	5000	2 73	5115	2 04	5171	1 30	5187	50	5175	-36	5145	-99	5103	-1 44	5053	-1 71	5000	-1 80
125	5097	5 06	5226	3 21	5276	1 64	5278	34	5249	-70	5200	-1 50	5139	-2 07	5071	-2 41	5000	-2 52
250	5354	6 83	5424	4 02	5433	1 73	5402	-03	5344	-1 27	5269	-2 24	5184	-2 93	5093	-3 34	5000	-3 46
375	5715	7 36	5692	4 02	5637	1 32	5557	-75	5460	-2 18	5351	-3 29	5236	-4 07	5118	-4 54	5000	-4 68
500	6134	6 69	6006	3 19	5874	33	5736	-1 89	5592	-3 46	5444	-4 66	5295	-5 51	5146	-6 01	5000	-6 16
625	6576	4 95	6344	1 52	6132	-1 31	5930	-3 55	5735	-5 19	5544	-6 43	5357	-7 31	5176	-7 83	5000	-7 99
750	7018	2 40	6690	-82	6399	-3 52	6132	-5 69	5883	-7 33	5647	-8 57	5422	-9 45	5207	-9 97	5000	-10 13
875	7448	-81	7030	-3 76	6663	-6 26	6334	-8 31	6032	-9 89	5751	-11 09	5487	-11 95	5237	-12 46	5000	-12 62
1 000	7855	-4 52	7356	-7 18	6919	-9 46	6530	-11 34	6177	-12 84	5852	-13 98	5550	-14 79	5287	-15 27	5000	-15 43
1 125	8235	-8 64	7662	-11 01	7162	-13 05	6717	-14 76	6316	-16 14	5949	-17 20	5611	-17 96	5296	-18 41	5000	-18 56
1 250	8583	-13 08	7945	-15 16	7387	-16 97	6891	-18 51	6446	-19 76	6041	-20 74	5668	-21 44	5323	-21 86	5000	-22 00
1 375	8895	-17 77	8202	-19 59	7593	-21 17	7052	-22 53	6587	-23 66	6126	-24 56	5721	-25 19	5348	-25 58	5000	-25 71
1 500	9177	-22 67	8432	-24 22	7778	-25 60	7199	-26 79	6678	-27 81	6204	-28 62	5771	-29 20	5371	-29 56	5000	-29 68
1 625	9418	-27 72	8633	-29 03	7944	-30 20	7331	-31 25	6779	-32 16	6278	-32 90	5817	-33 44	5393	-33 77	5000	-33 90
1 750	9620	-32 88	8806	-33 95	8089	-34 94	7450	-35 84	6873	-36 67	6347	-37 37	5862	-37 89	5414	-38 21	5000	-38 34
1 875	9782	-38 10	8949	-38 94	8215	-39 75	7558	-40 54	6965	-41 32	6415	-42 01	5908	-42 53	5437	-42 86	5000	-43 02
2 000	9901	-43 30	9065	-43 91	8325	-44 58	7659	-45 28	7050	-46 04	6486	-46 78	5959	-47 35	5463	-47 73	5000	-47 94
2 125	9975	-48 43	9153	-48 83	8422	-49 36	7757	-50 02	7143	-50 80	6569	-51 66	6023	-52 35	5499	-52 86	5000	-53 19
2 250	1 0000	-53 34	9218	-53 57	8510	-54 00	7858	-54 65	7249	-55 51	6671	-56 56	6112	-57 49	5560	-58 32	5000	-59 04
2 375	1 0000	-57 83	9271	-58 01	8596	-58 44	7968	-59 14	7374	-60 11	6805	-61 28	6248	-62 68	5686	-64 31	5097	-66 18
2 500	1 0000	-62 00	9321	-62 16	8687	-62 63	8091	-63 40	7524	-64 48	6977	-65 82	6442	-67 65	5905	-69 98	5354	-72 81
2 625	1 0000	-65 84	9374	-66 01	8785	-66 51	8228	-67 35	7697	-68 52	7186	-70 02	6689	-72 14	6200	-74 88	5715	-78 23
2 750	1 0000	-69 39	9429	-69 55	8890	-70 07	8378	-70 96	7891	-72 20	7424	-73 82	6975	-76 07	6544	-78 95	6134	-82 46
2 875	1 0000	-72 57	9487	-72 74	8999	-73 27	8537	-74 17	8097	-75 44	7680	-77 11	7285	-79 37	6915	-82 21	6576	-85 65
3 000	1 0000	-75 43	9544	-75 59	9111	-76 12	8699	-77 02	8309	-78 27	7943	-79 92	7603	-82 10	7292	-84 80	7018	-88 03
3 125	1 0000	-77 93	9501	-78 10	9221	-78 60	8860	-79 46	8521	-80 67	8205	-82 26	7918	-84 30	7663	-86 80	7448	-89 76
3 250	1 0000	-80 11	9556	-80 27	9327	-80 75	9016	-81 55	8726	-82 69	8460	-84 17	8222	-86 05	8018	-88 32	7855	-90 99
3 375	1 0000	-81 97	9708	-82 11	9427	-82 56	9164	-83 30	8920	-84 35	8700	-85 71	8508	-87 41	8351	-89 44	8255	-91 81
3 500	1 0000	-83 54	9755	-83 67	9521	-84 07	9301	-84 74	9100	-85 69	8923	-86 92	8773	-88 43	8658	-90 22	8583	-92 30
3 625	1 0000	-84 84	9798	-84 96	9605	-85 32	9426	-86 51	9264	-86 75	9125	-87 83	9014	-89 16	8936	-90 72	8898	-92 52
3 750	1 0000	-85 90	9837	-86 01	9680	-86 32	9537	-86 84	9410	-87 57	9305	-88 51	9228	-89 65	9183	-90 99	9177	-92 52
3 875	1 0000	-86 75	9870	-86 84	9746	-87 11	9634	-87 56	9538	-88 18	9462	-88 98	9414	-89 94	9397	-91 06	9418	-92 34
4 000	1 0000	-87 43	9898	-87 50	9802	-87 73	9717	-88 10	9646	-88 62	9596	-89 28	9571	-90 07	9577	-90 98	9620	-92 01
4 125	1 0000	-87 95	9922	-88 01	9849	-88 20	9786	-88 50	9736	-88 92	9705	-89 45	9698	-90 07	9722	-90 78	9782	-91 57
4 250	1 0000	-88 34	9942	-88 39	9887	-88 54	9842	-88 78	9808	-89 11	9792	-89 53	9798	-89 99	9831	-90 50	9901	-91 06
4 375	1 0000	-88 64	9957	-88 68	9917	-88 79	9885	-88 98	9864	-89 23	9857	-89 55	9869	-89 87	9905	-90 19	9975	-90 52
4 500	1 0000	-88 85	9969	-88 88	9941	-88 97	9919	-89 10	9905	-89 29	9904	-89 53	9917	-89 73	9948	-89 90	1 0000	-90 03
4 625	1 0000	-89 01	9978	-89 03	9968	-89 09	9943	-89 19	9935	-89 33	9935	-89 49	9946	-89 62	9969	-89 72	1 0000	-89 78
4 750	1 0000	-89 11	9984	-89 13	9971	-89 18	9961	-89 25	9956	-89 34	9957	-89 45	9965	-89 54	9980	-89 60	1 0000	-89 64
4 875	1 0000	-89 19	9989	-89 21	9980	-89 24	9975	-89 29	9970	-89 35	9971	-89 43	9977	-89 48	9987	-89 52	1 0000	-89 54
5 000	1 0000	-89 24	9993	-89 25	9986	-89 28	9982	-89 31	9980	-89 36	9981	-89 41	9985	-89 44	9992	-89 47	1 0000	-89 48
5 125	1 0000	-89 28	9995	-89 29	9991	-89 30	9988	-89 33	9986	-89 36	9987	-89 39	9990	-89 42	9995	-89 43	1 0000	-89 44
5 250	1 0000	-89 31	9997	-89 31	9994	-89 32	9992	-89 34	9991	-89 36	9992	-89 38	9994	-89 40	9997	-89 41	1 0000	-89 42
5 375	1 0000	-89 32	9998	-89 33	9996	-89 33	9995	-89 35	9994	-89 36	9995	-89 38	9996	-89 39	9998	-89 39	1 0000	-89 40
5 500	1 0000	-89 34	9999	-89 34	9997	-89 34	9997	-89 35	9996	-89 36	9996	-89 37	9997	-89 38	9999	-89 38	1 0000	-89 39
5 625	1 0000	-89 34	9999	-89 35	9998	-89 35	9998	-89 35	9998	-89 36	9998	-89 36	9999	-89 37	9999	-89 37	1 0000	-89 38
5 750	1 0000	-89 35	9999	-89 35	9999	-89 35	9999	-89 36	9999	-89 36	9999	-89 37	1 0000	-89 37	1 0000	-89 37	1 0000	-89 37
5 875	1 0000	-89 35	1 0000	-89 35	1 0000	-89 36	9999	-89 36	9999	-89 36	9999	-89 37	1 0000	-89 37	1 0000	-89 37	1 0000	-89 37
6 000	1 0000	-89 36	1 0000	-89 36	1 0000	-89 36	1 0000	-89 36	1 0000	-89 36	1 0000	-89 36	1 0000	-89 37	1 0000	-89 37	1 0000	-89 37



2306

TABLE II - DISTRIBUTION OF PHYSICAL COORDINATES x AND y IN TRANSFORMED $\phi\psi$ -PLANE FOR EXAMPLE III (ELBOW WITH INCOMPRESSIBLE FLOW)

[Prescribed variation in Q with arc length s along channel walls plotted in fig 2, $Q_u = 0.5$, $Q_d = 1.0$, $\Delta\theta = 89.36^\circ$]

ψ	0		0 125		0 250		0 375		0 500		0 625		0 750		0 875		1 000	
	x	y	x	y	x	y	x	y	x	y	x	y	x	y	x	y	x	y
-2 000	-3.978	-0.998	-3.978	-0.748	-3.978	-0.498	-3.978	-0.248	-3.978	0.002	-3.978	0.252	-3.978	0.502	-3.978	0.752	-3.978	1.002
-1 875	-3.727	-0.998	-3.728	-0.748	-3.728	-0.498	-3.728	-0.248	-3.728	0.002	-3.728	0.252	-3.728	0.502	-3.728	0.752	-3.727	1.002
-1 750	-3.477	-0.998	-3.478	-0.748	-3.478	-0.498	-3.478	-0.248	-3.478	0.002	-3.478	0.252	-3.478	0.502	-3.478	0.752	-3.477	1.002
-1 625	-3.227	-0.998	-3.228	-0.748	-3.228	-0.498	-3.228	-0.248	-3.228	0.002	-3.228	0.252	-3.228	0.502	-3.228	0.752	-3.227	1.002
-1 500	-2.977	-0.998	-2.977	-0.748	-2.978	-0.498	-2.978	-0.248	-2.978	0.002	-2.978	0.252	-2.978	0.502	-2.978	0.752	-2.977	1.002
-1 375	-2.727	-0.998	-2.728	-0.748	-2.728	-0.498	-2.728	-0.248	-2.728	0.002	-2.728	0.252	-2.728	0.502	-2.728	0.752	-2.727	1.002
-1 250	-2.477	-0.997	-2.478	-0.747	-2.478	-0.498	-2.478	-0.248	-2.478	0.002	-2.478	0.252	-2.478	0.502	-2.478	0.752	-2.477	1.002
-1 125	-2.227	-0.997	-2.228	-0.747	-2.228	-0.497	-2.228	-0.248	-2.228	0.002	-2.228	0.252	-2.228	0.502	-2.228	0.752	-2.227	1.002
-1 000	-1.977	-0.997	-1.978	-0.747	-1.978	-0.497	-1.978	-0.247	-1.978	0.002	-1.978	0.252	-1.978	0.501	-1.978	0.751	-1.977	1.001
-875	-1.727	-0.996	-1.728	-0.747	-1.728	-0.497	-1.728	-0.247	-1.728	0.002	-1.728	0.252	-1.728	0.501	-1.728	0.751	-1.727	1.001
-750	-1.477	-0.996	-1.478	-0.746	-1.479	-0.496	-1.479	-0.247	-1.480	0.002	-1.479	0.251	-1.479	0.501	-1.478	0.750	-1.477	1.000
-625	-1.227	-0.995	-1.229	-0.745	-1.230	-0.496	-1.230	-0.247	-1.231	0.002	-1.230	0.251	-1.230	0.500	-1.229	0.749	-1.227	999
-500	-0.977	-0.993	-0.979	-0.743	-0.981	-0.495	-0.982	-0.246	-0.982	0.002	-0.982	0.250	-0.981	0.499	-0.979	0.748	-0.977	997
-375	-0.727	-0.990	-0.730	-0.741	-0.733	-0.493	-0.734	-0.245	-0.735	0.002	-0.734	0.249	-0.732	0.497	-0.730	0.746	-0.727	996
-250	-0.478	-0.987	-0.482	-0.738	-0.485	-0.491	-0.487	-0.244	-0.488	0.002	-0.487	0.248	-0.484	0.495	-0.481	0.743	-0.477	992
-125	-0.228	-0.981	-0.235	-0.733	-0.239	-0.487	-0.242	-0.242	-0.243	0.001	-0.241	0.245	-0.238	0.491	-0.233	0.739	-0.227	987
0	0.022	-0.972	0.011	-0.726	0.004	-0.482	0.000	-0.240	0.000	0.003	0.242	0.008	0.486	0.015	0.732	0.023	981	
125	0.270	-0.955	0.254	-0.715	0.243	-0.476	0.239	-0.239	0.240	0.002	0.245	0.237	0.479	0.261	0.724	0.273	971	
250	0.510	-0.930	0.489	-0.700	0.477	-0.469	0.472	-0.238	0.476	-0.006	0.484	0.229	0.494	0.468	0.507	0.711	0.522	958
375	0.754	-0.901	0.713	-0.684	0.702	-0.463	0.700	-0.239	0.707	-0.013	0.719	0.218	0.734	0.454	0.751	0.695	0.772	941
500	0.942	-0.875	0.925	-0.670	0.918	-0.460	0.921	-0.244	0.933	-0.024	0.950	0.202	0.970	0.434	0.994	0.678	1.021	917
625	1.139	-0.855	1.129	-0.662	1.128	-0.461	1.136	-0.254	1.153	-0.041	1.177	0.180	1.204	0.409	1.234	0.643	1.269	886
750	1.322	-0.843	1.321	-0.660	1.327	-0.470	1.343	-0.271	1.367	-0.064	1.398	0.151	1.433	0.375	1.472	0.607	1.516	848
875	1.495	-0.840	1.502	-0.668	1.518	-0.486	1.542	-0.295	1.575	-0.095	1.614	0.113	1.658	0.332	1.707	0.560	1.761	798
1 000	1.658	-0.848	1.675	-0.684	1.701	-0.511	1.734	-0.328	1.776	-0.135	1.824	0.067	1.879	0.279	1.939	0.503	2.003	738
1 125	1.812	-0.866	1.840	-0.710	1.875	-0.545	1.918	-0.370	1.969	-0.185	2.028	0.010	2.094	0.216	2.165	0.435	2.242	665
1 250	1.958	-0.893	1.995	-0.747	2.041	-0.590	2.094	-0.423	2.156	-0.245	2.225	-0.068	2.302	0.142	2.386	0.354	2.477	578
1 375	2.096	-0.931	2.143	-0.793	2.198	-0.644	2.262	-0.485	2.334	-0.316	2.415	-0.137	2.504	0.055	2.601	0.260	2.706	477
1 500	2.226	-0.979	2.282	-0.849	2.348	-0.709	2.422	-0.558	2.504	-0.398	2.596	-0.228	2.697	-0.044	2.807	0.152	2.927	361
1 625	2.347	-1.036	2.413	-0.914	2.488	-0.783	2.572	-0.642	2.665	-0.491	2.768	-0.330	2.882	-0.156	3.005	0.030	3.139	229
1 750	2.461	-1.102	2.535	-0.989	2.621	-0.867	2.715	-0.735	2.816	-0.594	2.930	-0.444	3.055	-0.281	3.192	-0.106	3.341	082
1 875	2.566	-1.177	2.649	-1.073	2.741	-0.960	2.844	-0.838	2.957	-0.708	3.081	-0.569	3.218	-0.418	3.368	-0.255	3.531	-081
2 000	2.662	-1.260	2.753	-1.164	2.853	-1.061	2.964	-0.950	3.086	-0.831	3.219	-0.705	3.367	-0.567	3.529	-0.418	3.706	-259
2 125	2.749	-1.350	2.847	-1.264	2.955	-1.170	3.074	-1.070	3.202	-0.963	3.344	-0.850	3.501	-0.727	3.675	-0.594	3.865	-451
2 250	2.828	-1.447	2.932	-1.369	3.047	-1.286	3.172	-1.197	3.307	-1.102	3.455	-1.002	3.620	-0.895	3.803	-0.780	4.004	-658
2 375	2.899	-1.550	3.008	-1.481	3.128	-1.407	3.258	-1.329	3.398	-1.247	3.550	-1.160	3.721	-1.070	3.910	-0.977	4.119	-880
2 500	2.961	-1.659	3.075	-1.598	3.199	-1.533	3.332	-1.466	3.476	-1.395	3.631	-1.322	3.803	-1.249	3.994	-1.177	4.203	-1 105
2 625	3.016	-1.771	3.134	-1.718	3.260	-1.663	3.396	-1.605	3.541	-1.546	3.697	-1.485	3.869	-1.428	4.056	-1.374	4.259	-1 324
2 750	3.064	-1.886	3.184	-1.841	3.313	-1.794	3.450	-1.746	3.595	-1.697	3.751	-1.648	3.919	-1.604	4.100	-1.565	4.294	-1 532
2 875	3.105	-2.005	3.227	-1.966	3.357	-1.927	3.494	-1.887	3.638	-1.847	3.792	-1.808	3.966	-1.775	4.130	-1.748	4.314	-1 727
3 000	3.139	-2.125	3.263	-2.092	3.393	-2.060	3.530	-2.028	3.673	-1.996	3.824	-1.965	3.983	-1.941	4.150	-1.923	4.324	-1 911
3 125	3.168	-2.246	3.292	-2.219	3.423	-2.193	3.559	-2.167	3.700	-2.142	3.848	-2.119	4.002	-2.101	4.162	-2.089	4.328	-2 084
3 250	3.191	-2.369	3.317	-2.347	3.447	-2.326	3.582	-2.305	3.721	-2.285	3.866	-2.267	4.015	-2.256	4.168	-2.249	4.326	-2 247
3 375	3.211	-2.493	3.337	-2.475	3.466	-2.457	3.600	-2.411	3.737	-2.426	3.879	-2.413	4.024	-2.405	4.171	-2.401	4.323	-2 402
3 500	3.227	-2.617	3.352	-2.602	3.481	-2.588	3.614	-2.576	3.749	-2.564	3.888	-2.555	4.029	-2.549	4.172	-2.548	4.317	-2 551
3 625	3.239	-2.741	3.365	-2.729	3.493	-2.719	3.624	-2.709	3.758	-2.700	3.894	-2.693	4.032	-2.690	4.171	-2.690	4.311	-2 693
3 750	3.249	-2.865	3.375	-2.856	3.503	-2.848	3.633	-2.840	3.764	-2.834	3.898	-2.829	4.033	-2.827	4.169	-2.828	4.305	-2 832
3 875	3.257	-2.990	3.383	-2.983	3.510	-2.976	3.639	-2.971	3.769	-2.965	3.901	-2.962	4.033	-2.961	4.166	-2.962	4.299	-2 966
4 000	3.264	-3.115	3.389	-3.109	3.516	-3.104	3.644	-3.100	3.773	-3.096	3.903	-3.093	4.033	-3.093	4.164	-3.094	4.294	-3 097
4 125	3.269	-3.240	3.394	-3.235	3.520	-3.231	3.648	-3.228	3.776	-3.225	3.906	-3.223	4.033	-3.222	4.162	-3.223	4.290	-3 226
4 250	3.273	-3.365	3.398	-3.361	3.524	-3.358	3.651	-3.355	3.778	-3.352	3.906	-3.351	4.033	-3.350	4.160	-3.351	4.287	-3 353
4 375	3.276	-3.490	3.401	-3.487	3.527	-3.484	3.653	-3.482	3.780	-3.480	3.907	-3.478	4.033	-3.478	4.160	-3.478	4.286	-3 478
4 500	3.279	-3.615	3.404	-3.612	3.529	-3.610	3.655	-3.608	3.781	-3.606	3.908	-3.605	4.034	-3.604	4.159	-3.603	4.285	-3 603
4 625	3.281	-3.740	3.406	-3.738	3.531	-3.736	3.657	-3.734	3.783	-3.732	3.909	-3.731	4.034	-3.730	4.160	-3.729	4.285	-3 729
4 750	3.283	-3.865	3.408	-3.863	3.533	-3.861	3.659	-3.859	3.784	-3.858	3.910	-3.856	4.035	-3.855	4.161	-3.854	4.286	-3 853
4 875	3.285	-3.990	3.410	-3.988	3.535	-3.986	3.660	-3.985	3.786	-3.983	3.911	-3.982	4.036	-3.981	4.162	-3.979	4.287	-3 978
5 000	3.287	-4.115	3.412	-4.113	3.537	-4.111	3.662	-4.110	3.787	-4.108	3.912	-4.107	4.038	-4.106	4.163	-4.105	4.288	-4 103
5 125	3.288	-4.240	3.413	-4.238	3.538	-4.237	3.663	-4.235	3.788	-4.234	3.914	-4.232	4.039	-4.231	4.164	-4.230	4.289	-4 229
5 250	3.290	-4.365	3.415	-4.363	3.540	-4.362	3.665	-4.360	3.790	-4.359	3.915	-4.358	4.040	-4.356	4.165	-4.355	4.290	-4 353
5 375	3.291	-4.490	3.416	-4.488	3.541	-4.487	3.666	-4.485	3.791	-4.484	3.916	-4.482	4.041	-4.481	4.166	-4.480	4.292	-4 478
5 500	3.293	-4.615	3.418	-4.613	3.543	-4.612	3.668	-4.610	3.793	-4.609	3.918	-4.						

TABLE III - DISTRIBUTION OF VELOCITY q AND FLOW DIRECTION θ IN TRANSFORMED $\phi^*\psi^*$ -PLANE

FOR EXAMPLE IV (ELBOW WITH LINEARIZED COMPRESSIBLE FLOW)

[Prescribed variation in Q with arc length s along channel walls plotted in fig 2,
 $Q_u = 0.5$, $Q_d = 1.0$, $q_d = 0.80176$, $\Delta\psi^* = 0.73782$, $\Delta\theta = 104.07^\circ$]

$\frac{\psi^*}{\Delta\psi^*}$	0		1/6		1/3		1/2		2/3		5/6		1.0	
	q	θ	q	θ	q	θ	q	θ	q	θ	q	θ	q	θ
-11/6	0.4009	0	0.4009	0	0.4009	0	0.4009	0	0.4009	0	0.4009	0	0.4009	0
-10/6	4009	01	4009	01	4009	.00	4009	00	4009	00	4009	-01	4009	-01
-9/6	4009	01	4009	01	4010	01	4010	00	4010	-01	4009	-01	4009	-01
-8/6	4009	02	4010	02	4010	01	4010	00	4010	-01	4010	-02	4009	-02
-7/6	4009	03	4010	03	4011	01	4011	00	4011	-01	4010	-02	4009	-03
-6/6	4009	05	4011	04	4012	02	4013	00	4012	-02	4011	-04	4009	-05
-5/6	4009	08	4012	.07	4015	04	4015	00	4014	-04	4012	-07	4009	-08
-4/6	4009	14	4015	.12	4019	07	4020	00	4018	-07	4014	-11	4009	-13
-3/6	4009	24	4019	20	4025	11	4027	-01	4024	-11	4017	-18	4009	-21
-2/6	4009	.40	4026	.33	4037	17	4039	-03	4033	-20	4022	-31	4009	-35
-1/6	4009	70	4041	57	4057	27	4058	-05	4048	-33	4030	-50	4009	-56
0	4009	1.31	4070	96	4093	36	4090	-17	4071	-58	4042	-84	4009	-92
1/6	4072	2.82	4141	1.49	4155	43	4139	-40	4104	-99	4058	-1.34	4009	-1.45
2/6	4243	3.88	4268	1.77	4251	24	4207	-87	4148	-1.63	4080	-2.07	4009	-2.22
3/6	4489	4.00	4444	1.46	4377	-38	4295	-1.70	4202	-2.59	4106	-3.11	4009	-3.28
4/6	4780	3.17	4654	50	4526	-1.49	4396	-2.92	4265	-3.90	4135	-4.46	4009	-4.65
5/6	5094	1.44	4882	-1.17	4689	-3.16	4506	-4.62	4333	-5.63	4167	-6.21	4009	-6.41
6/6	5415	-0.98	5118	-3.43	4857	-5.34	4621	-6.76	4403	-7.75	4200	-8.33	4009	-8.52
7/6	5732	-4.00	5352	-6.23	5024	-8.01	4734	-9.35	4472	-10.29	4232	-10.85	4009	-11.04
8/6	6035	-7.48	5578	-9.48	5186	-11.10	4841	-12.34	4539	-13.22	4262	-13.74	4009	-13.91
9/6	6321	-11.35	5793	-13.12	5340	-14.57	4947	-15.70	4601	-16.49	4291	-16.97	4009	-17.13
10/6	6602	-15.52	5994	-17.09	5482	-18.37	5043	-19.38	4659	-20.09	4317	-20.52	4009	-20.67
11/6	6855	-19.96	6178	-21.33	5613	-22.46	5131	-23.34	4712	-23.98	4341	-24.37	4009	-24.49
12/6	7086	-24.62	6346	-25.80	5732	-26.79	5210	-27.56	4759	-28.12	4362	-28.46	4009	-28.58
13/6	7293	-29.46	6496	-30.47	5837	-31.32	5281	-32.00	4801	-32.49	4381	-32.79	4009	-32.89
14/6	7477	-34.45	6629	-35.31	5931	-36.03	5343	-36.62	4838	-37.05	4398	-37.31	4009	-37.40
15/6	7636	-39.56	6744	-40.27	6013	-40.89	5398	-41.39	4872	-41.77	4413	-42.00	4009	-42.08
16/6	7769	-44.16	6842	-45.34	6084	-45.86	5447	-46.30	4902	-46.64	4427	-46.85	4009	-46.93
17/6	7875	-50.02	6924	-50.47	6146	-50.90	5492	-51.30	4931	-51.63	4440	-51.85	4009	-51.93
18/6	7953	-55.27	6991	-55.61	6202	-55.98	5537	-56.36	4961	-56.72	4456	-56.98	4009	-57.08
19/6	8001	-60.49	7045	-60.72	6257	-61.06	5586	-61.47	4999	-61.91	4477	-62.28	4009	-62.44
20/6	8018	-65.55	7091	-65.68	6315	-66.03	5647	-66.53	5055	-67.13	4515	-67.79	4009	-68.16
21/6	8018	-70.32	7135	-70.45	6385	-70.85	5730	-71.49	5142	-72.37	4598	-73.46	4072	-74.80
22/6	8018	-74.81	7186	-74.96	6471	-75.43	5840	-76.22	5272	-77.36	4745	-78.91	4243	-81.03
23/6	8018	-78.97	7245	-79.15	6573	-79.68	5978	-80.59	5441	-81.93	4948	-83.79	4489	-86.33
24/6	8018	-82.82	7311	-83.01	6690	-83.59	6138	-84.57	5641	-86.02	5190	-88.01	4780	-90.69
25/6	8018	-86.28	7381	-86.48	6816	-87.07	6313	-88.08	5860	-89.55	5455	-91.55	5094	-94.16
26/6	8018	-89.37	7452	-89.56	6947	-90.15	6494	-91.14	6089	-92.57	5729	-94.48	5415	-96.93
27/6	8018	-92.07	7523	-92.25	7077	-92.81	6676	-93.75	6310	-95.10	6002	-96.88	5732	-99.11
28/6	8018	-94.40	7591	-94.57	7203	-95.09	6852	-95.97	6540	-97.21	6268	-98.83	6038	-100.83
29/6	8018	-96.39	7654	-96.54	7321	-97.02	7020	-97.82	6753	-98.94	6522	-100.39	6329	-102.17
30/6	8018	-98.05	7713	-98.20	7432	-98.62	7177	-99.34	6952	-100.34	6759	-101.63	6602	-103.19
31/6	8018	-99.44	7766	-99.56	7532	-99.94	7321	-100.58	7135	-101.46	6978	-102.59	6855	-103.95
32/6	8018	-100.56	7813	-100.67	7623	-101.01	7451	-101.56	7301	-102.33	7178	-103.31	7086	-104.49
33/6	8018	-101.47	7855	-101.57	7702	-101.85	7566	-102.33	7449	-102.99	7357	-103.83	7293	-104.84
34/6	8018	-102.18	7890	-102.26	7772	-102.51	7667	-102.91	7580	-103.47	7515	-104.18	7477	-105.03
35/6	8018	-102.73	7921	-102.80	7831	-103.00	7753	-103.34	7691	-103.80	7651	-104.39	7636	-105.10
36/6	8018	-103.14	7946	-103.20	7880	-103.37	7825	-103.64	7785	-104.01	7764	-104.48	7769	-105.05
37/6	8018	-103.45	7966	-103.49	7920	-103.62	7883	-103.83	7860	-104.12	7855	-104.49	7875	-104.91
38/6	8018	-103.66	7982	-103.69	7950	-103.79	7927	-103.95	7917	-104.16	7923	-104.42	7953	-104.71
39/6	8018	-103.81	7994	-103.83	7973	-103.90	7960	-104.02	7957	-104.16	7968	-104.33	8001	-104.49
40/6	8018	-103.90	8002	-103.92	7989	-103.97	7982	-104.05	7982	-104.14	7993	-104.23	8018	-104.28
41/6	8018	-103.97	8008	-103.98	8000	-104.01	7996	-104.06	7997	-104.11	8004	-104.16	8018	-104.18
42/6	8018	-104.00	8011	-104.01	8006	-104.03	8004	-104.06	8005	-104.09	8010	-104.12	8018	-104.13
43/6	8018	-104.03	8014	-104.03	8011	-104.05	8009	-104.06	8010	-104.08	8013	-104.10	8018	-104.10
44/6	8018	-104.04	8015	-104.05	8013	-104.05	8013	-104.06	8013	-104.08	8015	-104.08	8018	-104.09
45/6	8018	-104.05	8016	-104.05	8015	-104.06	8015	-104.07	8015	-104.07	8016	-104.08	8018	-104.08
46/6	8018	-104.06	8017	-104.06	8016	-104.06	8016	-104.07	8016	-104.07	8017	-104.07	8018	-104.07
47/6	8018	-104.06	8017	-104.06	8017	-104.06	8016	-104.07	8017	-104.07	8017	-104.07	8018	-104.07
48/6	8018	-104.06	8017	-104.06	8017	-104.06	8017	-104.07	8017	-104.07	8017	-104.07	8018	-104.07
49/6	8018	-104.06	8017	-104.06	8017	-104.06	8017	-104.07	8017	-104.07	8017	-104.07	8018	-104.07
50/6	8018	-104.06	8018	-104.06	8018	-104.06	8018	-104.07	8018	-104.07	8018	-104.07	8018	-104.07



TABLE IV - DISTRIBUTION OF PHYSICAL COORDINATES x AND y IN TRANSFORMED ψ^* -PLANE FOR

EXAMPLE IV (ELBOW WITH LINEARIZED COMPRESSIBLE FLOW)

[Prescribed variation in Q with arc length s along channel walls plotted in fig 2,
 $Q_u = 0.5$, $Q_d = 1.0$, $q_d = 0.80176$, $\Delta\psi^* = 0.73782$, $\Delta\theta = 104.07^\circ$]

$\frac{\psi^*}{\Delta\psi^*}$	0		1/6		1/3		1/2		2/3		5/6		1.0	
	x	y	x	y	x	y	x	y	x	y	x	y	x	y
-11/6	-2.466	-0.769	-2.466	-0.512	-2.466	-0.256	-2.466	0.001	-2.466	0.257	-2.466	0.513	-2.466	0.770
-10/6	-2.241	-.769	-2.241	-.512	-2.241	-.256	-2.241	0.001	-2.241	0.257	-2.241	.513	-2.241	.770
-9/6	-2.016	-.769	-2.016	-.512	-2.016	-.256	-2.016	0.001	-2.016	0.257	-2.016	.513	-2.016	.770
-8/6	-1.791	-.769	-1.791	-.512	-1.791	-.256	-1.791	0.001	-1.791	0.257	-1.791	.513	-1.791	.770
-7/6	-1.566	-.768	-1.566	-.512	-1.566	-.256	-1.566	0.001	-1.566	0.257	-1.566	.513	-1.566	.770
-6/6	-1.341	-.768	-1.341	-.512	-1.341	-.256	-1.341	0.001	-1.341	0.257	-1.341	.513	-1.341	.769
-5/6	-1.116	-.768	-1.116	-.512	-1.117	-.256	-1.117	0.001	-1.117	0.257	-1.116	.513	-1.116	.769
-4/6	-.891	-.768	-.892	-.511	-.892	-.255	-.892	0.001	-.892	0.256	-.892	.513	-.891	.769
-3/6	-.666	-.767	-.667	-.511	-.668	-.255	-.668	0.001	-.668	0.256	-.667	.512	-.666	.768
-2/6	-.441	-.766	-.443	-.510	-.444	-.254	-.444	0.001	-.444	0.256	-.443	.511	-.441	.767
-1/6	-.216	-.763	-.219	-.508	-.221	-.254	-.221	.000	-.220	0.255	-.219	.510	-.216	.765
0	.008	-.760	.003	-.505	.000	-.252	.000	.000	.002	0.253	.005	.507	.009	.763
1/6	.233	-.752	.223	-.500	.219	-.251	.213	-.001	.222	0.250	.220	.503	.234	.758
2/6	.450	-.739	.438	-.494	.434	-.249	.436	-.003	.441	0.245	.449	.496	.459	.751
3/6	.656	-.724	.645	-.488	.643	-.250	.648	-.008	.657	0.237	.670	.486	.684	.740
4/6	.851	-.712	.844	-.485	.846	-.253	.855	-.016	.870	0.225	.888	.472	.908	.725
5/6	1.033	-.704	1.033	-.485	1.042	-.261	1.057	-.029	1.079	0.208	1.104	.452	1.132	.703
6/6	1.205	-.703	1.213	-.492	1.230	-.274	1.254	-.049	1.284	0.184	1.318	.425	1.355	.674
7/6	1.366	-.710	1.385	-.507	1.411	-.295	1.445	-.076	1.485	0.152	1.529	.389	1.577	.636
8/6	1.519	-.725	1.548	-.529	1.586	-.325	1.630	-.111	1.681	0.112	1.737	.344	1.797	.587
9/6	1.663	-.749	1.704	-.560	1.753	-.363	1.809	-.156	1.871	0.061	1.940	.288	2.013	.527
10/6	1.798	-.781	1.852	-.600	1.913	-.410	1.981	-.210	2.056	0.000	2.138	.221	2.226	.455
11/6	1.926	-.822	1.992	-.649	2.065	-.466	2.146	-.274	2.235	-.072	2.331	.142	2.434	.368
12/6	2.046	-.871	2.124	-.706	2.209	-.532	2.304	-.349	2.406	-.156	2.517	.050	2.635	.268
13/6	2.157	-.928	2.247	-.772	2.346	-.608	2.453	-.435	2.569	-.251	2.694	-.055	2.829	.153
14/6	2.261	-.993	2.363	-.847	2.473	-.693	2.593	-.530	2.723	-.357	2.862	-.173	3.013	.024
15/6	2.356	-1.064	2.468	-.930	2.591	-.787	2.723	-.636	2.866	-.475	3.020	-.304	3.186	-.120
16/6	2.443	-1.143	2.567	-1.020	2.700	-.889	2.843	-.751	2.999	-.604	3.166	-.447	3.346	-.278
17/6	2.521	-1.228	2.655	-1.117	2.798	-1.000	2.952	-.875	3.118	-.743	3.298	-.601	3.492	-.449
18/6	2.590	-1.318	2.732	-1.220	2.885	-1.117	3.049	-1.007	3.225	-.890	3.416	-.766	3.623	-.632
19/6	2.650	-1.414	2.800	-1.330	2.960	-1.240	3.132	-1.146	3.317	-1.046	3.518	-.940	3.736	-.826
20/6	2.701	-1.514	2.858	-1.443	3.024	-1.369	3.203	-1.290	3.395	-1.208	3.603	-1.122	3.830	-1.030
21/6	2.743	-1.619	2.905	-1.561	3.076	-1.501	3.259	-1.438	3.456	-1.374	3.669	-1.309	3.901	-1.242
22/6	2.777	-1.726	2.942	-1.681	3.117	-1.635	3.303	-1.588	3.501	-1.541	3.715	-1.496	3.947	-1.455
23/6	2.803	-1.836	2.970	-1.803	3.147	-1.770	3.333	-1.737	3.531	-1.707	3.743	-1.680	3.969	-1.661
24/6	2.820	-1.947	2.990	-1.926	3.167	-1.905	3.353	-1.885	3.548	-1.869	3.755	-1.858	3.974	-1.856
25/6	2.831	-2.059	3.001	-2.048	3.177	-2.038	3.362	-2.030	3.554	-2.026	3.756	-2.027	3.966	-2.038
26/6	2.835	-2.171	3.005	-2.169	3.181	-2.169	3.363	-2.171	3.552	-2.177	3.747	-2.189	3.950	-2.209
27/6	2.834	-2.283	3.003	-2.290	3.177	-2.297	3.357	-2.308	3.542	-2.322	3.732	-2.342	3.927	-2.369
28/6	2.827	-2.396	2.996	-2.409	3.168	-2.423	3.345	-2.440	3.527	-2.461	3.712	-2.487	3.900	-2.520
29/6	2.817	-2.508	2.984	-2.527	3.155	-2.547	3.330	-2.570	3.508	-2.596	3.688	-2.626	3.871	-2.663
30/6	2.803	-2.619	2.969	-2.643	3.139	-2.668	3.311	-2.695	3.485	-2.725	3.662	-2.760	3.841	-2.799
31/6	2.786	-2.731	2.951	-2.756	3.119	-2.787	3.289	-2.818	3.461	-2.851	3.635	-2.888	3.809	-2.929
32/6	2.766	-2.841	2.931	-2.872	3.097	-2.904	3.266	-2.938	3.435	-2.973	3.606	-3.012	3.777	-3.055
33/6	2.744	-2.952	2.908	-2.985	3.074	-3.019	3.241	-3.055	3.409	-3.093	3.577	-3.133	3.746	-3.176
34/6	2.721	-3.062	2.885	-3.097	3.049	-3.133	3.215	-3.171	3.381	-3.209	3.548	-3.250	3.714	-3.294
35/6	2.697	-3.172	2.860	-3.208	3.024	-3.246	3.188	-3.284	3.353	-3.324	3.518	-3.366	3.683	-3.409
36/6	2.672	-3.281	2.834	-3.319	2.998	-3.358	3.161	-3.397	3.325	-3.437	3.489	-3.479	3.653	-3.522
37/6	2.646	-3.391	2.808	-3.430	2.971	-3.469	3.134	-3.509	3.297	-3.549	3.460	-3.591	3.623	-3.633
38/6	2.620	-3.500	2.782	-3.540	2.944	-3.579	3.107	-3.619	3.269	-3.660	3.432	-3.701	3.594	-3.744
39/6	2.593	-3.608	2.755	-3.643	2.917	-3.689	3.079	-3.730	3.241	-3.770	3.403	-3.811	3.565	-3.853
40/6	2.566	-3.719	2.728	-3.759	2.890	-3.799	3.052	-3.839	3.214	-3.880	3.376	-3.921	3.537	-3.962
41/6	2.539	-3.828	2.701	-3.868	2.862	-3.908	3.024	-3.949	3.186	-3.990	3.348	-4.030	3.510	-4.071
42/6	2.512	-3.937	2.673	-3.977	2.835	-4.018	2.997	-4.058	3.159	-4.099	3.320	-4.139	3.482	-4.180
43/6	2.484	-4.046	2.646	-4.087	2.808	-4.127	2.970	-4.168	3.131	-4.208	3.293	-4.249	3.455	-4.289
44/6	2.457	-4.155	2.619	-4.196	2.780	-4.236	2.942	-4.277	3.104	-4.317	3.266	-4.358	3.427	-4.398
45/6	2.430	-4.264	2.591	-4.305	2.753	-4.345	2.915	-4.386	3.077	-4.426	3.238	-4.467	3.400	-4.507
46/6	2.402	-4.374	2.564	-4.414	2.726	-4.455	2.887	-4.495	3.049	-4.536	3.211	-4.576	3.372	-4.617
47/6	2.375	-4.483	2.537	-4.523	2.698	-4.564	2.860	-4.604	3.022	-4.645	3.183	-4.685	3.345	-4.726
48/6	2.348	-4.592	2.509	-4.632	2.671	-4.673	2.833	-4.713	2.994	-4.754	3.156	-4.794	3.318	-4.835
49/6	2.320	-4.701	2.482	-4.741	2.644	-4.782	2.805	-4.822	2.967	-4.863	3.129	-4.903	3.290	-4.944
50/6	2.293	-4.810	2.455	-4.851	2.616	-4.891	2.778	-4.932	2.940	-4.972	3.101	-5.013	3.263	-5.053

2306

TABLE V - DISTRIBUTION OF VELOCITY q AND FLOW DIRECTION θ IN TRANSFORMED $\phi\psi$ -PLANE FOR

EXAMPLE V (ELBOW WITH COMPRESSIBLE FLOW ($\gamma=1.4$))

[Prescribed variation in Q with arc length s along channel walls plotted in fig 2, $Q_u = 0.5$, $Q_d = 1.0$, $q_d = 0.79927$, $\Delta\psi = 0.71054$, $\Delta\theta = 105.31^\circ$]

$\frac{\psi}{\Delta\psi}$	0		1/6		1/3		1/2		2/3		5/6		1.0	
	q	θ	q	θ	q	θ	q	θ	q	θ	q	θ	q	θ
-12/6	0.3996	0	0.3996	0	0.3996	0	0.3996	0	0.3996	0	0.3996	0	0.3996	0
-11/6	3996	00	3997	00	3997	00	3997	00	3997	00	3997	00	3996	00
-10/6	3996	01	3997	01	3997	00	3997	00	3997	00	3997	-01	3996	-01
-9/6	3996	.01	3997	01	3997	01	3997	00	3997	-01	3997	-01	3996	-01
-8/6	3996	02	3997	02	3998	01	3998	00	3998	-01	3997	-02	3996	-02
-7/6	3996	03	3998	03	3999	02	3999	00	3998	-02	3998	-02	3996	-03
-6/6	3996	05	.3998	04	4000	03	4000	00	4000	-03	3998	-04	3996	-05
-5/6	3996	09	4000	08	4002	04	.4003	00	4002	-04	4000	-07	3996	-08
-4/6	3996	15	4002	13	4006	07	4008	00	4006	-07	4002	-12	3996	-14
-3/6	3996	25	4007	22	4014	12	4015	-01	4012	-12	4005	-20	3996	-23
-2/6	3996	43	4015	.36	4026	18	4028	-03	4022	-22	4011	-34	3996	-38
-1/6	3996	77	4030	62	4047	30	4049	-06	4038	-36	4019	-55	3996	-62
0	3996	1.45	4062	1.06	4086	39	.4082	-19	4062	-64	4031	-92	3996	-102
1/6	4066	3.13	.4137	1.64	4152	46	.4134	-45	4097	-1.09	4049	-1.48	3996	-1.61
2/6	4253	4.28	.4275	1.93	4255	.24	4207	-98	4144	-1.81	4072	-2.30	3996	-2.46
3/6	4519	4.31	4464	1.54	4389	-48	4300	-1.92	4202	-2.89	4099	-3.46	3996	-3.64
4/6	4830	3.26	4687	40	4547	-1.74	4408	-3.30	4268	-4.35	4131	-4.97	3996	-5.17
5/6	.5162	1.21	4928	-1.53	4719	-3.64	4524	-5.21	4340	-6.29	4164	-6.92	3996	-7.13
6/6	5499	-1.61	5175	-4.11	4895	-6.10	4643	-7.61	4413	-8.66	4198	-9.28	3996	-9.49
7/6	5828	-5.05	5419	-7.27	5069	-9.09	4762	-10.50	4485	-11.49	4231	-12.08	3996	-12.28
8/6	6144	-8.99	5652	-10.92	5236	-12.55	4875	-13.82	4554	-14.74	4263	-15.29	3996	-15.47
9/6	.6441	-13.32	5871	-14.98	5393	-16.40	4981	-17.54	4618	-18.37	4292	-18.86	3996	-19.03
10/6	6717	-17.98	6074	-19.38	5538	-20.61	5078	-21.61	4677	-22.34	4319	-22.79	3996	-22.94
11/6	6970	-22.89	6258	-24.06	5669	-25.12	5166	-25.98	4730	-26.62	4343	-27.02	3996	-27.15
12/6	7197	-28.02	6424	-28.98	5786	-29.87	5245	-30.62	4777	-31.18	4364	-31.52	3996	-31.63
13/6	7399	-33.31	6569	-34.09	5889	-34.84	5314	-35.48	4818	-35.96	4383	-36.26	3996	-36.36
14/6	7573	-38.74	6696	-39.35	5978	-39.98	5375	-40.52	4855	-40.94	4400	-41.20	3996	-41.30
15/6	7719	-44.26	6803	-44.74	6056	-45.25	5428	-45.72	4888	-46.09	4415	-46.33	3996	-46.41
16/6	7836	-49.84	6891	-50.20	6123	-50.62	5476	-51.03	4918	-51.37	.4429	-51.61	3996	-51.70
17/6	7922	-55.44	.6963	-55.70	6182	-56.04	.5522	-56.43	4951	-56.80	4446	-57.07	3996	-57.18
18/6	7975	-60.96	7019	-61.13	6238	-61.44	5573	-61.85	4990	-62.30	.4468	-62.69	3996	-62.86
19/6	7993	-66.35	7066	-66.45	6297	-66.76	5635	-67.25	5047	-67.87	4507	-68.57	3996	-68.97
20/6	7993	-71.43	7110	-71.53	6367	-71.88	5720	-72.51	5138	-73.42	4595	-74.59	4066	-76.09
21/6	.7993	-76.19	7163	-76.31	6456	-76.73	5835	-77.50	5274	-78.69	4753	-80.35	4253	-82.69
22/6	7993	-80.67	7224	-80.80	6562	-81.27	5979	-82.14	.5453	-83.48	4969	-85.45	4519	-88.20
23/6	7993	-84.69	7292	-84.83	6684	-85.33	6145	-86.27	5662	-87.72	5225	-89.79	4830	-92.62
24/6	7993	-88.32	7366	-88.47	6816	-88.97	6327	-89.92	5892	-91.38	.5503	-93.41	.5162	-96.11
25/6	7993	-91.55	7442	-91.69	6952	-92.17	.6516	-93.06	6129	-94.41	5789	-96.29	5499	-98.75
26/6	.7993	-94.33	7516	-94.46	7087	-94.90	6705	-95.72	6366	-96.96	.6073	-98.65	5828	-100.82
27/6	7993	-96.70	7587	-96.81	7219	-97.21	.6888	-97.94	6597	-99.04	.6347	-100.52	.6144	-102.39
28/6	7993	-98.68	.7653	-98.78	7342	-99.14	7062	-99.77	6815	-100.72	.6607	-101.99	.6441	-103.57
29/6	7993	-100.31	7714	-100.40	7456	-100.71	7223	-101.25	7019	-102.06	6849	-103.13	6717	-104.45
30/6	7993	-101.64	.7769	-101.72	7559	-101.97	.7370	-102.43	7205	-103.10	7070	-103.99	.6970	-105.07
31/6	7993	-102.68	7817	-102.75	7651	-102.97	7502	-103.34	7373	-103.89	.7270	-104.61	7197	-105.49
32/6	7993	-103.48	.7858	-103.54	7731	-103.72	7617	-104.03	7520	-104.47	7446	-105.05	7399	-105.75
33/6	7993	-104.09	7893	-104.14	7800	-104.28	7716	-104.53	7648	-104.88	7599	-105.33	7573	-105.87
34/6	7993	-104.53	7922	-104.58	7856	-104.67	7799	-104.87	7754	-105.14	.7726	-105.49	7719	-105.89
35/6	7993	-104.83	7945	-104.86	7901	-104.95	7865	-105.09	7839	-105.29	.7828	-105.54	7836	-105.84
36/6	7993	-105.04	7962	-105.05	7935	-105.11	7914	-105.21	7903	-105.35	7904	-105.52	7922	-105.71
37/6	7993	-105.16	7975	-105.17	7959	-105.21	7948	-105.28	7945	-105.36	7953	-105.46	7975	-105.56
38/6	7993	-105.22	7983	-105.24	7974	-105.26	.7969	-105.30	7970	-105.34	7977	-105.39	.7993	-105.41
39/6	7993	-105.26	7987	-105.27	7983	-105.28	.7981	-105.31	7982	-105.33	7986	-105.35	7993	-105.35
40/6	7993	-105.29	7990	-105.29	7988	-105.30	.7987	-105.31	7987	-105.31	7990	-105.33	7993	-105.33
41/6	7993	-105.30	7991	-105.30	7990	-105.30	.7990	-105.31	7990	-105.31	.7991	-105.32	7993	-105.32
42/6	7993	-105.31	.7992	-105.31	7992	-105.31	7991	-105.31	7992	-105.31	.7992	-105.31	.7993	-105.31
43/6	7993	-105.31	7993	-105.31	7992	-105.31	7992	-105.31	7992	-105.31	7993	-105.31	7993	-105.31
44/6	7993	-105.31	7993	-105.31	7993	-105.31	7993	-105.31	7993	-105.31	.7993	-105.31	7993	-105.31

TABLE VI - DISTRIBUTION OF PHYSICAL COORDINATES x AND y IN TRANSFORMED $\phi\psi$ -PLANE FOR

EXAMPLE V (ELBOW WITH COMPRESSIBLE FLOW ($\gamma=1.4$))

[Prescribed variation in Q with arc length s along channel walls plotted in fig 2,
 $Q_u = 0.5$, $Q_d = 1.0$, $q_d = 0.79927$, $\Delta\psi = 0.71054$, $\Delta\theta = 105.31^\circ$]

$\frac{\psi}{\Delta\psi}$	0		1/6		1/3		1/2		2/3		5/6		1.0	
	x	y	x	y	x	y	x	y	x	y	x	y	x	y
	-12/6	-2.832	-0.770	-2.832	-0.513	-2.832	-0.256	-2.832	0.001	-2.832	0.258	-2.832	0.514	-2.832
-11/6	-2.595	-0.770	-2.595	-0.513	-2.595	-0.256	-2.595	0.001	-2.595	0.258	-2.595	0.514	-2.595	0.771
-10/6	-2.358	-0.770	-2.358	-0.513	-2.358	-0.256	-2.358	0.001	-2.358	0.258	-2.358	0.514	-2.358	0.771
-9/6	-2.122	-0.770	-2.122	-0.513	-2.122	-0.256	-2.122	0.001	-2.122	0.258	-2.122	0.514	-2.122	0.771
-8/6	-1.885	-0.770	-1.885	-0.513	-1.885	-0.256	-1.885	0.001	-1.885	0.258	-1.885	0.514	-1.885	0.771
-7/6	-1.648	-0.770	-1.648	-0.513	-1.648	-0.256	-1.648	0.001	-1.648	0.257	-1.648	0.514	-1.648	0.771
-6/6	-1.411	-0.769	-1.411	-0.513	-1.411	-0.256	-1.412	0.001	-1.411	0.257	-1.411	0.514	-1.411	0.771
-5/6	-1.174	-0.769	-1.175	-0.512	-1.175	-0.256	-1.175	0.001	-1.175	0.257	-1.175	0.514	-1.174	0.771
-4/6	-0.937	-0.769	-0.938	-0.512	-0.939	-0.256	-0.939	0.001	-0.938	0.257	-0.938	0.513	-0.937	0.770
-3/6	-0.701	-0.768	-0.702	-0.511	-0.702	-0.255	-0.703	0.001	-0.702	0.257	-0.702	0.513	-0.701	0.769
-2/6	-0.464	-0.767	-0.466	-0.510	-0.467	-0.255	-0.467	0.001	-0.467	0.256	-0.465	0.512	-0.464	0.768
-1/6	-0.227	-0.764	-0.230	-0.508	-0.232	-0.254	-0.233	0.001	-0.232	0.255	-0.230	0.510	-0.227	0.766
0	0.009	-0.760	0.004	-0.505	0.000	-0.252	0.000	0.000	0.002	0.253	0.005	0.507	0.010	0.763
1/6	0.245	-0.750	0.235	-0.499	0.230	-0.250	0.230	-0.001	0.234	0.250	0.240	0.502	0.247	0.758
2/6	0.473	-0.735	0.460	-0.492	0.456	-0.249	0.458	-0.004	0.463	0.244	0.473	0.495	0.484	0.749
3/6	0.688	-0.719	0.677	-0.485	0.675	-0.249	0.680	-0.009	0.690	0.235	0.704	0.483	0.720	0.737
4/6	0.891	-0.705	0.884	-0.482	0.887	-0.253	0.897	-0.019	0.913	0.220	0.934	0.466	0.956	0.719
5/6	1.080	-0.697	1.081	-0.483	1.091	-0.263	1.109	-0.035	1.132	0.200	1.161	0.443	1.192	0.693
6/6	1.257	-0.698	1.268	-0.492	1.287	-0.270	1.314	-0.058	1.347	0.172	1.385	0.411	1.426	0.659
7/6	1.424	-0.707	1.446	-0.510	1.475	-0.304	1.513	-0.089	1.556	0.135	1.605	0.369	1.659	0.615
8/6	1.581	-0.726	1.615	-0.537	1.656	-0.338	1.705	-0.130	1.760	0.088	1.822	0.317	1.888	0.558
9/6	1.729	-0.755	1.775	-0.574	1.828	-0.383	1.890	-0.182	1.958	0.099	2.033	0.252	2.115	0.488
10/6	1.867	-0.794	1.926	-0.620	1.992	-0.438	2.067	-0.245	2.149	-0.042	2.239	0.174	2.336	0.403
11/6	1.997	-0.842	2.069	-0.677	2.148	-0.503	2.236	-0.320	2.332	-0.125	2.437	0.082	2.550	0.303
12/6	2.117	-0.899	2.202	-0.743	2.295	-0.579	2.396	-0.406	2.507	-0.221	2.627	-0.024	2.757	0.187
13/6	2.229	-0.966	2.326	-0.820	2.432	-0.666	2.546	-0.503	2.671	-0.330	2.806	-0.145	2.953	0.055
14/6	2.331	-1.040	2.441	-0.905	2.558	-0.763	2.686	-0.612	2.824	-0.452	2.974	-0.279	3.137	-0.094
15/6	2.424	-1.122	2.545	-0.999	2.674	-0.869	2.814	-0.732	2.965	-0.585	3.129	-0.420	3.308	-0.259
16/6	2.506	-1.211	2.638	-1.100	2.778	-0.984	2.929	-0.862	3.092	-0.730	3.270	-0.589	3.463	-0.436
17/6	2.579	-1.306	2.720	-1.209	2.870	-1.108	3.031	-1.000	3.205	-0.886	3.394	-0.762	3.601	-0.629
18/6	2.642	-1.407	2.791	-1.325	2.949	-1.238	3.118	-1.147	3.301	-1.050	3.501	-0.946	3.719	-0.834
19/6	2.694	-1.513	2.850	-1.445	3.015	-1.374	3.191	-1.299	3.381	-1.221	3.588	-1.138	3.816	-1.050
20/6	2.737	-1.624	2.898	-1.570	3.068	-1.514	3.248	-1.456	3.443	-1.398	3.654	-1.335	3.887	-1.274
21/6	2.770	-1.738	2.935	-1.697	3.107	-1.656	3.290	-1.614	3.486	-1.572	3.698	-1.533	3.928	-1.499
22/6	2.794	-1.854	2.961	-1.826	3.135	-1.799	3.319	-1.772	3.513	-1.747	3.722	-1.727	3.945	-1.714
23/6	2.809	-1.971	2.977	-1.956	3.152	-1.940	3.334	-1.927	3.527	-1.917	3.729	-1.912	3.944	-1.916
24/6	2.816	-2.089	2.985	-2.085	3.159	-2.081	3.339	-2.079	3.528	-2.081	3.724	-2.089	3.929	-2.106
25/6	2.816	-2.208	2.985	-2.212	3.157	-2.218	3.336	-2.226	3.520	-2.238	3.710	-2.256	3.906	-2.281
26/6	2.810	-2.326	2.978	-2.339	3.149	-2.353	3.325	-2.369	3.505	-2.389	3.689	-2.414	3.878	-2.446
27/6	2.799	-2.444	2.965	-2.463	3.135	-2.484	3.308	-2.507	3.484	-2.533	3.664	-2.564	3.846	-2.601
28/6	2.783	-2.561	2.948	-2.586	3.116	-2.613	3.287	-2.641	3.460	-2.672	3.635	-2.708	3.812	-2.748
29/6	2.763	-2.678	2.928	-2.708	3.094	-2.739	3.263	-2.771	3.433	-2.807	3.604	-2.845	3.777	-2.887
30/6	2.740	-2.794	2.904	-2.828	3.069	-2.862	3.236	-2.898	3.404	-2.936	3.573	-2.977	3.742	-3.021
31/6	2.715	-2.910	2.879	-2.947	3.043	-2.984	3.208	-3.022	3.374	-3.063	3.540	-3.105	3.707	-3.150
32/6	2.689	-3.025	2.851	-3.064	3.014	-3.104	3.178	-3.144	3.342	-3.186	3.507	-3.229	3.672	-3.274
33/6	2.660	-3.140	2.822	-3.181	2.985	-3.222	3.148	-3.264	3.311	-3.307	3.474	-3.351	3.637	-3.396
34/6	2.631	-3.255	2.793	-3.297	2.954	-3.339	3.117	-3.382	3.279	-3.425	3.441	-3.470	3.603	-3.515
35/6	2.601	-3.369	2.762	-3.412	2.924	-3.455	3.085	-3.498	3.247	-3.542	3.409	-3.587	3.570	-3.632
36/6	2.570	-3.484	2.731	-3.527	2.893	-3.571	3.054	-3.614	3.215	-3.658	3.376	-3.703	3.537	-3.748
37/6	2.540	-3.598	2.701	-3.642	2.862	-3.685	3.023	-3.729	3.184	-3.773	3.344	-3.818	3.505	-3.862
38/6	2.509	-3.712	2.669	-3.756	2.830	-3.800	2.991	-3.844	3.152	-3.888	3.313	-3.932	3.474	-3.977
39/6	2.477	-3.827	2.638	-3.871	2.799	-3.915	2.960	-3.959	3.121	-4.003	3.281	-4.047	3.442	-4.091
40/6	2.446	-3.941	2.607	-3.985	2.768	-4.029	2.929	-4.073	3.089	-4.117	3.250	-4.161	3.411	-4.205
41/6	2.415	-4.055	2.576	-4.099	2.736	-4.143	2.897	-4.187	3.058	-4.232	3.219	-4.275	3.380	-4.319
42/6	2.384	-4.169	2.544	-4.213	2.705	-4.257	2.866	-4.301	3.027	-4.345	3.187	-4.389	3.348	-4.433
43/6	2.352	-4.284	2.513	-4.328	2.674	-4.372	2.835	-4.416	2.995	-4.460	3.156	-4.504	3.317	-4.548
44/6	2.321	-4.398	2.482	-4.442	2.643	-4.486	2.803	-4.530	2.964	-4.574	3.125	-4.618	3.286	-4.662



2306

2306

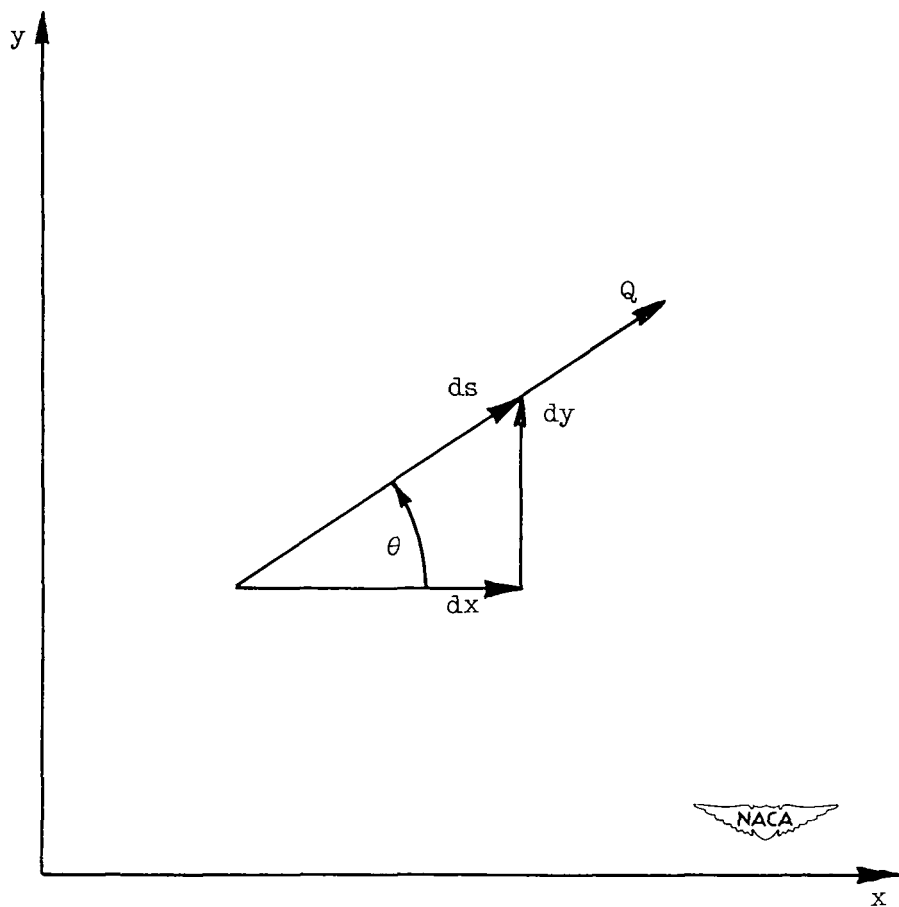


Figure 1. - Magnitude and direction of velocity at point in xy -plane.

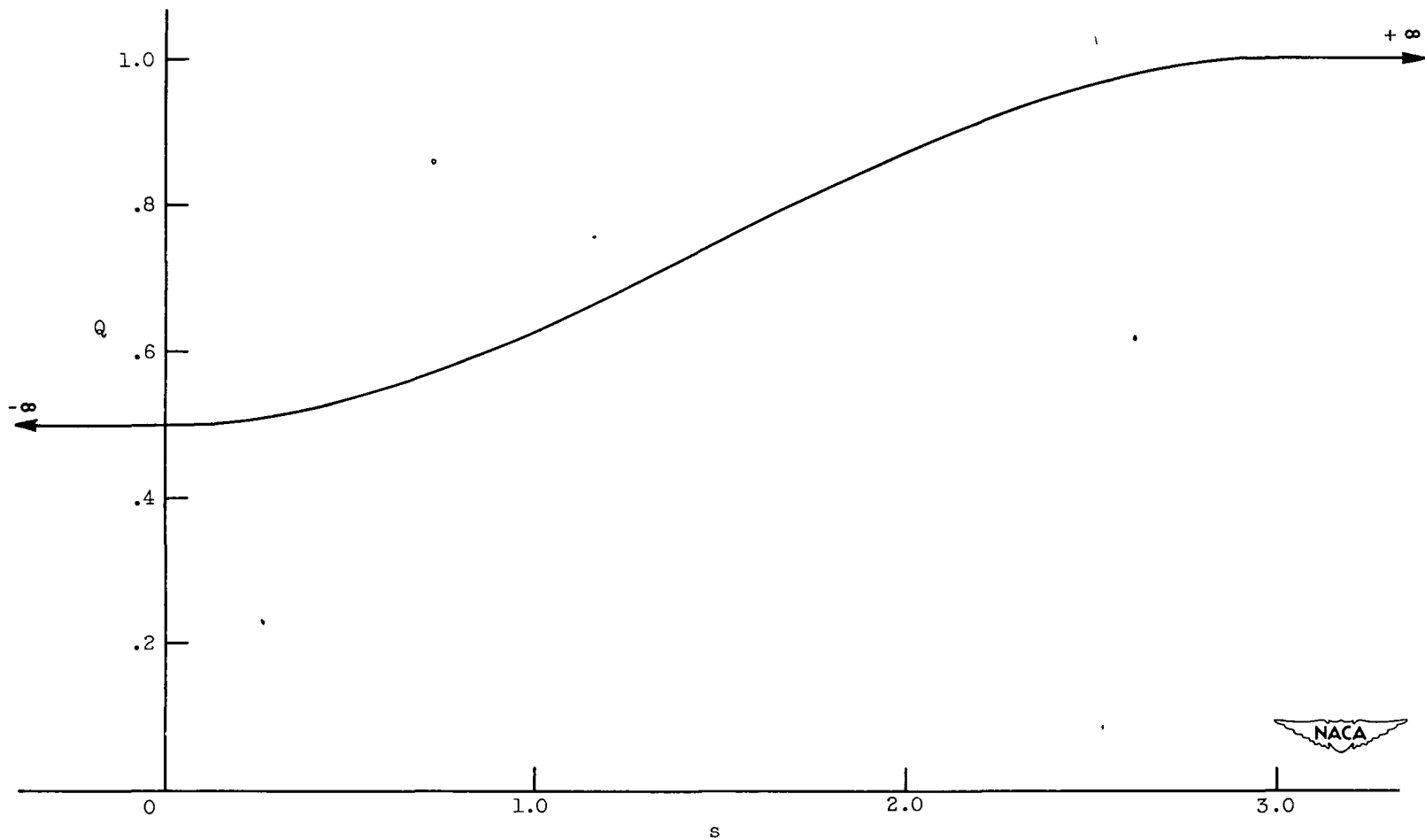


Figure 2. - Prescribed velocity distribution as function of arc length along channel wall for examples I, III, IV, and V. Equation (35).

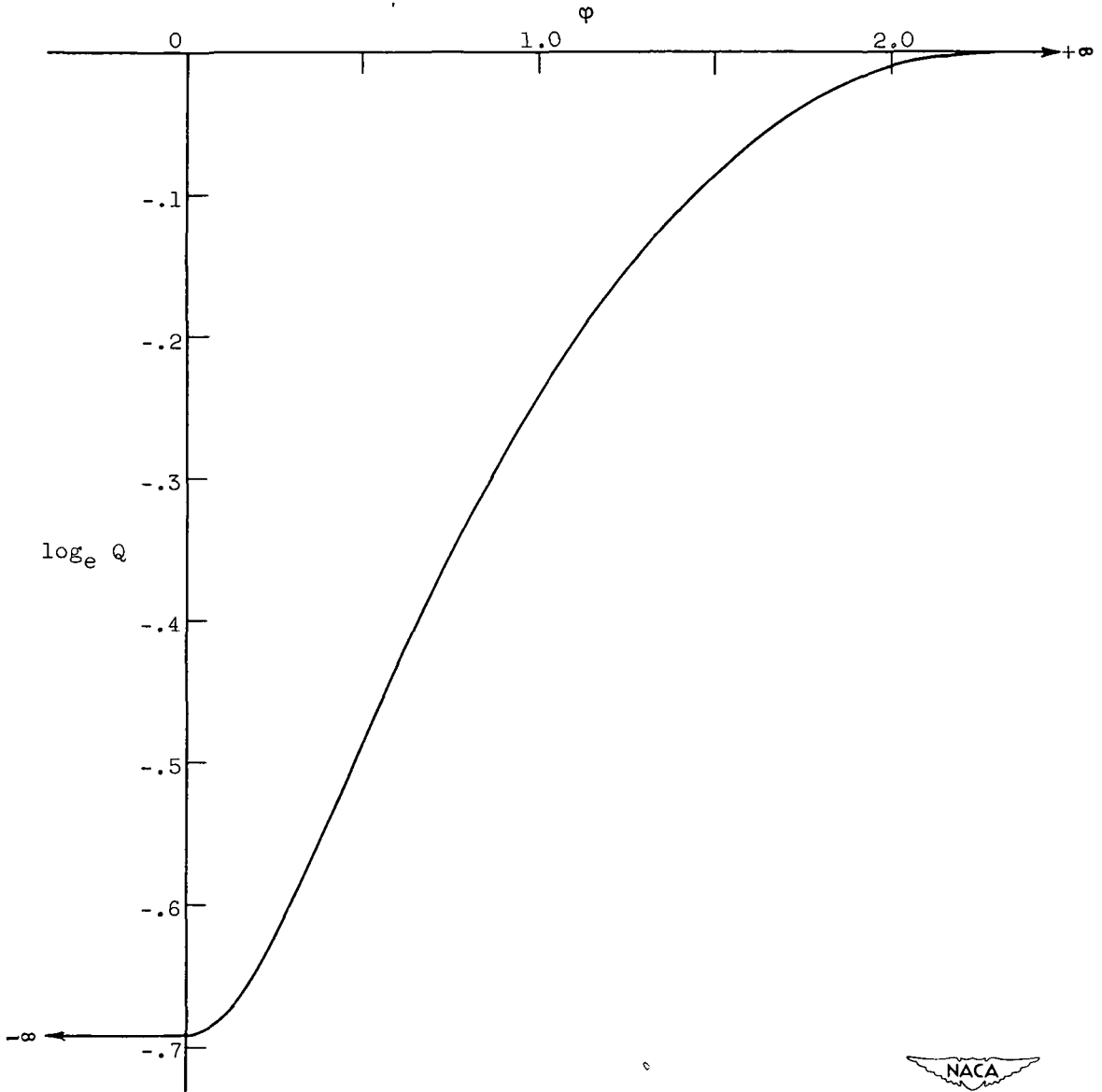


Figure 3. - Prescribed distribution of $\log_e Q$ as function of ϕ along channel walls for example I.

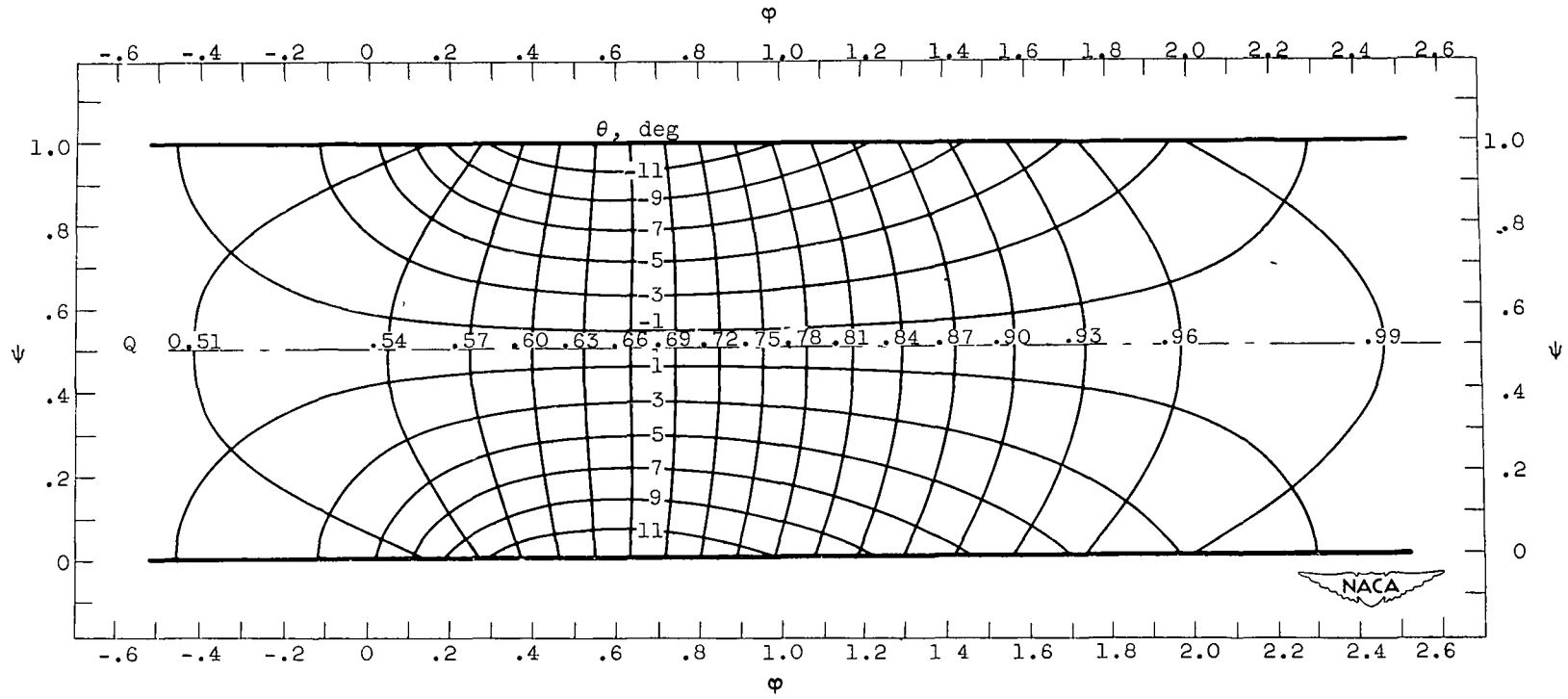


Figure 4. - Lines of constant velocity Q and flow direction θ in transformed $\phi\psi$ -plane for example I. Incompressible flow; prescribed velocity given in figure 2.

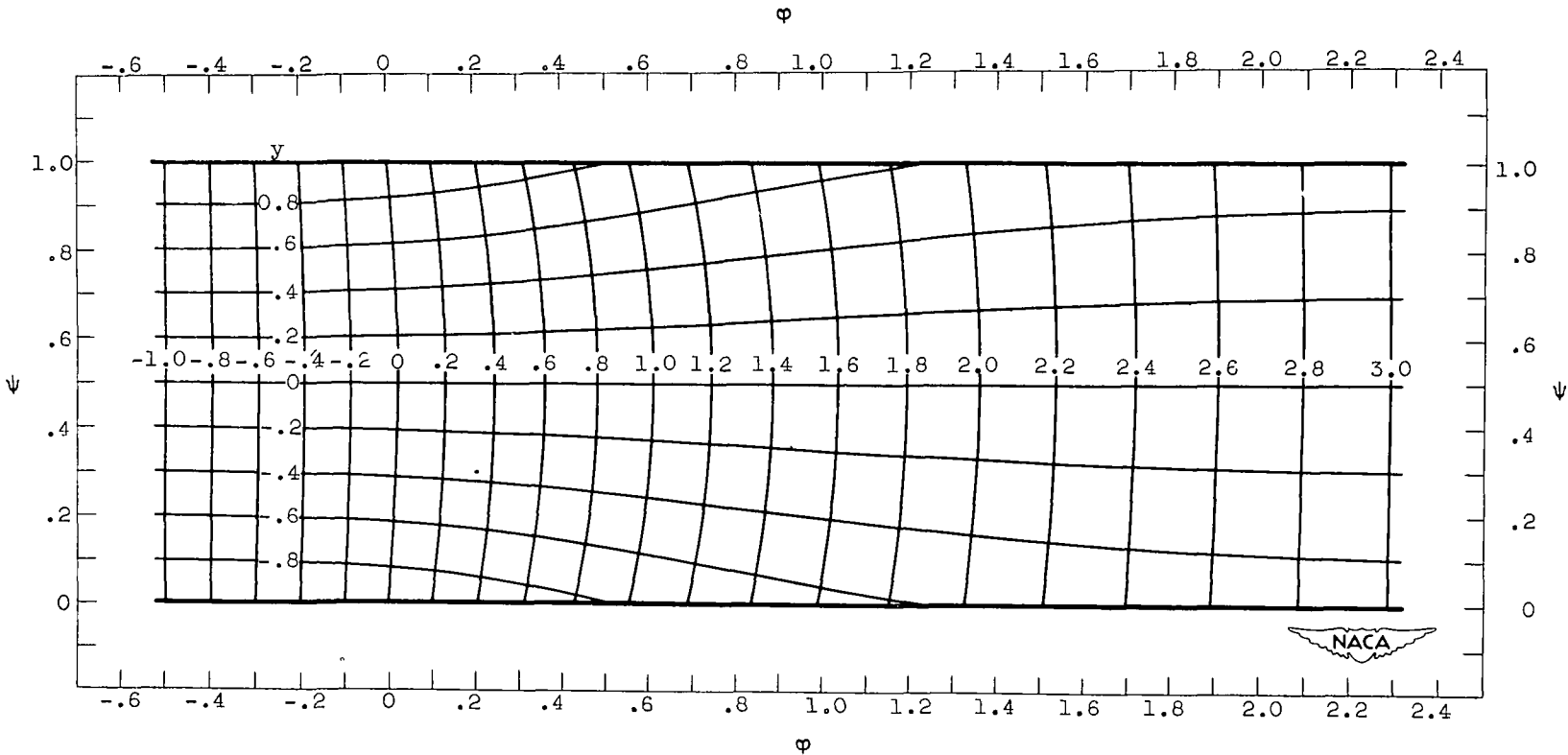


Figure 5. - Lines of constant x and y coordinates in transformed $\phi\psi$ -plane for example I. Incompressible flow; prescribed velocity given in figure 2.

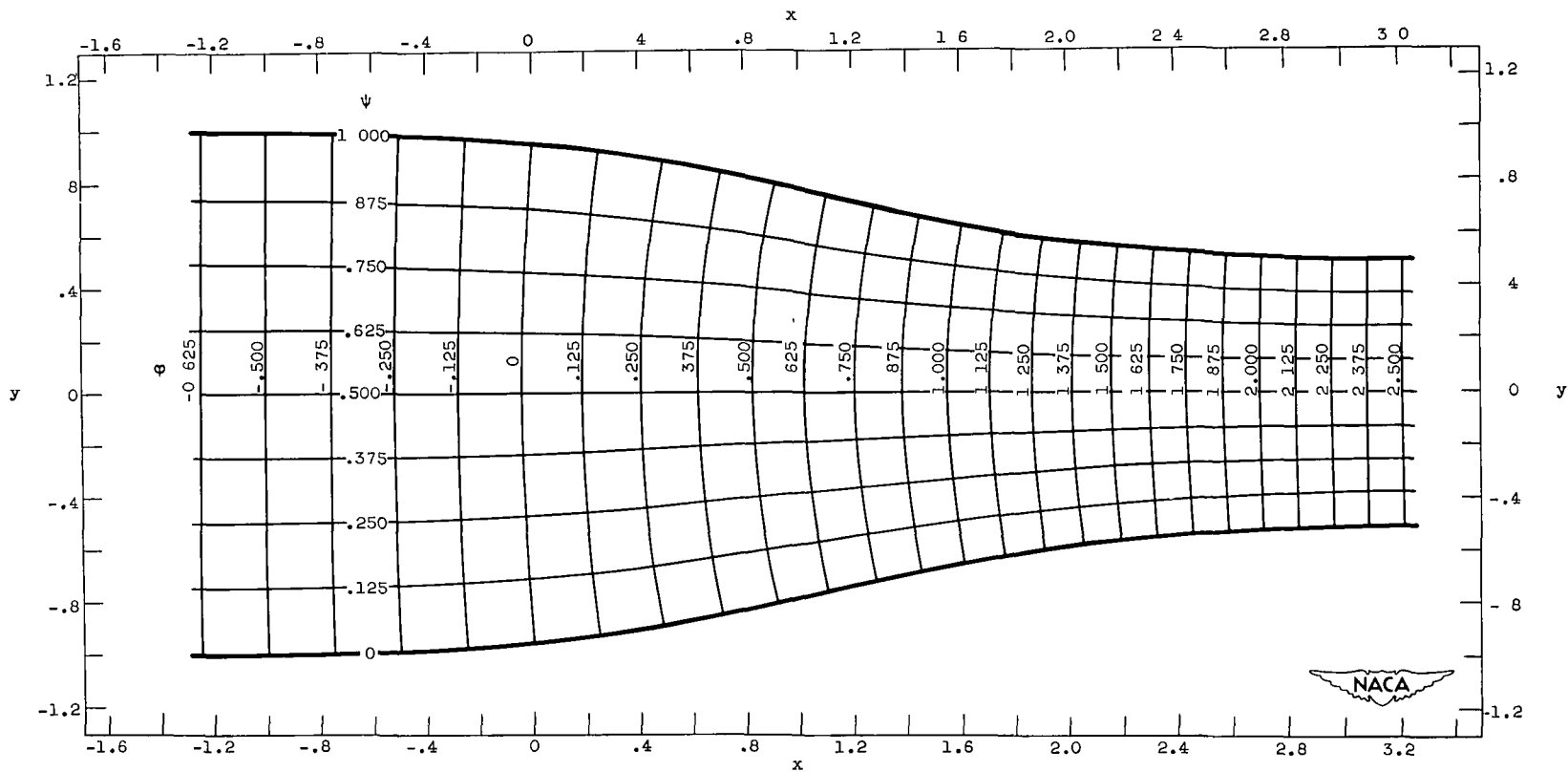


Figure 6. - Streamlines and velocity-potential lines on physical xy -plane for example I. Incompressible flow, prescribed velocity given in figure 2.

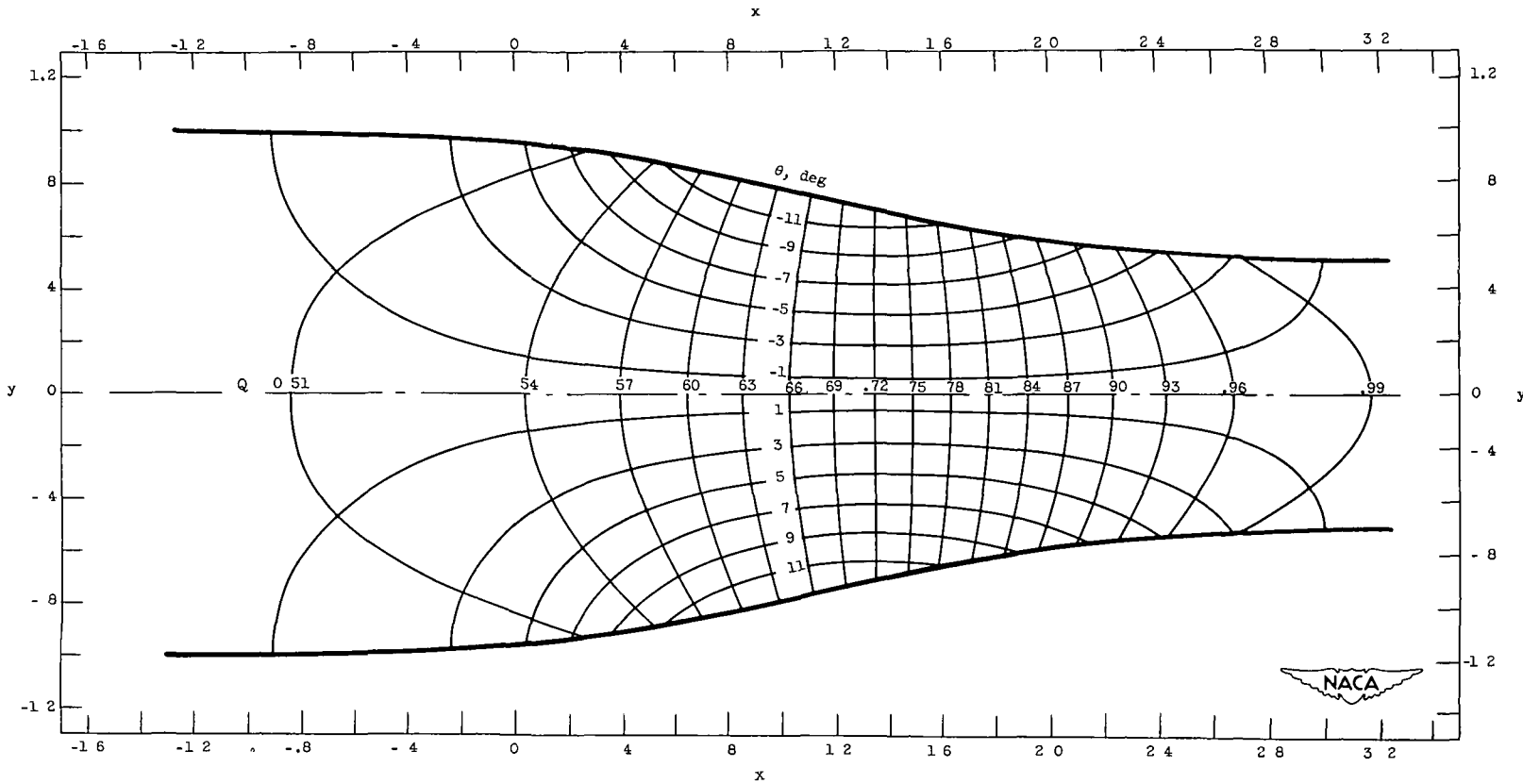


Figure 7 - Lines of constant velocity Q and flow direction θ in physical xy -plane for example I
Incompressible flow, prescribed velocity given in figure 2

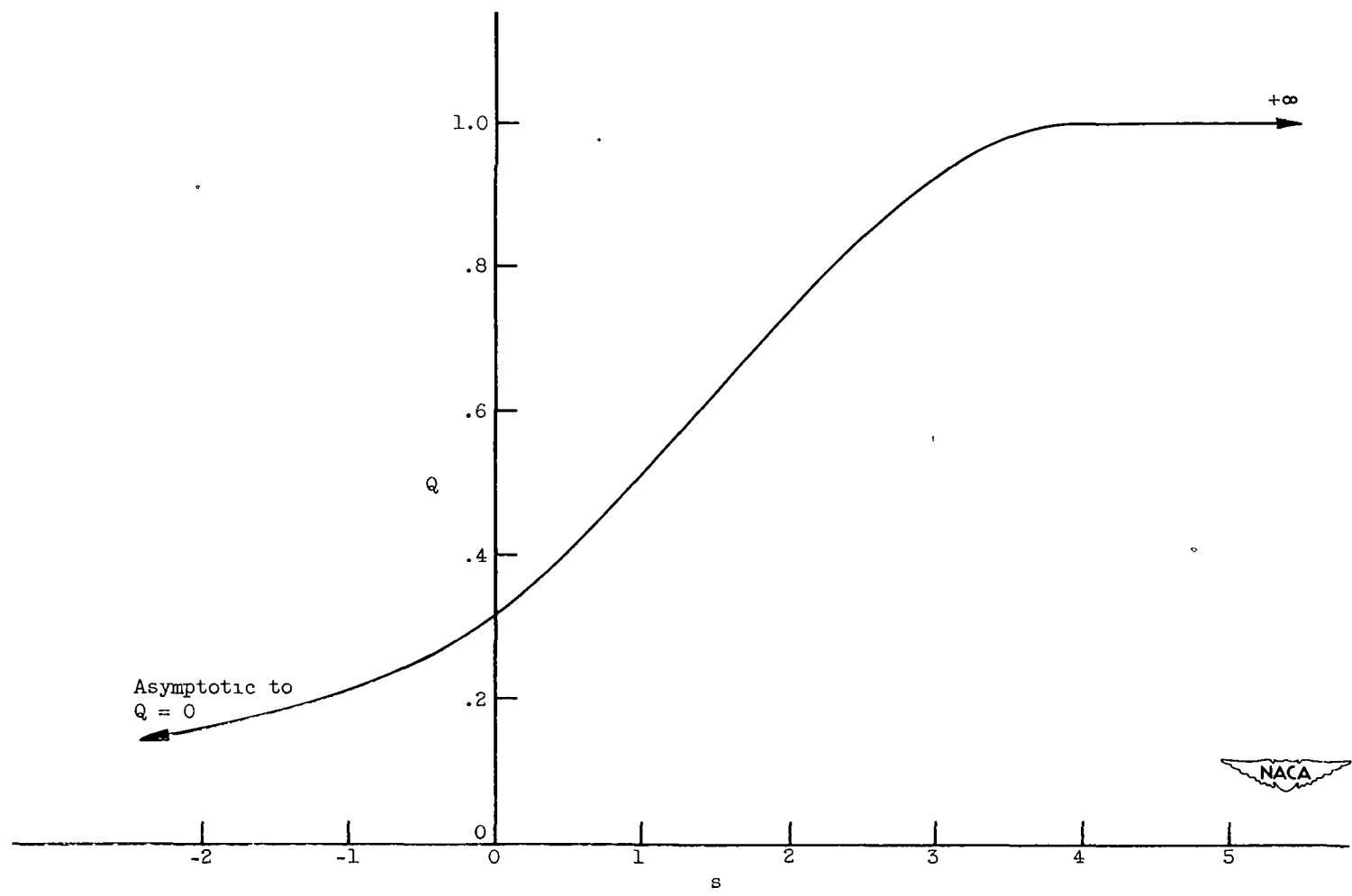


Figure 8. - Prescribed velocity distribution as function of arc length along channel wall for example II. Equation (38).

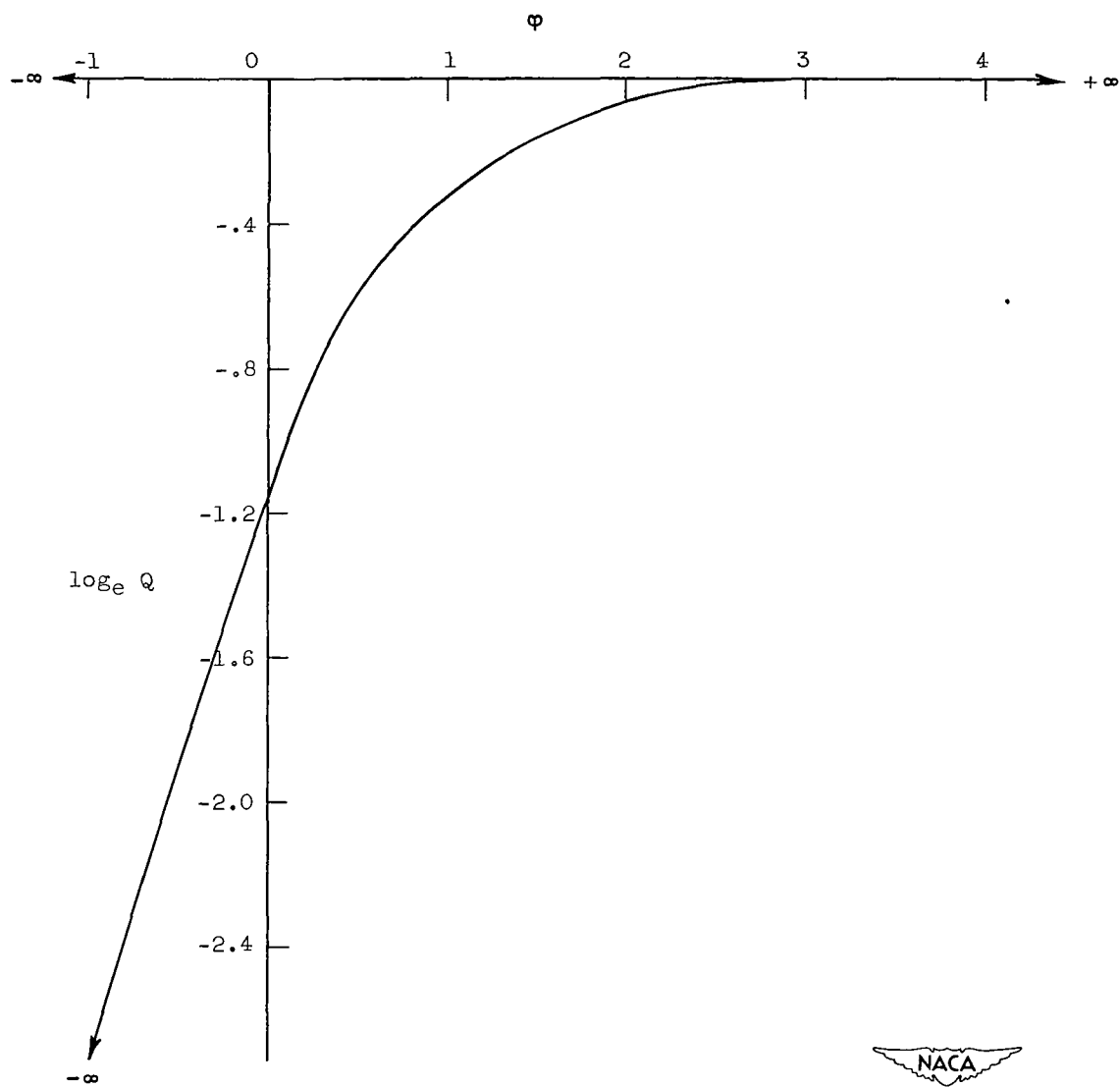


Figure 9. - Prescribed distribution of $\log_e Q$ as function of ϕ along channel walls for example II.

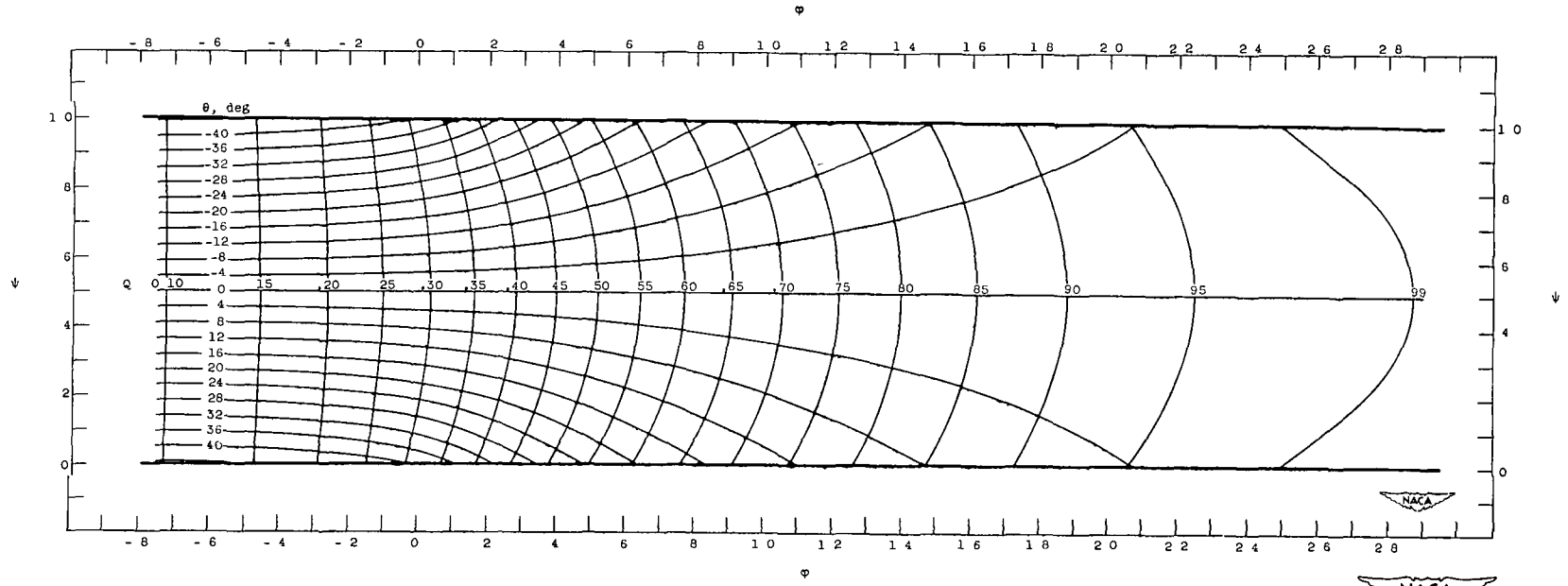


Figure 10. - Lines of constant velocity Q and flow direction θ in transformed $\phi\psi$ -plane for example II. Incompressible flow, prescribed velocity given in figure 8. (An enlarged print of this figure is enclosed.)

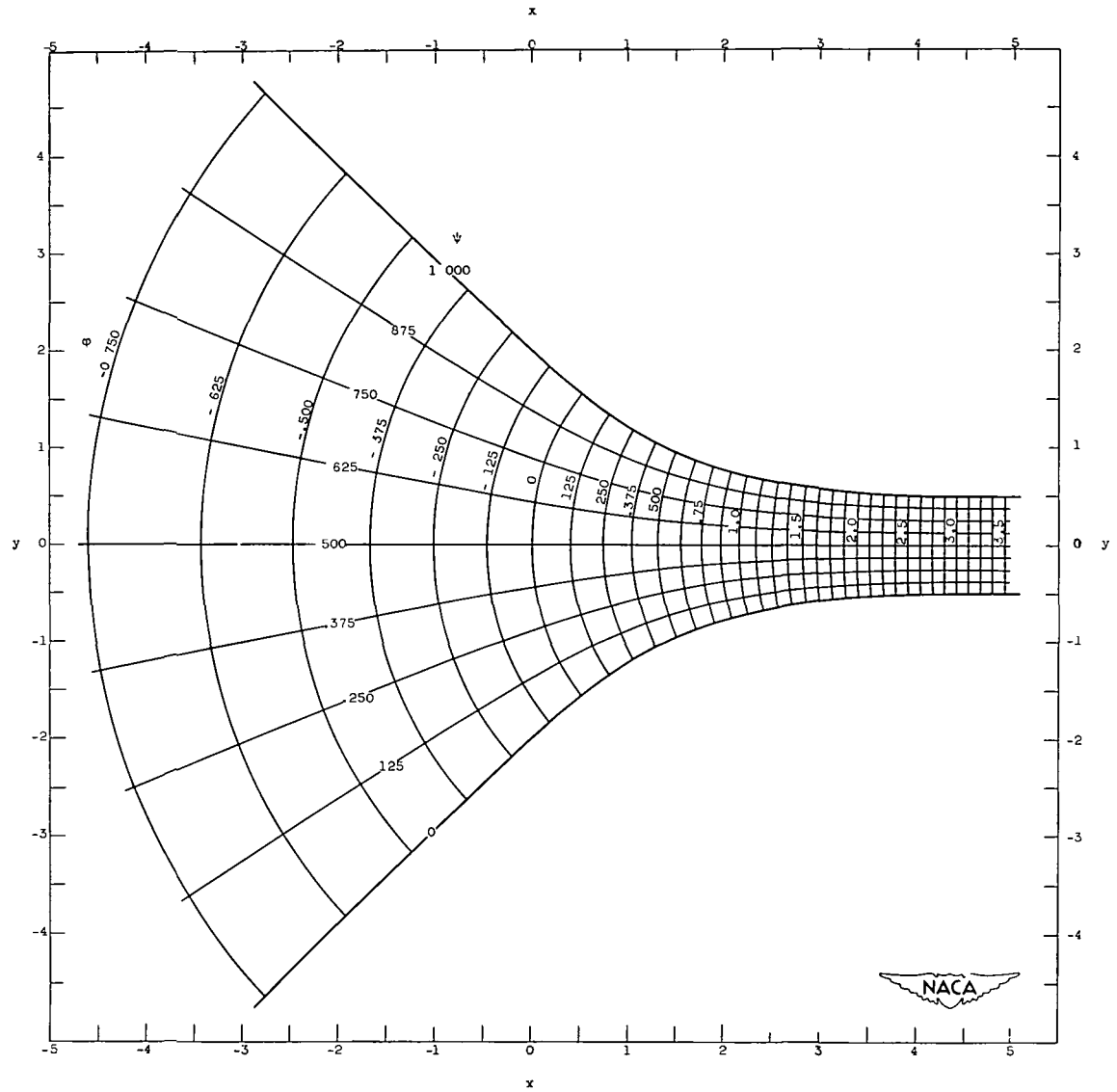


Figure 11. - Streamlines and velocity-potential lines in physical xy -plane for example II. Incompressible flow, prescribed velocity given in figure 8.

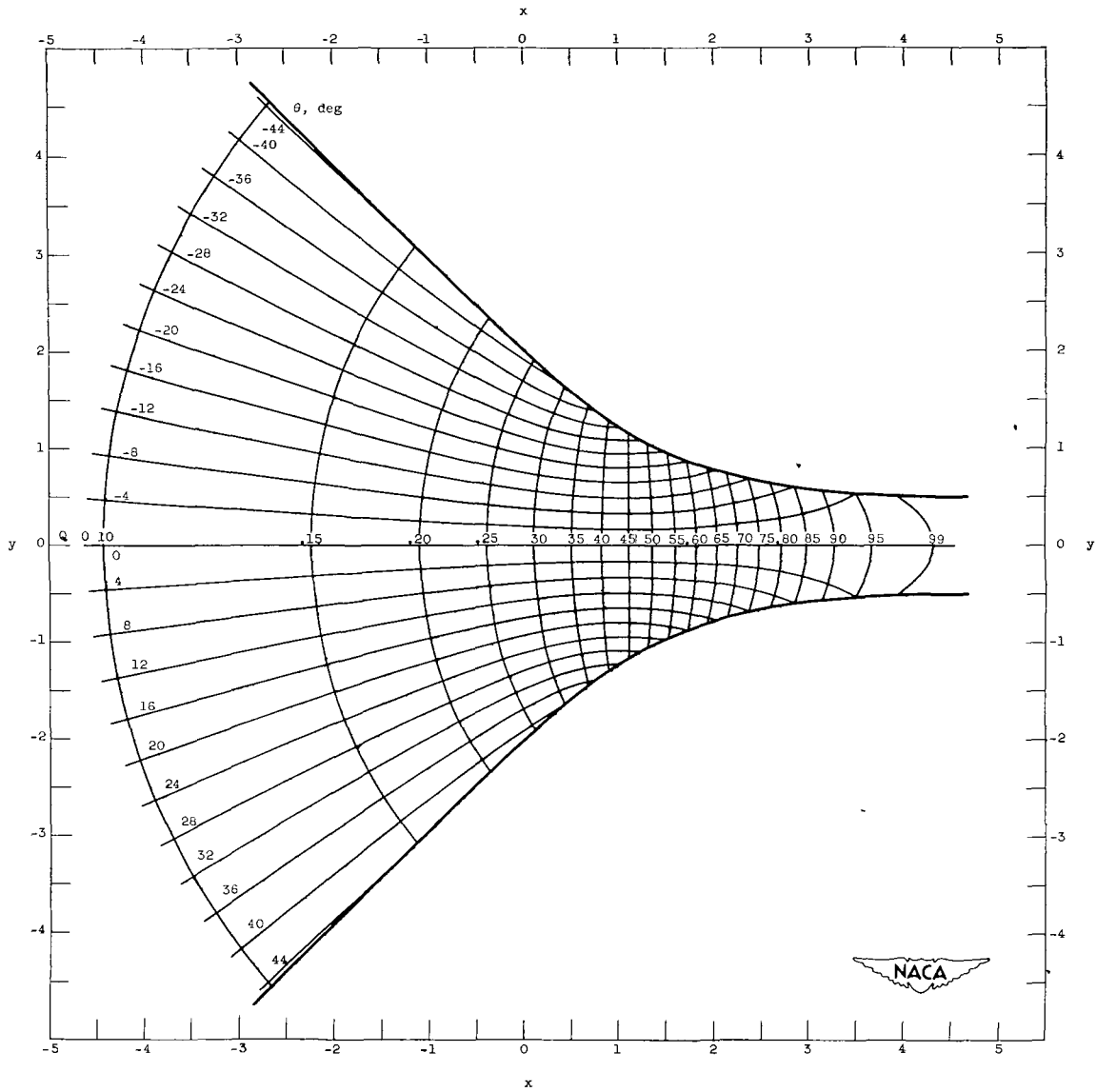


Figure 12 - Lines of constant velocity Q and flow direction θ in physical xy -plane for example II. Incompressible flow, prescribed velocity given in figure 8.

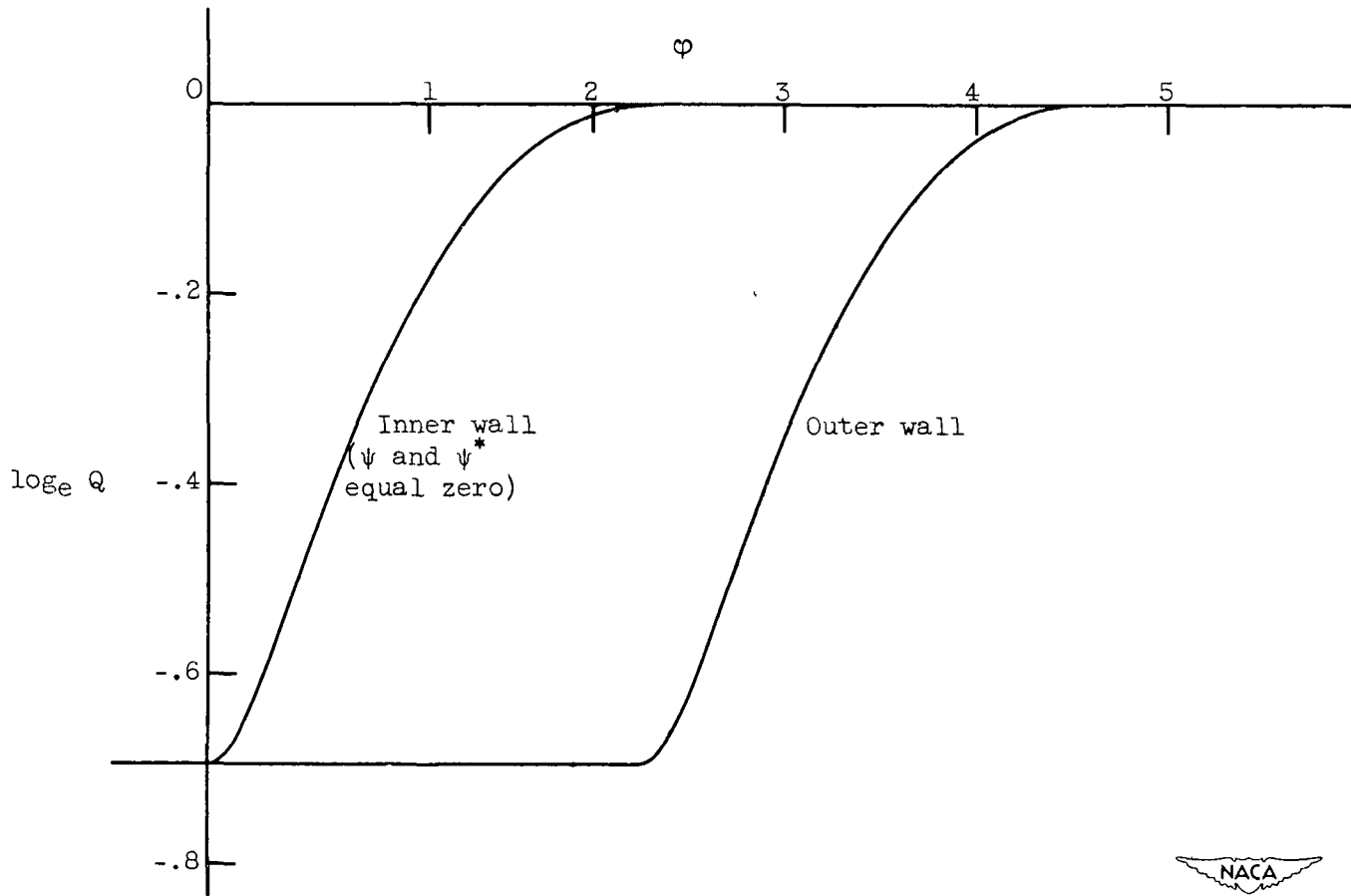


Figure 13. - Prescribed distribution of $\log_e Q$ as function of ϕ along channel walls for examples III, IV, and V.

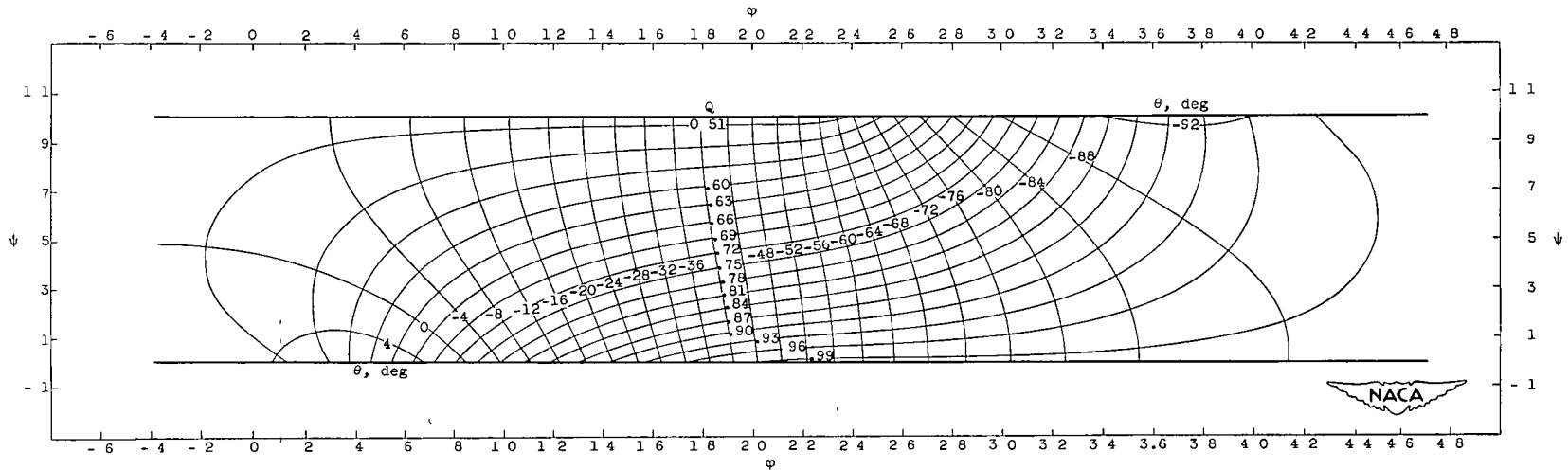


Figure 14. - Lines of constant velocity Q and flow direction θ in transformed $\phi\psi$ -plane for example III. Incompressible flow, prescribed velocity given in figures 2 and 13. (An enlarged print of this figure is enclosed.)

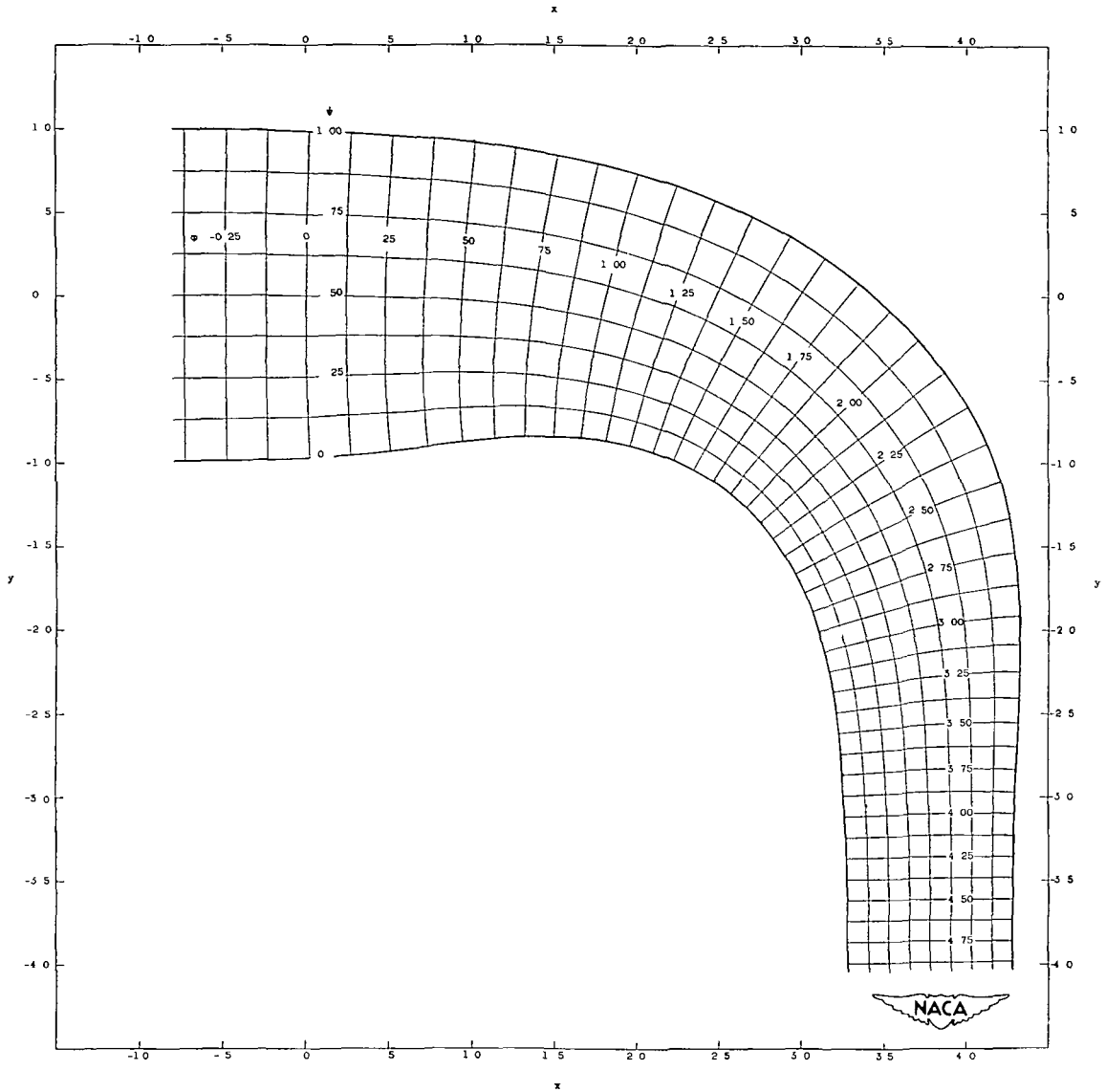


Figure 15. - Streamlines and velocity-potential lines in physical xy -plane for example III
Incompressible flow; prescribed velocity given in figures 2 and 13

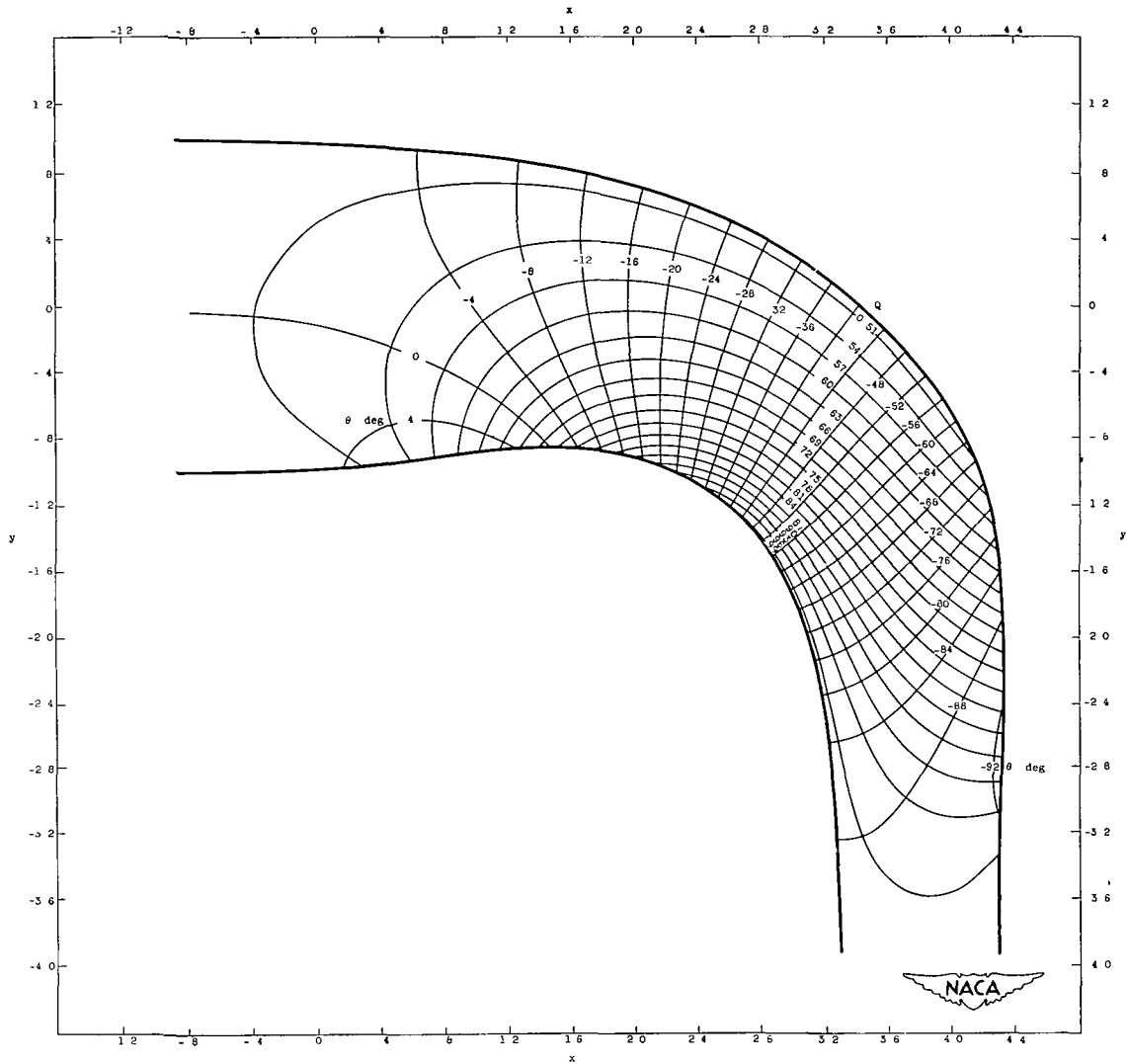


Figure 16. - Lines of constant velocity Q and flow direction θ in physical xy -plane for example III. Incompressible flow, prescribed velocity given in figures 2 and 13

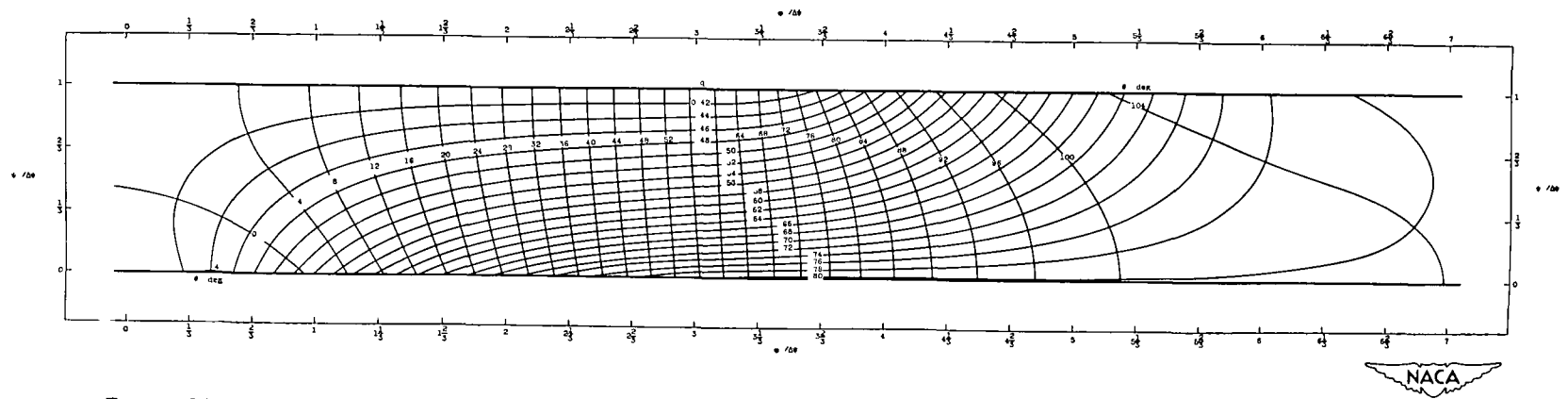


Figure 17. - Lines of constant velocity q and flow direction θ in transformed $\psi^*\eta$ -plane for example IV Linearized compressible flow, prescribed velocity as function of arc length along channel walls same as for example III (fig. 2) and with q_d equal to 0.80176 (An enlarged print of this figure is enclosed.)

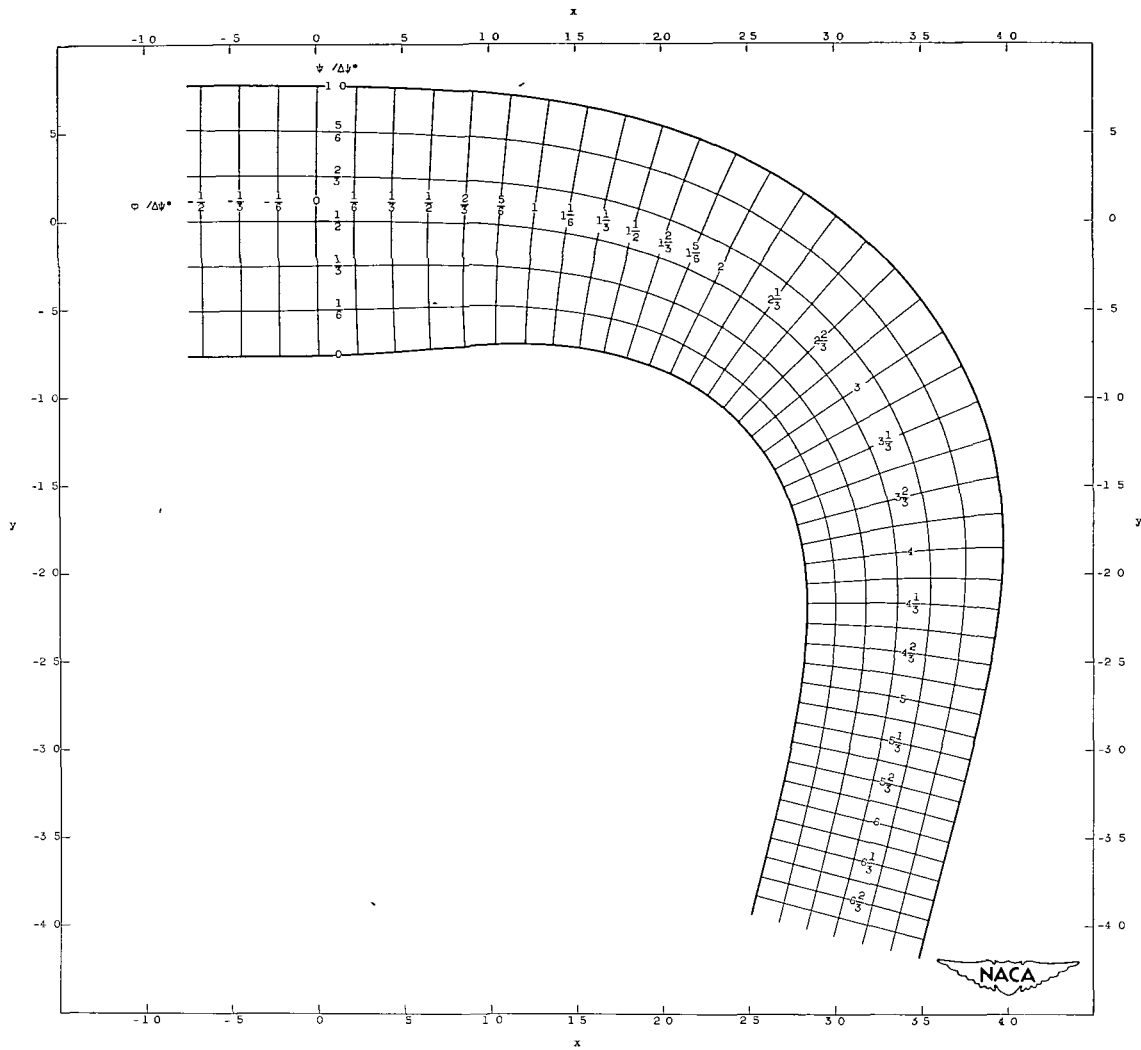


Figure 18. - Streamlines and velocity-potential lines in physical xy -plane for example IV
 Linearized compressible flow, prescribed velocity as function of arc length along channel
 walls same as for example III (fig. 2) and with q_d equal to 0.80176.

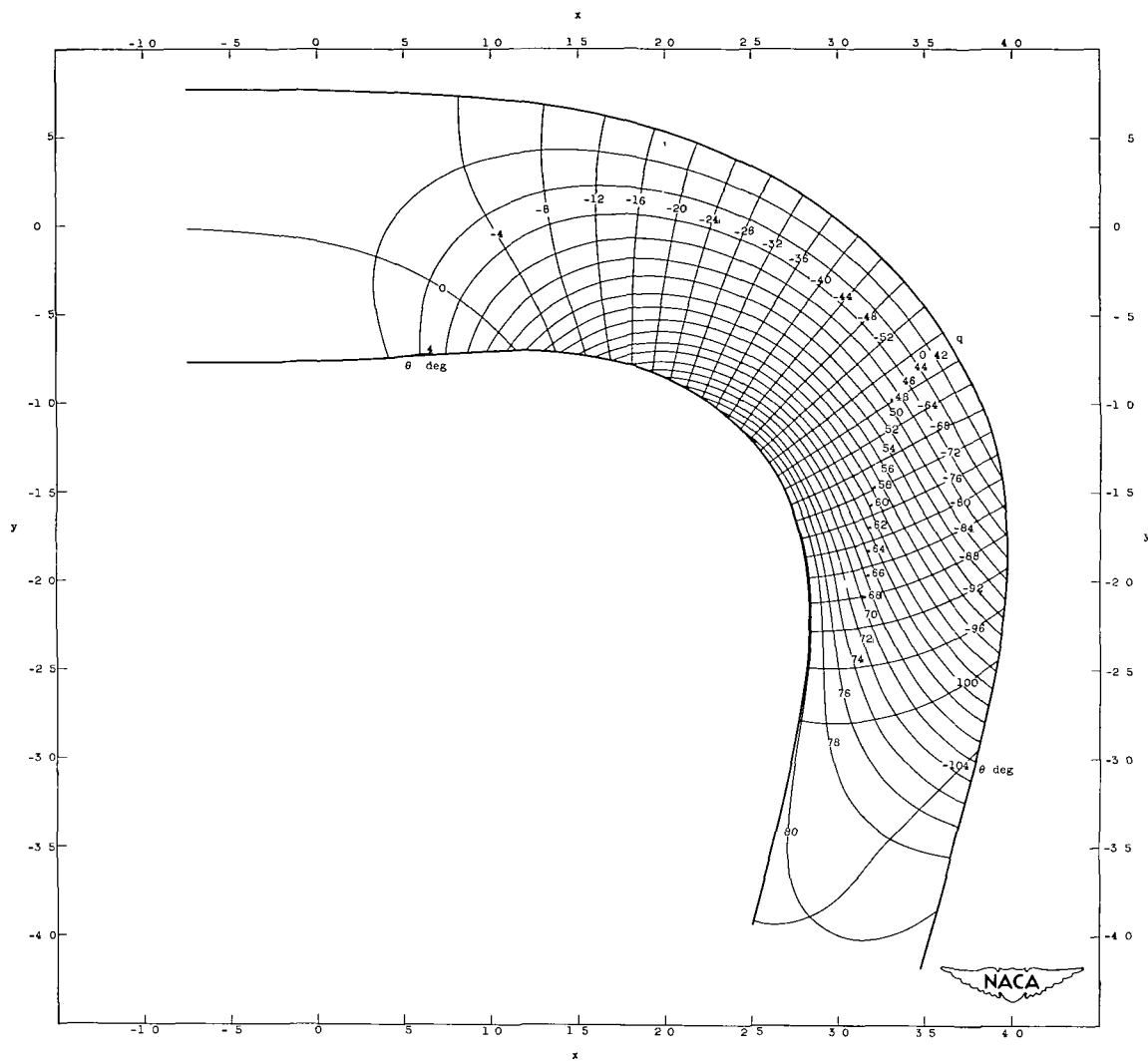


Figure 19. - Lines of constant velocity q and flow direction θ in physical xy -plane for example IV. Linearized compressible flow, prescribed velocity as function of arc length along channel walls same as for example III (fig. 2) and with q_d equal to 0.80176.

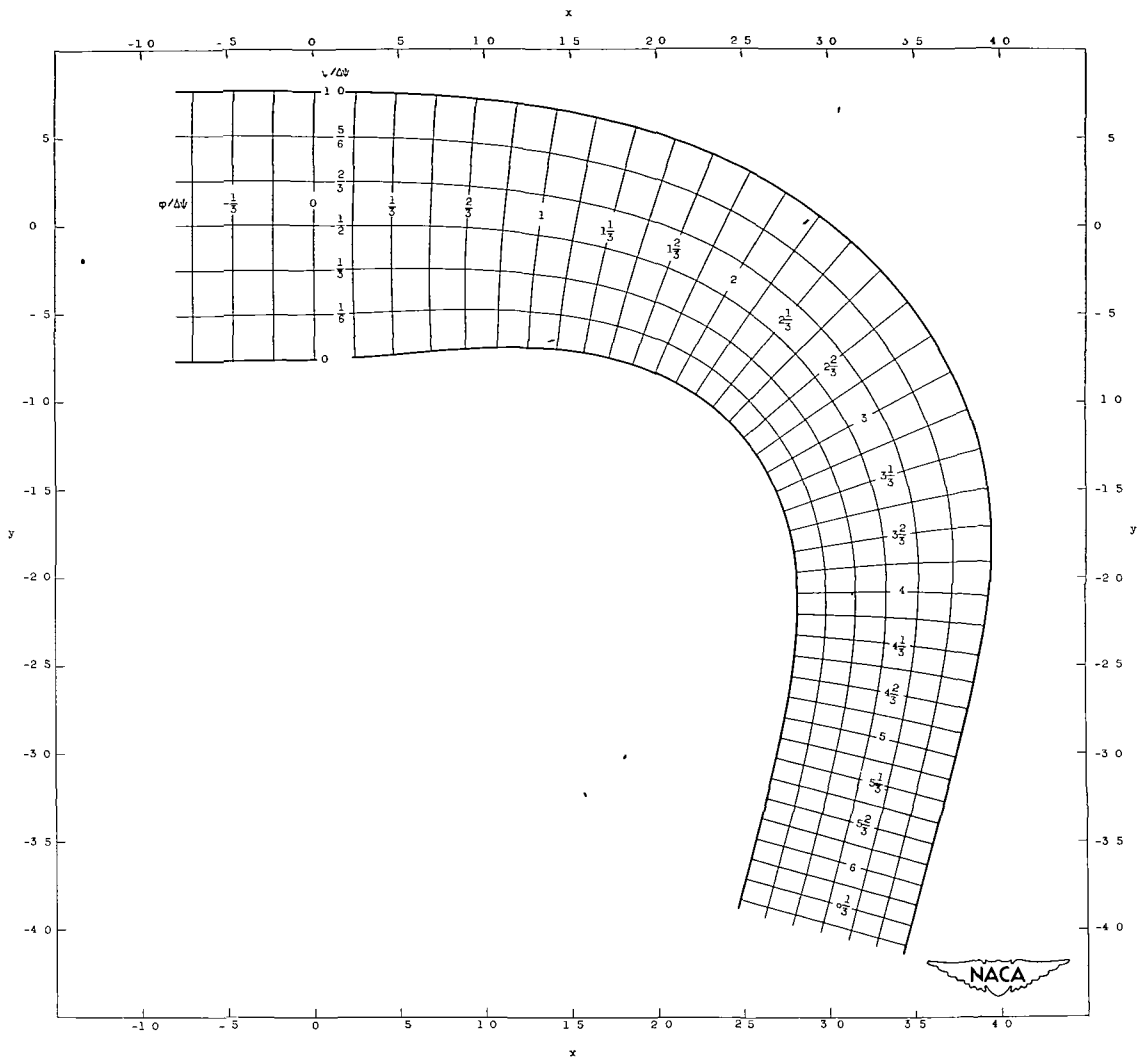


Figure 20 - Streamlines and velocity-potential lines in physical xy -plane for example V Compressible flow ($\gamma = 1.4$), prescribed velocity as function of arc length along channel walls same as for examples III and IV (fig. 2) but with q_d equal to 0.79927.

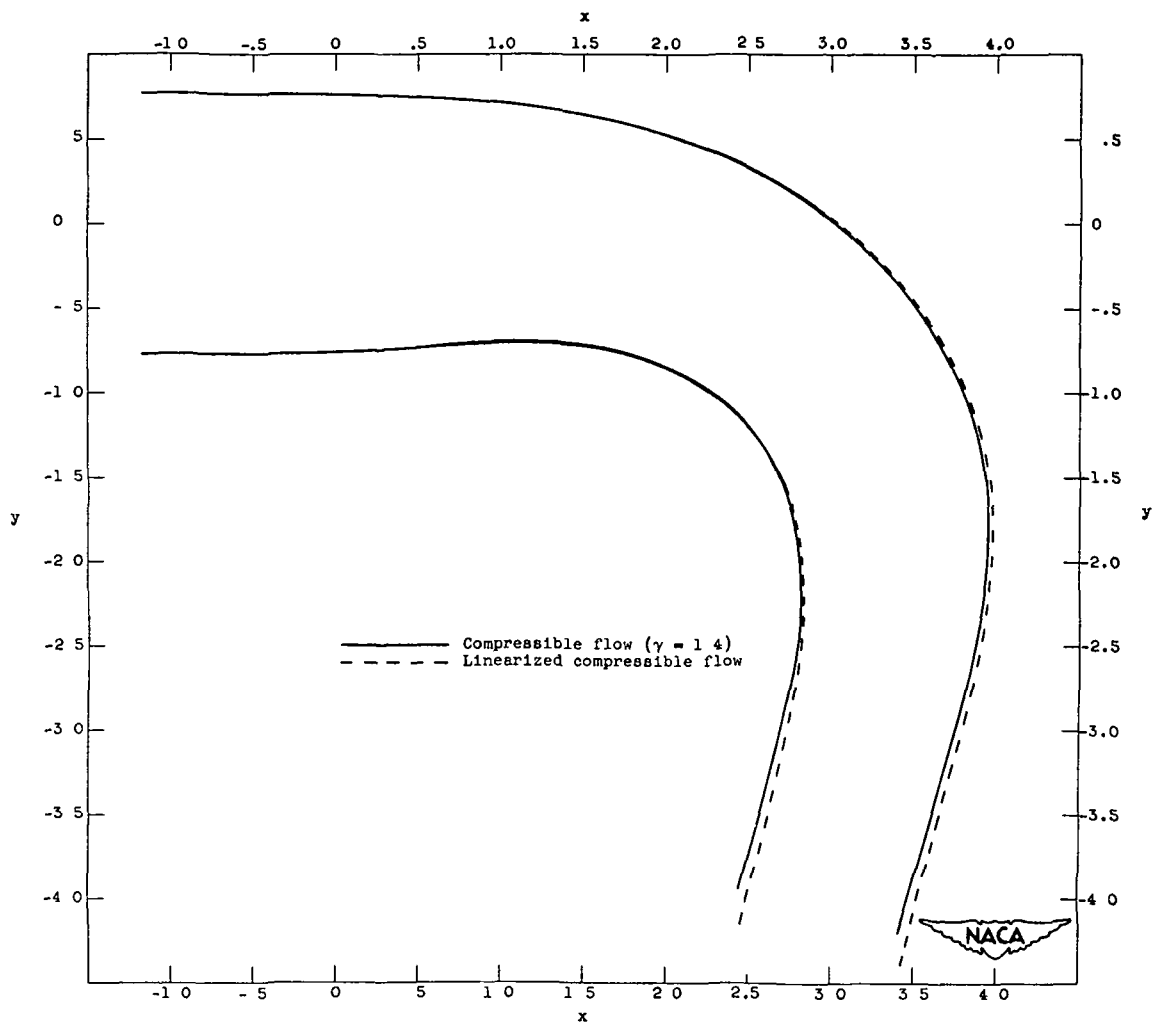


Figure 21 - Comparison of channel wall shapes for compressible flow (example V) with γ equal to 1.4 and for linearized compressible flow (example IV) for same prescribed velocity as function of arc length along channel walls (fig. 2)

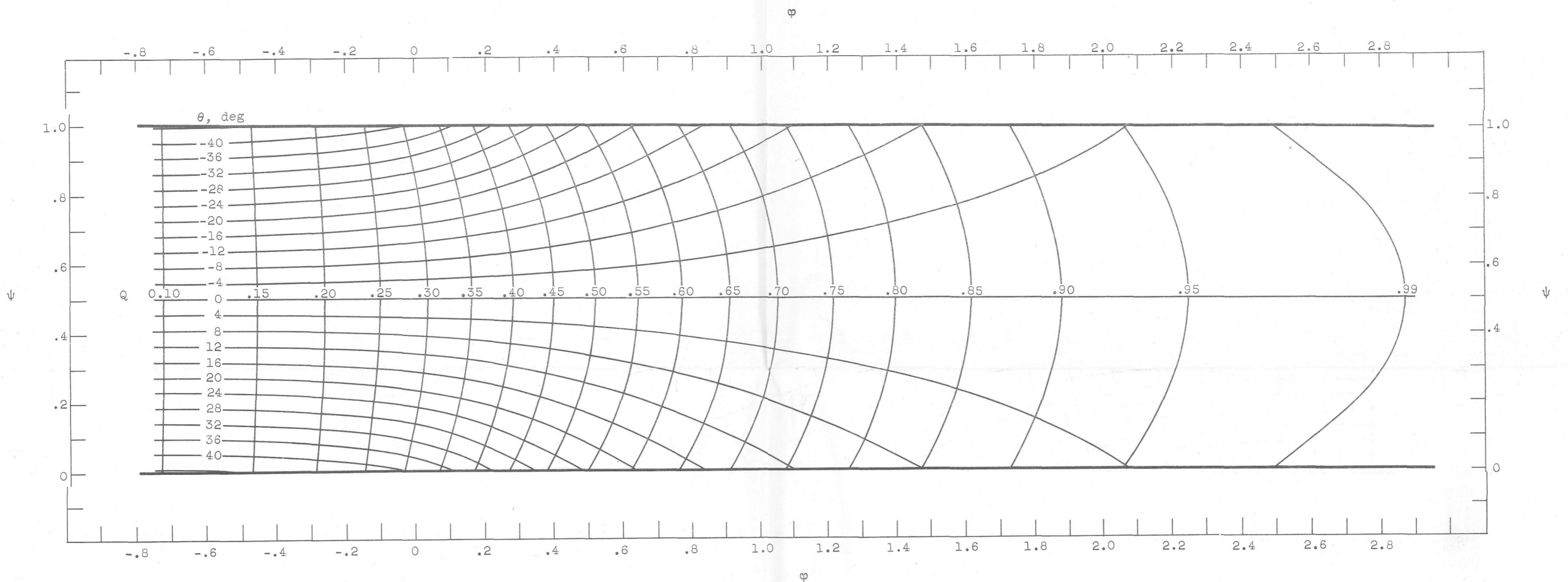


Figure 10. - Lines of constant velocity Q and flow direction θ in transformed $\phi\psi$ -plane for example II. Incompressible flow; prescribed velocity given in figure 8.

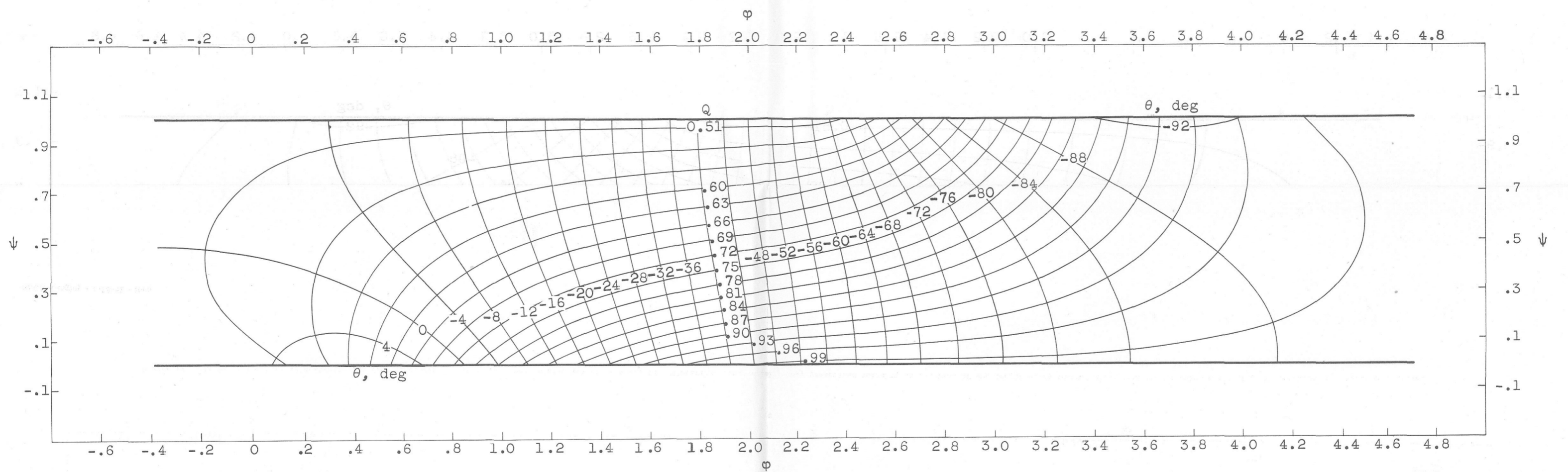


Figure 14. - Lines of constant velocity Q and flow direction θ in transformed $\phi\psi$ -plane for example III. Incompressible flow; prescribed velocity given in figures 2 and 13.

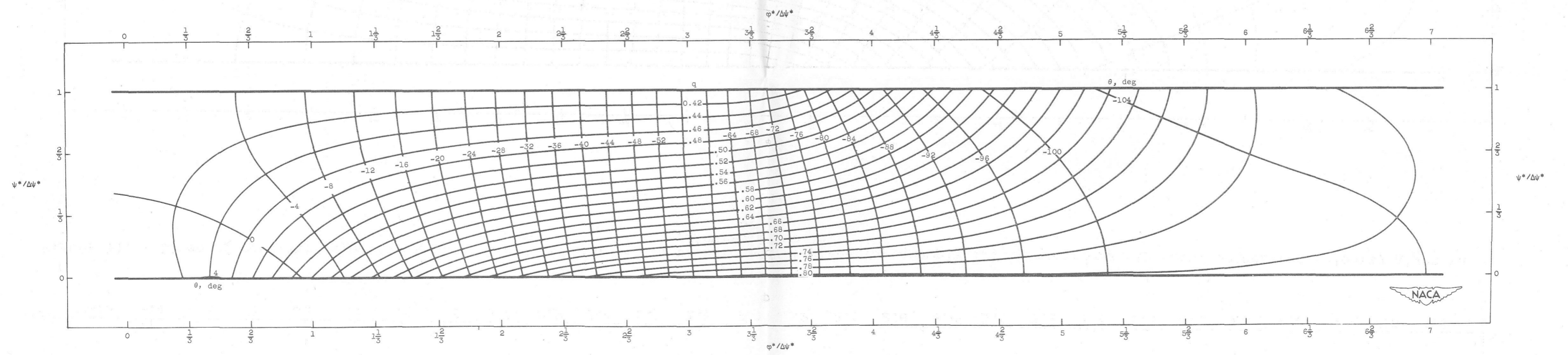


Figure 17. - Lines of constant velocity q and flow direction θ in transformed $\phi^*\psi^*$ -plane for example IV. Linearized compressible flow; prescribed velocity as function of arc length along channel walls same as for example III (fig. 2) and with q_1 equal to 0.80176.